

NUMERICAL STUDY OF NANOPARTICLE CONCENTRATION
EFFECT ON HEAT TRANSFER ENHANCEMENT IN MINI-
CHANNEL FLOW

A Thesis by

Tewodros Fiseha Wondimu

Bachelor of Science, Bahir Dar University, 2008

Submitted to the Department of Mechanical Engineering
and the faculty of the Graduate School of
Wichita State University
in partial fulfillment of
the requirements for the degree of
Master of Science

December 2014

© Copyright 2014 by Tewodros Fiseha Wondimu

All Rights Reserved

NUMERICAL STUDY OF NANOPARTICLE CONCENTRATION EFFECT ON HEAT TRANSFER ENHANCEMENT IN MINI- CHANNEL FLOW

The following faculty members have examined the final copy of this thesis for form and content, and recommend that it be accepted in partial fulfillment of the requirement for the degree of Master of Science with a major in Mechanical Engineering.

T. S. Ravigururajan, Committee Chair

Gisuk Hwang, Committee Member

M. B. Yildirim, Committee Member

DEDICATION

I would like to dedicate this work to my beloved family who supported me throughout all the time with encouragement and prayer

ACKNOWLEDGMENTS

I want to express my gratitude to my adviser, T. S. Ravigururajan, for his excellent guidance, thoughts, and support. I am also grateful to my family who were willing to sacrifice their time and money to support me and achieve my goals. I must express my gratitude to Duane Davies who took his time to review and comment on this research paper despite his tight schedule. I also thank National Institute for Aviation Research, computational mechanics lab for allowing me to use their work station computer and software resource for my research without any difficult. Finally I would like to extend my thankfulness to all good friends who supported me with their heartening thoughts.

ABSTRACT

The study conducted in this research focuses primarily on the discussion and statistical analysis of thermophysical physical properties in published literature, development of a mathematical correlation for estimating thermophysical and rheological properties, numerical study of heat transfer enhancement, and comparison of results between experimental and theoretical studies of nanofluids. Specifically suspensions of nanoparticles of Al_2O_3 , CuO and TiO_2 in a base fluid of water up to a concentration of 5% by volume are studied. Due to their properties of creating a well diluted solution with a base fluid, good thermal conductivity enhancement, ease of synthesis, abundance, low cost, and extensive possible applications, these three metal oxide nanoparticles are currently the preferred nanofluids in industries. Adequate experimental observations of thermophysical properties are gathered from literature to develop a comprehensive model of thermal conductivity and viscosity of nanofluids. This study will offer baseline information for further research and study in the fields of microelectronics, aerospace and automotive industries that implement micron and millimeter size cooling circuits in their thermal management system. In this study, a rectangular channel with 1.651mm hydraulic diameter is used to test and compare the heat transfer performance of the subject nanofluids in a high flux density of heat dissipation. A steady state of 150 watt heat load is used to observe the heat transfer enhancement relative to the conventional cooling processes. Accordingly, conditions that are selected and imposed on the study environment make this research result in a virtuous benchmark, especially perhaps to mini embedded cooling circuits potentially used in microelectronics and related fields.

TABLE OF CONTENTS

Chapter	Page
1. INTRODUCTION	1
2. REVIEW OF LITERATURE	5
2.1 Overview	5
2.2 Theoretical Thermal Conductivity Models	7
2.3 Potential Mechanisms of Thermal Performance Enhancement	10
2.3.1 Brownian Motion of Particles	11
2.3.2 Liquid Molecular Layering	12
2.3.3 Nanoparticle Clustering	13
2.3.4 Ballistic Transport of Energy	15
2.4 Theoretical Viscosity Models	17
2.5 Density of Nanofluid	20
2.6 Specific Heat Capacity of Nanofluid	21
2.7 Synthesis of Nanofluid	21
2.8 Application of Nanofluid	23
3. STATISTICAL MODELING OF NANOFLUID PROPERTIES	27
3.1 Experimental Evidence Review	27
3.2 Data Collection and Processing	30
3.2.1 Experiment Observation	30
3.2.2 Experimental Results	31
3.2.2.1 Effective Dynamic Viscosity of Nanofluids	32
3.2.2.2 Effective Thermal Conductivity of Nanofluids	40
3.2.3 Data Process Summary	46
3.3 Statistical Modeling	47
3.3.1 Regression Modeling of Al ₂ O ₃ Nanofluid Properties	47

TABLE OF CONTENTS (continued)

Chapter	Page
3.3.2 Regression Modeling of CuO Nanofluid Properties.....	51
3.3.3 Regression Modeling for TiO ₂ nanofluid properties	55
4. FINITE ELEMENT MODELING AND GRID VALIDATION.....	59
4.1 Computational Fluid Dynamics.....	59
4.1.1 Domain Discretization Methods	60
4.2 Grid Selection and Validation	62
4.2.1 Domain Size and Specification.....	63
4.2.2 Grid Validation	65
4.3 Mathematical Modeling	69
4.3.1 Governing Equation	71
4.3.2 Effective Nanofluid Viscosity Model	72
4.3.3 Effective Nanofluid Thermal Conductivity Model.....	73
4.3.4 Effective Nanofluid Density Model.....	73
4.3.5 Effective Specific Heat Capacity Model.....	74
4.4 Boundary Conditions.....	74
4.4.1 Inlet and Outlet Boundary Conditions	74
4.4.2 Thermal Load Condition.....	75
4.5 Computation Goals Convergence and Goals Criteria	76
5. NUMERICAL ANALYSIS RESULT	77
5.1 Numerical Simulation Matrix.....	78
5.2 Numerical Results and Discussion	79
5.2.1 Numerical Results of Al ₂ O ₃ Nanofluid.....	79
5.2.1.1 Heat Transfer Enhancement of Al ₂ O ₃ Nanofluid.....	83
5.2.2 Numerical Result of CuO Nanofluid	85
5.2.2.1 Heat Transfer Enhancement of CuO Nanofluid.....	89
5.2.3 Numerical Result of TiO ₂ Nanofluid	90

TABLE OF CONTENTS (continued)

Chapter	Page
5.2.3.1 Heat Transfer Enhancement of TiO ₂ Nanofluid	95
5.2.4 Heat Transfer Enhancement Summary	96
6. HEAT TRANSFER ENHANCEMENT COMPARISON	99
6.1 Previous Studies and Developed Correlations	100
6.2 Developing Nusselt Number Correlation	101
6.2.1 Data Correlation Methodology	103
6.3 Comparison of Correlations from Literature	106
7. CONCLUSION	109
REFERENCES	112
APPENDIX	121

LIST OF TABLES

Table	Page
2.1 Effective thermal conductivity models based on EMT.....	8
2.2 Theoretical models for effective thermal conductivity.....	16
3.1 Thermal conductivity comparison of solids and liquids at room temperature.....	42
3.2 ANOVA table of Al ₂ O ₃ nanofluid effective viscosity.....	49
3.3 ANOVA table of Al ₂ O ₃ nanofluid effective conductivity.....	51
3.4 ANOVA table of CuO nanofluid effective viscosity.....	53
3.5 ANOVA table of CuO nanofluid effective conductivity.....	55
3.6 ANOVA table of TiO ₂ nanofluid effective viscosity.....	57
3.7 ANOVA table of TiO ₂ nanofluid effective conductivity.....	58
4.1 Grid 1 CFD result data of different thermo-physical properties.....	66
4.2 Error comparison between different grids.....	67
4.3 New effective dynamic viscosity models of nanofluids.....	72
4.4 New effective thermal conductivity models of nanofluids.....	73
4.5 Numerical analysis goal convergence criterion.....	76
5.1 Numerical analysis result matrix table.....	78
5.2 Numerical result for 1% concentration of Al ₂ O ₃ nanofluids at Re=540.....	79
5.3 Numerical result for 5% concentration of Al ₂ O ₃ nanofluids at Re=645.....	80
5.4 Numerical result for 1% concentration of CuO nanofluids at Re=525.....	85
5.5 Numerical result for 5% concentration of CuO nanofluids at Re=645.....	86
5.6 Numerical result for 1% concentration of TiO ₂ nanofluids at Re=510.....	91

LIST OF TABLES (continued)

Table	Page
5.7 Numerical result for 5% concentration of TiO ₂ nanofluids at Re=625	92
6.1 New Developed Nusselt number correlation based on Numerical analysis result	104

LIST OF FIGURES

Figure	Page
2.1 Size comparison of nanoparticles.	5
2.2 TEM image of some nanofluids.....	6
2.3 Thermal conductivity enhancement due to solid-liquid layer structure.....	13
2.4 Schematic representation of nanoparticle cluster and their phenomenon.....	14
2.5 Relative viscosity comparison between theoretical models.....	20
3.1 Schematics of transient hot wire experiment setup.....	28
3.2 Paralle plate steady state conductivity measurement.....	29
3.3 Stress - strain dependence of different classification of fluids.	34
3.4 Comparison of the experimental data of relative viscosity for Al_2O_3	38
3.5 Comparison of the experimental data of relative viscosity for CuO	39
3.6 Comparison of the experimental data of relative viscosity for TiO_2	40
3.7 Comparison of relative conductivity of experimental data for Al_2O_3	43
3.8 Comparison of relative conductivity of experimental data for CuO	44
3.9 Comparison of relative conductivity of experimental data for TiO_2	45
3.10 Regressed viscosity model plot for Al_2O_3 - water nanofluid.....	48
3.11 Regressed conductivity model plot for Al_2O_3 - water nanofluid.....	50
3.12 Regressed Viscosity model plot for CuO - water nanofluid.....	52
3.13 Regressed conductivity model plot for CuO - water nanofluid.....	54
3.14 Regressed Viscosity model plot for TiO_2 - water nanofluid.....	56
3.15 Regressed conductivity model plot for TiO_2 - water nanofluid.....	57

LIST OF FIGURES (continued)

Figure	Page
4.1 FloEFD V13.0 manual mesh setup window	62
4.2 (a) Circular flow cross section tube in a structured grid domain	63
4.3 Optimized grid of fluid flow cross section in square channel.	64
4.4 CFD result comparison with a theoretical Nusselt number correlation.	67
4.5 Error comparison with different grids.....	68
4.6 Applicable mathematical models for solid-fluid mixture	69
4.7 Geometrical configuration of 3D numerical analysis setup.....	75
5.1 Heat transfer variation along the channel length at 1% concentration of Al_2O_3	81
5.2 Heat transfer variation along the channel length of Al_2O_3	82
5.3 Heat transfer coefficient of Al_2O_3 nanofluid at different volume fraction.	84
5.4 Heat transfer variation along the channel length at 1% concentration of CuO	87
5.5 Heat transfer variation along the channel length of CuO	88
5.6 Heat transfer coefficient of CuO nanofluid at different volume fraction.	89
5.7 Heat transfer variation along the channel length at 1% concentration of TiO_2	93
5.8 Heat transfer variation along the channel length of TiO_2	94
5.9 Heat transfer coefficient of TiO_2 nanofluid at different volume fraction.	95
5.10 Heat transfer enhancement comparison per nanoparticle volume fraction.....	98
6.1 Heat transfer performance comparison between studied nanofluid types.	105
6.2 Nusselt number response at different volume fraction.	106
6.3 Nusselt number comparison of different models at $\phi=1.0\%$	107
6.4 Nusselt number comparison of different models at $\phi=3.0\%$	108

LIST OF FIGURES (continued)

Figure	Page
6.5 Nusselt number comparison of different models at $\phi=5.0\%$	108

LIST OF ABBREVIATIONS

3D	Three Dimensional
ANOVA	Analysis of Variance
BC	Boundary Condition
CAD	Computer Aided Design
CFD	Computational Fluid Dynamics
CWHF	Constant Wall Heat Flux
DBC	Dirchlet Boundary Condition
DF	Degree of Freedom
EMA	Effective Medium Approximation
EMT	Effective Medium Theory
FD	Finite Difference
FE	Finite Element
FEM	Finite Element Model
FV	Finite Volume
HTC	Heat Transfer Coefficient
MBC	Mixed Boundary Condition
MS	Mean Square Error
NBC	Neuman Boundary Condition
PDE	Partial Differential Equation
POLY	Polynomial Function
RBC	Robin Boundary Condition
SS	Sum Square Error
TEM	Transmission Electron Microscopy

LIST OF NOMENCLATURE

a	Partial Regression Coefficient (–)
A	Surface Area (m^2)
C_p	Specific Heat Capacity ($J/kg.K$)
D	Diffusion Constant (m^2/s)
D_h	Hydraulic Diameter (m)
d_p	Particle Diameter (nm)
E	Heat Transfer Enhancement (–)
g	Gravitational Force (m/s^2)
h	Heat Transfer Coefficient($w/m^2.K$)
K	Thermal Conductivity($w/m.k$)
K_B	Boltzmann Constant($1.3806E - 23 J/K$)
K_{bf}	Base Fluid Thermal Conductivity ($w/m.k$)
K_{eff}	Effective Thermal Conductivity ($w/m.k$)
K_{layer}	Nano-Layer Thermal Conductivity ($w/m.k$)
K_{nf}	Nanofluid Thermal Conductivity ($w/m.k$)
K_p	Particle Thermal Conductivity ($w/m.k$)
L	Channel Length (m)
m_{bf}	Mass of Base Fluid (kg)
m_p	Mass of Particle (kg)
n	Particle Shape Constant (–)
Nu	Nusselt Number (–)
P	Pressure (Pa)
Pe	Peclet Number ($w/m.k$)
Pr	Prandtl Number (–)
Q	Heat (w)
q''	Heat Flux (w/m^2)
R	Regression Coefficient (–)

LIST OF NOMENCLATURE (continued)

Re	Reynolds Number (–)
r_p	Radius of Particle (m)
t	Nano Layer Thickness (nm)
T	Temperature (k)
U	Flow Velocity (m/s)
x	Local Length (m)
Y	Statistical Dependent Variable (–)
Y*	Inverse of Dependent Variable (–)
γ	Fluid Shear Strain ($1/s$)
δ_t	Boundary Layer Thickness (m)
ε	Statistical Error (–)
μ_{bf}	Base Fluid Viscosity ($Pa \cdot s$)
μ_{nf}	Nanofluid Viscosity ($Pa \cdot s$)
ρ_{bf}	Base Fluid Density (kg/m^3)
ρ_{nf}	Nanofluid Density (kg/m^3)
ρ_p	Particle Density (kg/m^3)
τ	Fluid Shear Stress (Pa)
φ	Solid Particle Volumetric Concentration (–)

CHAPTER 1

INTRODUCTION

The performance of mechanical and electrical equipment used in microelectronics, transportation, defense, and space applications is dependent on the effectiveness of their associated thermal management. Limited heat transfer performance puts a restrictive boundary on further development to those emerging technologies. According to many studies, cooling is the biggest technical challenge facing those technologies. In many published literature, the enhancements thus far of heat transfer performance of a given unit is mostly related to a small number of factors such as extended surface area of a heat transfer, boundary layer disturbance using tube inserts, or tube roughness. Conventionally, an improved design varies those parameters to enhance the heat transfer capability of equipment despite the fact that the performance improvement achieved is significantly limited due to the size and weight restraint, power consumption, efficiency, or effectiveness.

A nanofluid cooling medium is a state-of-the-art heat transfer technology which opens a new gate for enormous innovations specifically in the engineering and technology domain. Nanofluids technically are composite materials that have solid particles in suspension, usually with a diameter size of 1-100nm, diluted inside a conventional cooling or heating liquids [1]. The dispersion of those solid particles contributes to the exploitation of their inherent high thermal conductivity behavior. In nature, solid particles have higher thermal conductivity than liquids and in some cases metallic nanoparticles have a thermal conductivity of three orders of magnitude higher than a conventional cooling liquid, [2]. A curious study of mixtures of solid particles and liquid is dated back to the classical work of Maxwell [3]. He developed one of the

first models of effective thermal conductivity of solid/fluid mixtures based on the conventional concept of the heat conduction equation under the condition of static and random spherical solid particles. Burggman [4] developed a model for the effective conductivity of a solid/fluid mixture based on the work from Maxwell [3]. Burggman [4] model is applicable to mixtures with higher volume concentration of solid particles. Hamilton and Crosser [5] modified the Maxwell [3] model to come up with a new effective thermal conductivity model that can be exploited for non-spherical solid particle suspensions in liquid. Although major studies on this effective medium theory gives a coherent result for millimeter or micron size particles, the basic Maxwell [3] concept of heat conduction for those classical formulation fails to explain the thermal conductivity enhancement in nanofluids. While fluid mixtures with a suspension of millimeter and micron sized particles have shown a good thermal conductance behavior, their application is at present not widely explored due to their adverse rheological and stability problems. Because of their relative greater size and weight, the particles tend to quickly sediment in response of the forces acting on them. This inimical characteristic of such suspensions then set the stage for nanofluids to become the novel approach to-ward robust engineering fluids for improved heat transfer properties. The ultrafine solid particles in nanofluid can be well-diluted to give an extremely stable solution during operation as well as in static conditions for longer periods of time without any sign of sedimentation [2]. Moreover, the thermal performance of nanofluids is superior to other fluids with a suspension of micron or millimeter sized particles [1].

Since the earliest observation of thermal conductivity enhancement of fluid with suspended nanoparticles by Masuda et al. [6], published literature can be found on the theories of the possible heat transfer mechanism in nanofluid. Although most recent studies have ruled out the classical approaches suggested by Maxwell [3], Lorenz and Clausius in the 19th century to

describe the thermal performance enhancement of mixtures, published results are in disagreement regarding the mechanism of heat transfer due to significant discrepancies of result between studies. Literature reports dissimilar results on the thermal conductivity enhancement when compared to different research for identical nanoparticles and base fluids. Poor characterization of nanoparticle suspensions in a fluid and lack of a basic theoretical understanding on the mechanism of heat transfer obstructs the science of nanotechnology. So far, there is no accurate theoretical model that comprehensively governs nanofluids and determines the conductivity enhancement satisfactorily [7].

However, continuing research and development in the field of nanotechnology reveals many possible contributing factors in the mechanism of heat transfer. Those factors are likely involved in explaining the inadequacy of the classical macroscopic analysis of heat transfer [1]. Major factors in heat transfer of a nanofluid that are thoroughly discussed in literature are the Brownian motion of particle, molecular level layering of the liquid at the liquid-particle interface, ballistic heat transport in nanoparticles, and the effect of clustering of nanoparticles. Researchers put forth an effort to come up with a sound heat transfer model using those premises as a standalone or by integrating their effect with the conventional heat transfer theory on a static and random particle approach. Thus far, fairly improved results on the thermal conductivity enhancement are being able to be estimated from those theoretical models. Yu and Choi [8] have developed a new thermal conductivity model based on a proposition that the solid like nano layer acts like a thermal bridge between the nanoparticle and the bulk fluid, and this phenomenon plays a key role in enhancing the overall thermal conductivity. The nano-layer around the solid particle will be in transitional physical state between solid and bulk liquid. And it is expected to have a higher thermal conductivity than the bulk fluid. Similar thermal conductivity models based on nano-

layer effects are also developed by Xue and Xu [9] through modifying the Burggman classical theoretical model. A Brownian motion is also one of the major hypotheses proposed by different literature. By incorporating the thermal conductive enhancement due to random motion of particles in to the conventional models of heat transfer Xuan et al. [10] proposed an effective thermal conductive model including the effect of particle size, concentration and temperature. Wang et al. [11] also developed a thermal conductivity model based on the effective medium approximation and the fractal theory by introducing the effect of particle size and the surface adsorption property of nanoparticles. Comparable studies also present several models that can be used to approximate the nanofluid property. Although present studies are not in the vicinity of a comprehensive, accurate, and robust nanofluid theoretical model the astounding progress in understanding the mechanism leads to a promising nanotechnology based applications.

The wide and intriguing applications of nanofluid drive the technology research in seeking a comprehensive governing model. A complete understanding of these novel composite materials will enlighten the technology industry and boost the capability, efficiency and quality of their products to the next level. For example, microelectronic devices that operates at a multi-Giga Hertz range needing a super conducting fluid for cooling, or higher power output engines or optical devices that emit high flux density of heat requiring a liquid with ultra-high cooling performance. Other examples can be found in new applications in the biomedical field such as cancer imaging and drug delivery, using a magnetic nanofluid guided through the blood stream to the location of tumor using controlled magnetic fields. In general, liquids with a suspension of solid nanoparticles are being studied comprehensively and will be developed to meet those challenges.

CHAPTER 2

REVIEW OF LITERATURE

2.1 Overview

A suspension of nanoparticles with a diameter size less than 100nm inside a base fluid of water, ethylene glycol or engine oil can be considered as a nanofluid. Generally, nanofluids are composite materials that are laboratory engineered to enhance their heat transfer behavior by altering their thermo-physical and rheological properties. By introducing a quantifiable volumetric fraction of solid particles (nano-metric size in diameter) into the base fluid, an increase in the conductivity and convective film coefficient of heat transfer can be achieved. In general this will elevate the efficiency of the heat transfer achieved in the system. This novel technology enormously enriches the ability of industries that specialize in products that are highly dependent on heat transfer capability, such as microelectronics, aerospace industries, nuclear reactors, micro-reactors, automotive, industrial heat exchangers and so on. The ultrafine size of the particles dispersed in the base fluid makes the nanofluids preeminent alternatives especially in microelectronics where clogging, settling, and clustering are the main issue.

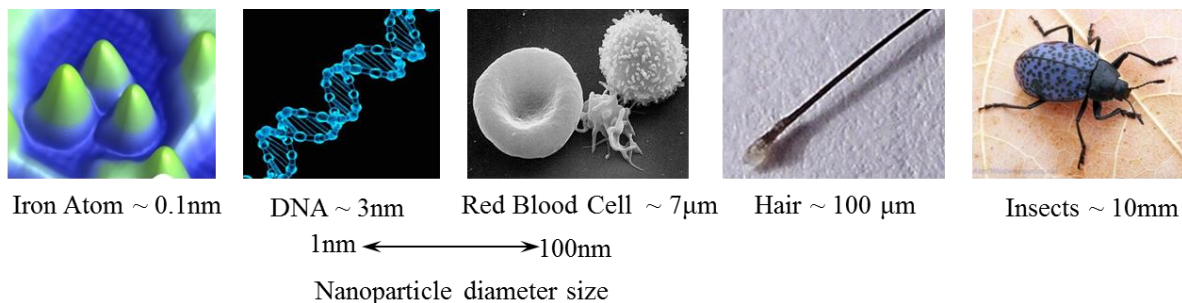


Figure 2.1 Size comparison of nanoparticles.

The application of nanofluids also extends to the medical field. Magnetic nanofluids are used to deliver a drug in a blood stream with the guide of controlled magnetic field to the exact location of tumor in cancer therapeutics [12]. The thermophysical property of a nanofluid is highly dependent on the characteristics of its constituents. Present literature shows that the thermophysical properties of nanoparticle and base fluid, volume fraction of nanoparticle, nanoparticle size, shape and temperature are the major factors that influence the property of nanofluids [11].

Nanofluids can be synthesized from numerous combinations of nanoparticles and base fluids. Particles can be a type of metallic oxides, nonmetallic oxide, metals, nonmetals, and metal carbides. The most common base fluids used in the nanotechnology industries are water, ethylene glycol, and oil [1]. Some of the common nanoparticles used in heat transfer industries are Al_2O_3 , CuO , TiO_2 , SiC , TiC in the compound form and Ag , Au , Cu , and in the elemental form.

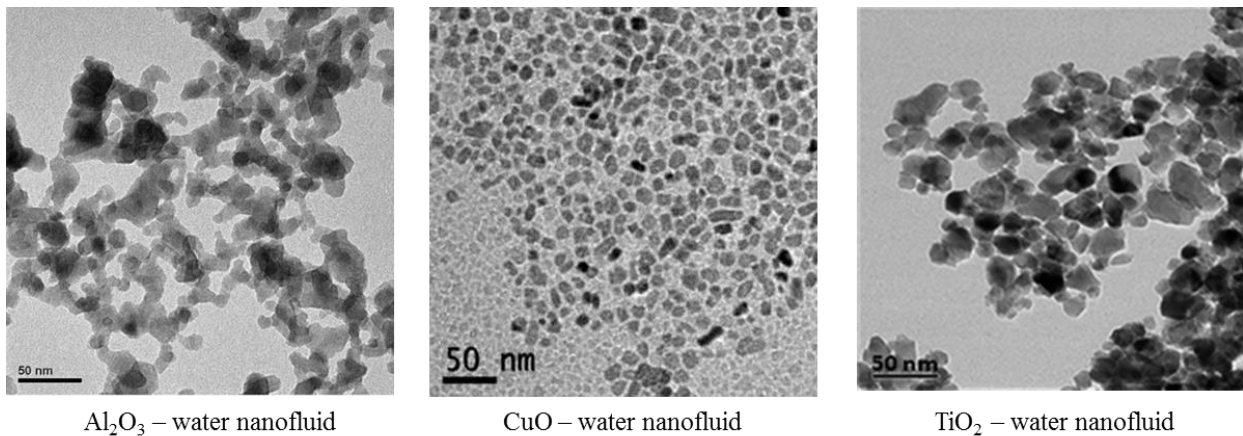


Figure 2.2 TEM image of some nanofluids. (Source: Teng et al., Pastoriza et al., and Sotto respectively.)

2.2 Theoretical Thermal Conductivity Models

The history of diluted liquid suspension of nanoparticles is dates back to the late 19th century. A pioneering work from Maxwell [3] in 1873, on the effective medium theory established a firm base for the current understanding of nanofluids. Effective medium theory (EMT) or effective medium approximation (EMA) is a theoretical modeling of composite materials behavior based on the macroscopic properties and the relative amount of fraction of its constituent [11]. Maxwell [3] has approached the mixture medium in his work on dielectric properties of composite material, small solid particles dispersed with a random fashion in the fluid medium where the distance between each particle is far enough to avoid any interference due to the local distortion in the matrix (base fluid). Based on this approach numerous derivations of composite materials are developed. Detailed research from Bruggman [4] in 1935 strengthens the concept of Maxwell [3] by considering the interaction between solid particles which makes it applicable to high concentrations of particles [13]. Hamilton and Crosser [5] developed an effective conductivity model based on the Maxwell formulation. Hamilton and Crosser [5] model incorporates the effect of particle shape into their new equation. The shape factor explains the surface area of the non-spherical particles relative to the basic spherical particles. Higher shape factor magnitude implies an enhancement of effective thermal conductivity. The hypothesis suggested by Hamilton and Crosser [5] model will be less valuable on the application of nanofluids, where synthesized nanoparticles are more or less spherical, and thermal conductivity enhancement due to nonsphericity loses its valid ground.

Unfortunately, all EMT models don't provide an accurate thermal conductivity prediction for nano sized particles in spite of their robust mathematical modeling assessment of

micron and millimeter size particle solutions. This demonstrates that the heat transfer mechanism in nanofluid is beyond the concept of a macroscopic conventional heat transfer theory.

Table 2.1 Effective thermal conductivity models based on EMT

Model	Expression	Description
Maxwell [3]	$\frac{K_{eff}}{K_{bf}} = \frac{K_p + 2K_{bf} + 2(K_p - K_{bf})\varphi}{K_p + 2K_{bf} - (K_p - K_{bf})\varphi}$	Spherical particles φ Solid volume fraction
Hamilton and Crosser [5]	$\frac{K_{eff}}{K_{bf}} = \frac{K_p + (n - 1)K_{bf} - (n - 1)\varphi(K_{bf} - K_p)}{K_p + (n - 1)K_{bf} + \varphi(K_{bf} - K_p)}$	N depends on particle shape and $K_p/K_{bf} > \sim 100$, $n=3$ for other cases, ψ -sphericity.
Jeffrey [91]	$\frac{K_{eff}}{K_{bf}} = 1 + \frac{3\varphi(K_p/K_{bf} - 1)}{K_p/K_{bf} + 2} + 3\varphi^2 \left(\frac{K_p/K_{bf} - 1}{K_p/K_{bf} + 2} \right)^2 \cdot [1 + \frac{1}{4} \left(\frac{K_p/K_{bf} - 1}{K_p/K_{bf} + 2} \right) + \frac{3}{16} \left(\frac{K_p/K_{bf} - 1}{K_p/K_{bf} + 2} \right) \left(\frac{K_p/K_{bf} + 2}{K_p/K_{bf} + 3} \right) + \dots]$	High order terms due to pair interaction of randomly dispersed particles.
Davis [92]	$\frac{K_{eff}}{K_{bf}} = 1 + \frac{3(K_p/K_{bf} - 1) \cdot [\varphi + f \cdot \varphi^2 + O(\varphi^3)]}{(K_p/K_{bf} + 2) - (K_p/K_{bf} - 1)\varphi}$	High order terms due to pair interaction of randomly dispersed spheres, $f=2.5$ & 0.5 for $K_p/K_{bf}=10$ and ∞ , respectively.
Bruggeman [4]	$\frac{K_{eff}}{K_{bf}} = [(3\varphi - 1) \frac{K_p}{K_{bf}} + (2 - 3\varphi) + \sqrt{(\Delta)}] / 4$ $\Delta = (3\varphi - 1)^2 (K_p/K_{bf})^2 + (2 - 3\varphi)^2 + 2(2 + 9\varphi - 9\varphi^2)(K_p/K_{bf})$	Spherical particles, interaction between particles considered, applicable to high concentration.

After Choi et al. [14] wrote the first review article on nanofluid, numerous literature has been published regarding all aspects of nanofluids. Most literature is focused on the study of the

mechanism of heat transfer between the bulk liquid and particles, and also investigates the anomalous conductivity enhancement phenomenon. Studies reported that the enhancement of thermal performance is highly dependent on the concentration of nanoparticles blended in the base fluid. Higher volumetric concentration of particles is directly proportional to the thermal conductivity improvement. Concentration of volumetric fraction of the nanoparticles is usually limited to 5% in order to keep the rheological property of the solution fairly close to a nanofluid with low concentration [15]. Higher concentration of nanoparticle suspension changes the fluid viscosity behavior drastically which adversely affects the thermal performance of the nanofluid. Masuda et al. [6] conducted a pioneering investigation on the conductivity of Al_2O_3 (Alumina) nanoparticles and reported that the volumetric concentration significantly affects the thermal conductivity of the nanofluid. In their report experimentally they have shown a concentration of 4.3% by volume can enhance the thermal conductivity by 30%. Das et al. [16] also shows a thermal conductivity of alumina nanofluid is significantly dependent on temperature. In their experiment 9.4% enhancement of thermal conductivity is observed at room temperature and 24.3% enhancement at 51°C . Timofeeva et al. [17] conducted an experiment on alumina nanofluid with a 5% volume fraction of 40nm diameter size nanoparticles, and they reported a 10% increment in the effective thermal conductivity. Accordingly, various literature reports an anomalous enhancement of thermal conductivity. Choi et al. [18], Chon et al. [19], and Li et al. [20], also reported a thermal conductivity augmentation of 11%, 28.8% and 26.1% respectively. The irregularity of thermal conductivity enhancement between studies may arise from different factors such as, nanoparticle manufacturing, nanofluid synthesis, experiment setup and preparation, testing condition and so on. Nonetheless, the improvement of the thermal conductivity is yet to be explained by existing theories. A full understanding of an atomic scale

of heat transfer in the near future might give a new insight toward unlocking the secret behind nanofluids [1]. Hypotheses have been developed in regards to explaining the heat transfer mechanism in a nano scale, however scientists are far from getting a definitive accurate model of these novel fluids. Major premises available in literature are discussed briefly in the following chapter.

2.3 Potential Mechanisms of Thermal Performance Enhancement

Although it is recognized that the dispersion of solid particles in a base fluid such as water or engine oil will potentially intensify the heat transfer in the system, the lack of a concrete theoretical basis to support the heat transfer makes a comprehensive understanding challenging. The mechanisms of heat transfer in fluids with suspended solid particles have been studied going back to the classic work of Maxwell [3], and others. The classical theories of effective medium theory are limited to a suspension of millimeter or micron size solid particles in a base fluid [2]. The stability and rheology properties of solid particles with larger size are different from nano size particles despite the fact that the heat transfer enhancement can be achieved. Particles with micron size will not create a completely diluted solution in the base fluid, and consequently the rate of sedimentation of those particles will be faster in comparison with nano scale particles. This phenomenon yields a variation of viscosity and severe clogging, especially in micro channels.

EMT models that are listed above are only consider the nanoparticle concentration and their shape effect as a factor for conductivity enhancement. This theory assumes classical heat transport between solid and liquid phases, and theoretically it doesn't take into account for the solid/liquid interface, random particle motion, and other atomic scale level phenomenon in their

formulation. In spite of its reasonable approach for micron size particle suspension in fluid, effective medium theories fail to explain the mechanism of heat transfer in nanofluids.

Despite the inconsistency of research results and their unconvincing hypotheses presented in papers, literature has put forth an effort to study the tangible mechanism of heat transfer in nanofluids in the last few decades. Below, the major mechanics of heat transfer widely found in literature that satisfactorily explain the anomalous increment of thermal conductivity observed in nanofluid are discussed in detail.

2.3.1 Brownian Motion of Particles

A Brownian motion is a movement of nano sized particles in random fashion suspended in the base fluid medium. The phenomenon is named after Robert Brown, a well-known botanist who observed the random movement of pollen grains in a fluid medium. However, he was unable to explain this random motion phenomenon. The movement of these particles through liquids, with a continuous collision between same particles, base fluid molecules, and the surrounding wall, will help to transport the thermal energy in the system. Some research credit the collision of those particles for the enhancement of effective thermal conductivity of a nanofluid [1]. The energy exchange between colliding particles could result in an improved thermal conductance in the nanofluid. This phenomenon is not accounted for as a factor in the conventional theories during the estimation of effective thermal conductivity of a mixture. The Stokes – Einstein formula defines the Brownian motion as a diffusion constant D with a factor of temperature, Boltzmann constant, particle diameter and viscosity of the base fluid.

$$D = \frac{K_B T}{3\pi\mu_{bf}d_p} \quad (2.1)$$

This equation estimates the effect of Brownian motion on the improvement of the effective thermal conductance by comparing the rate of heat diffusion in fluid with particle slip velocity. Nevertheless, Keblinski et al. [2] demonstrates that the diffusion of nanoparticles due to the Brownian motion is much slower when it is directly compared to the diffusion of heat in a liquid. And their study suggests that the random motion of particle is too slow to transport heat energy in the nanofluid. This phenomenon cannot be considered as a major mechanism of heat transfer enhancement in a nanofluid problem. Despite the deduction of Keblinski et al. [2], Xuan et al. [21] shows an indirect role of Brownian motion might affect the heat transfer enhancement. In their premise, nanofluids due to the chaotic movement of nanoparticles form a cluster of particles which might act as a thermal bridge and leads to a heat transfer augmentation.

2.3.2 Liquid Molecular Layering

The formation of structural ordering of nano particles close to a solid surface is an occurrence in nanofluids. Yu and Choi [8] suggest a new approach on the study of a nano-layer effect. In this approach the nanofluid is subdivided into three main structures consisting of solid nanoparticles, bulk liquid, and solid like-liquid layer. And this solid like-liquid layer near to the solid surface acts like a thermal bridge and assists the heat transfer between the fluid and the solid particles.

In their studies, they have improved the original Maxwell [3] effective thermal conductivity theory by adding the effect of the nano-layer on the thermal conductance of the solution. Keblinski et al. [2] reports layer effect at the wall might have a positive outcome on enhancing the thermal conductivity. Henderson et al. [23] explains that the structured arrangement of the solid-liquid layer is more ordered than the bulk liquid in atomic scale size.

This phenomenon creates a higher thermal transport at the solid/liquid interface when compared to pure liquids.

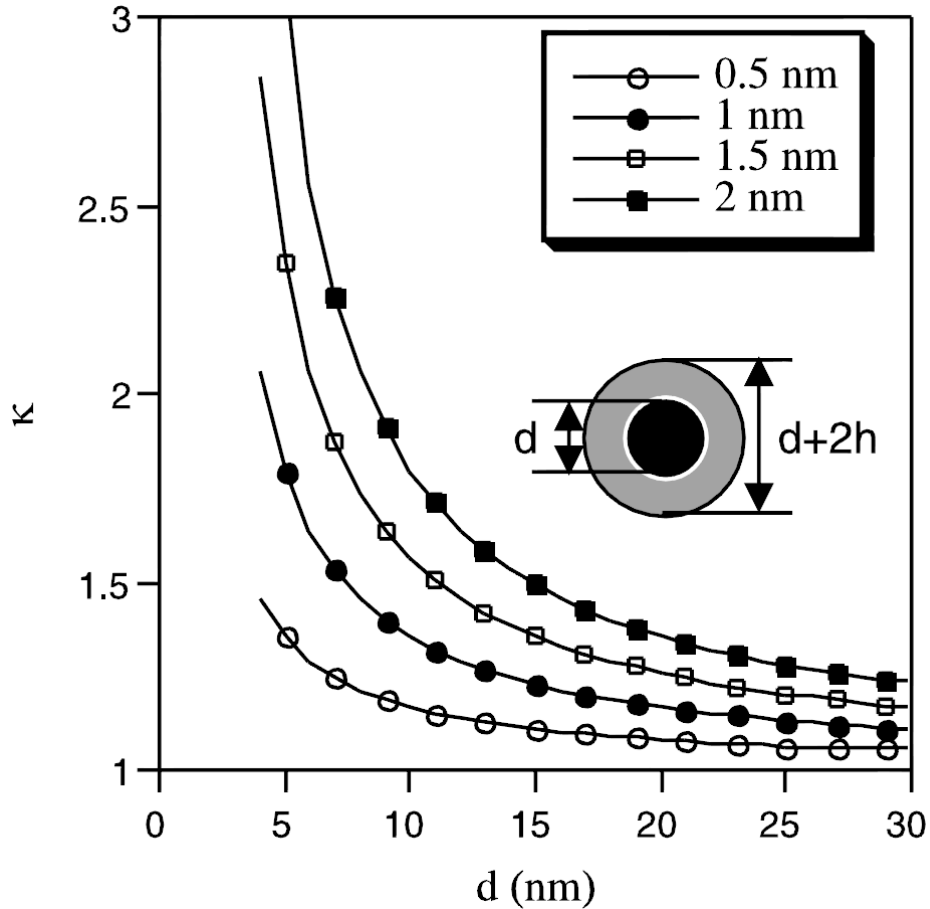


Figure 2.3 Thermal conductivity enhancement due to solid-liquid layer structure at various layer thickness h and particle diameter, d . (Source: Keblinski et al. [2], *Mechanism of heat flow in suspensions of nano-sized particles.*)

2.3.3 Nanoparticle Clustering

The agglomeration of nanoparticles in the base fluid can result in an improved heat transfer in some circumstances. The mechanism of heat transfer in clustered particles is thoroughly investigated by Evans et al. [24], using Monte Carlo simulations for model aggregates. Based on their studies the size and the shape of the cluster is the main factor on the

enhancement of conductivity. A long continuous path in the cluster of nanoparticles promotes rapid heat conduction.

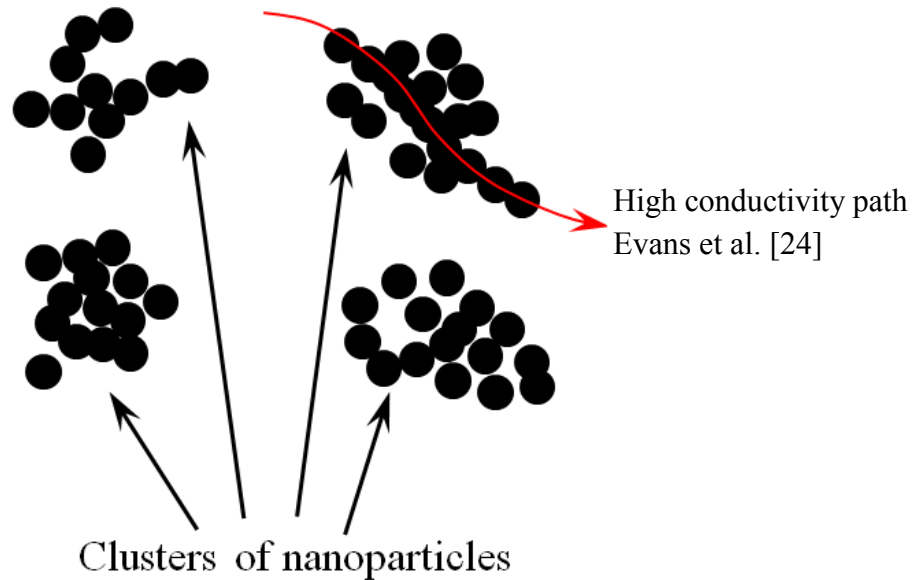


Figure 2.4 Schematic representation of nanoparticle cluster and their phenomenon.

Eastman et al. [1] reports a conductivity enhancement due a cluster of nanoparticle in nanofluid. A closely packed cluster of nanoparticle has lower conductivity than clusters that have a thin liquid layer separation between particles. Based on their studies, if ~25% of the volume of a cluster is filled with a liquid between nanoparticles, it might increase the highly conductive region volume by ~30%.

Despite the heat transfer enhancement study due to clustering, some researches refute the phenomenon by listing the effect of nanoparticle clusters on the deterioration of thermal conductivity. Koblinski et al. [2] concluded the agglomerates of particles in a nanofluid will adversely affect the heat transfer enhancement due to sedimentation of clusters, which will leave

the nanofluid only with a high thermal resistance base fluid. Clusters also create uneven viscosity and thermal conductivity in the system.

2.3.4 Ballistic Transport of Energy

In this mechanism, researchers reported that the heat in the solid particles is transported by a means of phonons. By the propagation of lattice vibration, the phonon carries the heat energy to the next available particle. Eastman et al. [1] explains when the mean free path of a phonon becomes greater than the size of the nanoparticles, the phonon energy transport will be incapable through diffusion, but will transmit the energy ballistically. Keblinski et al. [2] presented in their studies that the ballistic photon effect could strongly enhance the thermal conductivity if a nanofluid. If the separation between particles is on the order of $\sim 1\text{-}2\text{nm}$ layer thickness, the phonon mean free path is much shorter in the liquid than in the solid particle which leads to a significant thermal conductance increment. However, Yulong et al. [13] reports that ballistic energy transport has no effect on the enhancement of thermal conductance since it is explained that the thermal conductivity of nanoparticle decreases when the particle size decreases which opposes the ballistic energy transport assumption.

Based on available heat transfer hypotheses in nanofluids, some effective thermal models have been proposed in literature. Some of the developed expressions are tabulated as show below.

Table 2.2 Theoretical models for effective thermal conductivity

Models	Expressions	Description
Yu and Choi [8]	$\frac{K_{nf}}{K_{bf}} = \frac{K_{pe} + 2K_{bf} + 2\varphi(K_{pe} - K_{nf})\varphi}{K_{pe} + 2K_{bf} - \varphi(K_{pe} - K_{bf})(1 + \beta)^3}$ $\frac{K_{pe}}{K_p} = \frac{2(1 - \gamma) + (1 + \beta)^3(1 + 2\gamma)\gamma}{-(1 - \gamma) + (1 + \beta)^3(1 + 2\gamma)}$ $\beta = \frac{t}{r_p} \text{ and } \gamma = \frac{K_{layer}}{K_p}$	Modified Maxwell [3] model, considering spherical particles and nano-layer theory.
Xue [25]	$9 \left(1 - \frac{\varphi}{\lambda}\right) \frac{k_{nf} - K_{bf}}{2K_{nf} + K_{bf}} + \frac{\varphi}{\lambda} \frac{k_{nf} - K_{px}}{K_{nf} + B_{2x}(K_{px} - K_{nf})}$ $+ \frac{\varphi}{\lambda} 4 \frac{k_{nf} - K_{py}}{2K_{nf} + (1 - B_{2x})(K_{px} - K_{nf})} = 0$	Modified Maxwell [3] model, considering spherical particles and nano-layer theory
Xie et al [26]	$\frac{K_{nf} - K_{bf}}{K_{bf}} = 3\theta\varphi_T + \frac{3\theta^2\varphi_T^2}{1 - \theta\varphi_T}$ $\varphi_T = \frac{4}{3}\pi(r_p + t)^3 N_p = \varphi_p(1 + \beta)^3, \beta = \frac{t}{r_p}$	Low particle loading and nano-layer theory
Xuan et al [10]	$\frac{K_{nf}}{K_{bf}} = \frac{K_p + 2K_{bf} - 2\varphi(K_{bf} - K_p)\varphi}{K_p + 2K_{bf} + \varphi(K_{bf} - K_p)\varphi} + \frac{\rho_p\varphi_p C_p}{2K_{bf}} \sqrt{\frac{K_B T}{3\pi r_c \mu}}$	Includes the effect of Brownian motion, particle size, concentration, and temperature.
Prasher et al. [27]	$\frac{K_{eff}}{K_{bf}} = (1 + AR e^m Pr^{0.33} \varphi)$ $\times \left[\frac{K_p + 2K_{bf} - 2\varphi(K_{bf} - K_p)\varphi}{K_p + 2K_{bf} + \varphi(K_{bf} - K_p)\varphi} \right]$	Modified Maxwell [3] model, considers a convection caused by the Brownian motion from multiple nanoparticles

2.4 Theoretical Viscosity Models

Determining the viscosity of a nanofluid is essential in establishing the fluidic, thermodynamic and heat transfer properties. The non-dimensional properties similar to Prandtl number, Reynolds number and Nusselt number which are used to estimate convective heat transfer coefficient of a fluid are a function of viscosity. Most studies struggle to provide the viscosity of a nanofluid by comparing experimental data to theoretical models. The most significant factor that dictates the viscosity of a nanofluid is the concentration of particles suspended in the base fluid. The concentration of the particles is described using the volume fraction relative to the nanofluid. The other factors affecting the viscosity of the fluid are temperature, particle and agglomerate size of the particles. Even though the main factor in determining the viscosity is the particle volume fraction dispersed in the fluid, other factors listed above also play an important role in the rheological properties of the nanofluid.

Einstein [28], in 1906 proposed this pioneering equation to correlate the viscosity of a particle suspension in a base fluid to the viscosity of the base fluid, for a volume fraction of particles in small quantity.

$$\mu_{nf} = \mu_{bf}(1 + 2.5\varphi) \quad (2.2)$$

Einstein [28], formulates this equation based on the assumption of a linear viscous fluid containing suspended spherical particles in small amount of volume fraction ($\varphi < 2\%$). The Brownian molecular movement of particles suspended in the fluid is hypothesized to be the major basis in determining the viscosity of a nanofluid. Most viscosity theoretical models are a derived form of the basic Einstein equation.

$$\mu_{nf} = \mu_{bf} \frac{1}{(1 - \varphi)^{2.5}} \quad (2.3)$$

Brinkman [29] extended Einstein's [28] viscosity equation for higher particle concentration as shown in equation (2.3). This model can estimate a viscosity of nanofluid with a solid particle up to 5% volume concentration. As explained in the mathematical model of Einstein's [28] viscosity, the Brinkman model is also based on solid particle molecular kinetic theory or Brownian motion.

As discussed above in Einstein's and Brinkman's model, the Batchelor's [30] model similarly considers a two phase fluid property and treats the mixture as solid liquid slurry.

$$\mu_{nf} = \mu_{bf}(1 + 2.5\varphi + 6.5\varphi^2) \quad (2.4)$$

The viscosity of the mixture (nanofluid) is only a function of the base fluid viscosity and concentration of the solid particle. The higher order term in the equation will approach zero when the volume fraction of the particles suspended in the base fluid gets lower. For small particle quantities Batchelor's [30] model will be reduced to Einstein's [28] equation.

$$\mu_{nf} = \mu_{bf}(1 + 2.5\varphi + 14.1\varphi^2) \quad (2.5)$$

Guth and Simha [31] formulated equation (2.5) by considering suspended solid particles in a base fluid, and also studied the interaction between particles. This allows their model to handle nanofluids with higher quantity of solid particles by volume.

Equation (2.6) is the mathematical model of viscosity of nanofluid proposed by Krieger and Dougherty [32] which takes into consideration the strong interaction between particles and aggregation of these particles.

$$\mu_{nf} = \mu_{bf} \left(1 - \frac{\varphi_a}{\varphi_m}\right)^{-[\epsilon]\varphi_m} \quad (2.6)$$

φ_a is the volume fraction of particle in agglomerate form, $[\epsilon]$ is the intrinsic viscosity for rigid spherical particles and φ_m is the maximum particles volume fraction. A simplified equation of the above model is

$$\mu_{nf} = \mu_{bf} \left(1 - \frac{\varphi}{\varphi_m}\right)^{-2} \quad (2.7)$$

Kitano et al. [33] suggested an equation to calculate the maximum solid particle volume fraction suspended in the base fluid. φ_m can be estimated by $\varphi_m = \frac{1-\beta}{\alpha}$. Where α and β are estimated from experimental data collected.

$$\alpha = 0.07298$$

$$\beta = 0.03402$$

Kitano et al. [33] correspondingly proposed an empirical equation (2.8) to estimate a viscosity of nanofluid at higher solid particle concentration.

$$\mu_{nf} = \mu_{bf} \left(1 - \frac{\varphi}{A}\right)^{-2} \quad (2.8)$$

where $A=0.68$ for spherical shape particles.

$$\mu_{nf} = \mu_{bf} (1 + 2.5\varphi - 10.05\varphi^2 + A \cdot e^{B \cdot \varphi}) \quad (2.9)$$

Further modification of the above mathematical models, equation (2.9) is offered by Thomas [34] using a regressed model from experimental observation, where, $A=0.00273$ and $B=16.6$.

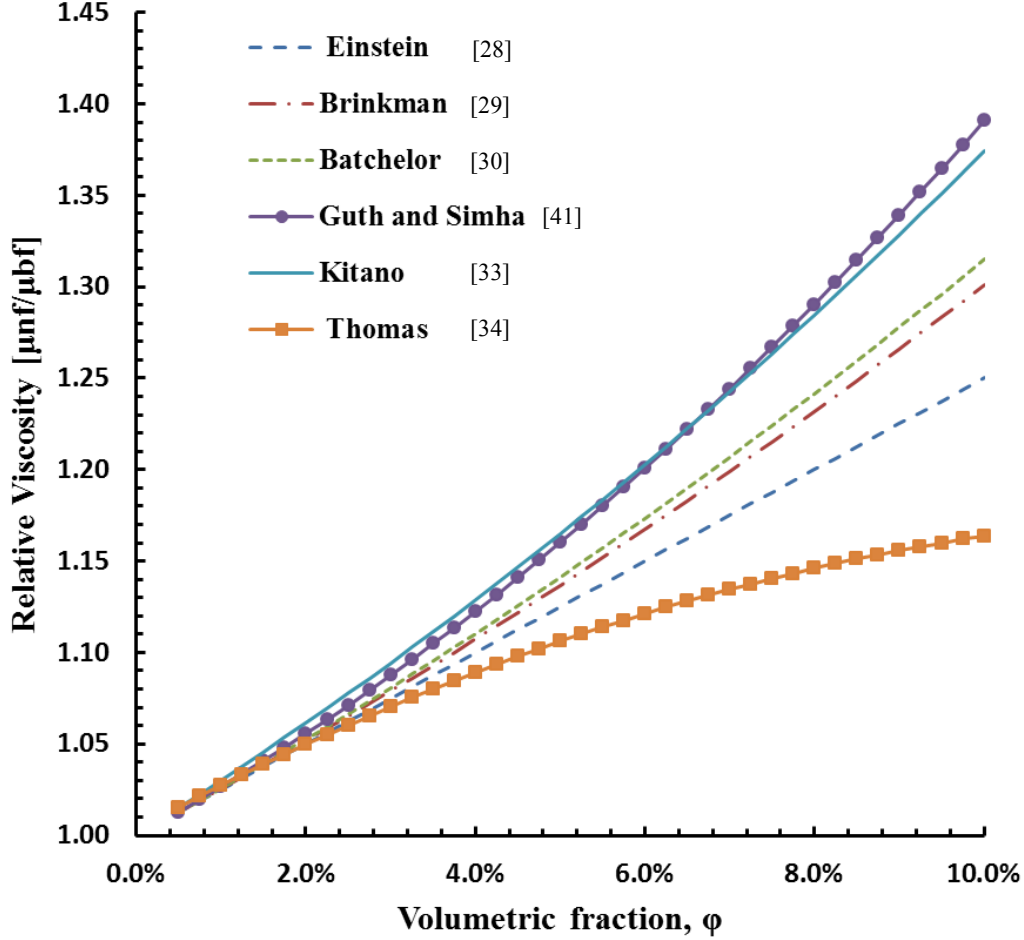


Figure 2.5 Relative viscosity comparison between theoretical models.

2.5 Density of Nanofluid

The density of a nanofluid can be approximated using the principle of fluid solid mixture property (conservation of mass). Considering the nanofluid as slurry, the density can be formulated from the mass constituent and volume fraction of the fluid and solid particle.

$$m_{nf} = m_p + m_{bf} \quad (2.10)$$

$$\rho_{nf} = \rho_p \phi + \rho_{bf}(1 - \phi) \quad (2.11)$$

Equation (2.11) precisely estimates the density of the nanofluid as a function of volume fraction of the nanoparticle. Pak and Cho [35] and Ho et al. [36] conducted experimental studies to measure the density of Al_2O_3 - water nanofluid at room temperature. At a constant temperature, the experiment demonstrates the mathematical model shown in equation (2.11) flawlessly agrees with the experiment conducted.

2.6 Specific Heat Capacity of Nanofluid

The specific heat capacity of a nanofluid is a physical property that can be estimated from the effective medium theory. The formulation can be done by assuming equilibrium of heat transfer between nanoparticles and the base fluid.

$$(\rho C_p)_{nf} = \rho_{nf} \left(\frac{Q}{m \Delta T} \right)_{nf} = \rho_{nf} \left(\frac{Q_{bf} + Q_p}{(m_{bf} + m_p) \Delta T} \right) = \rho_{nf} \left(\frac{(m C_p)_{bf} \Delta T + (m C_p)_p \Delta T}{(m_{bf} + m_p) \Delta T} \right)$$

$$C_{p_{nf}} = \frac{(C_p \rho)_p \varphi + (C_p \rho)_{bf} (1 - \varphi)}{\rho_{nf}} \quad (2.12)$$

Zhou and Ni [37] conducted an experiment to estimate the specific heat capacity using Al_2O_3 – water nanofluid. The test was conducted at different volume fractions and the mathematical model shown in equation (2.12) matches very well with the test result.

2.7 Synthesis of Nanofluid

Manufacturing process is one of the basic factors that determine the quality of a nanofluid. Due to variability in manufacturing nanofluids exhibits an observable performance difference in experiments. Different researchers developed various processes for appropriate nanofluid synthesis. The most common methodologies used in studies and industries are a two-step and single step process [1].

The two step technique starts with the production of nanoparticles via the physical or chemical processes and proceeds with dispersing the produced nanoparticles in to the base fluid. Some of the physical processes used in making the nanoparticles are mechanical grinding, and inert gas condensation technique. Chemical processes that are also used to make nanoparticles include chemical vapor deposition, micro emulsions, chemical precipitation, and thermal spraying [38]. The challenge in making nanofluids in a two-step method is a quick agglomeration of nanoparticles before a complete dispersion in to the base fluid. The Van der Waals force between each particle creates a cluster of nanoparticles and the clusters will sediment out of the liquid rapidly [39].

In the second technique of making nanofluids, nanoparticles are formed and dispersed into the base fluid with a single process. A condensation of vapor is used to form the nanoparticles within contact of the liquid. In this technique a well dispersed and stable nanoparticle can be achieved due to a continuous liquid flow. Although agglomeration is greatly reduced in this process, the low vapor pressure needed to keep the liquid introduces a limitation in this technique. Research and development on this valuable process for large volume production and commercial availability is yet a challenge facing researchers in the technology [39].

Although most nanofluid production processes use one or two step techniques, there are various processes used in the manufacturing of nanofluid based on the nanoparticle and base liquid material type. Some of the processes are electrolysis metal deposition, templating, microdroplet drying, layer-by-layer assembly, and so on.

2.8 Application of Nanofluid

Nanofluids have wide application in emerging technology, and despite that the intention of dispersing ultrafine particles in base fluid was to enhance the effective capability of heat dissipation in machineries, it's currently extended to a topnotch application in the fields of biomedical and micro scale fluidic applications like electro wetting.

One of the most common applications of nanofluid is cooling. Blending a limited amount of nanoparticles into a conventional cooling liquid result in an immense heat transfer enhancement in the automotive engine, transmission, boiler flue gas recovery, nuclear system, refrigeration, microwave tubes, thermal storage, space, and so on [40].

Ethylene glycol and water mixtures are the universal coolant in the automotive industry. The heat transfer enhancement of automotive engines based on conventional coolants has been exploited for a century and has reached to its limit. The addition of nanoparticles to those conventional engine coolants improves the capability of the heat dissipation. This enhancement yields a smaller and lighter cooling system which leads to higher performance fuel efficient vehicle. Tzeng et al. [41] offers research on the effect of Al_2O_3 and CuO nanoparticles dispersed in engine transmission oil for the cooling of an automatic transmission. The test was conducted on the torque coupling where high local heat flux is generated and temperature is measured at different engine rotational speed. The investigation shows transmission oil with a dispersed copper oxide particle results in a significantly lower transmission temperature when compared to the conventional coolant. In Automotive lubrication, nanofluids also play an important role in enhancing the tribological properties such as wear resistance, load carrying capacity and friction reduction between moving mechanical parts. The capability of TiO_2 nanofluid in reducing

friction between two pieces of cast iron is studied by Mu-Jung Kao et al. [42]. A suspension of TiO_2 nanoparticles in a base fluid of paraffin oil results in reduced friction between moving parts. The study reports that the nanoparticles can amend and fill rough cracks in the metal surface and consequently reduce the friction coefficient. Audi Le mans Quattro implemented a magnetic nanofluid for its shock absorber systems. This magneto rheological nanofluid can change its viscosity based on the magnetic field applied on it, and the control unit adjusts the shock absorber damping property according to the information provided from the sensors [43]. nanofluids are also used in advanced brake systems and as fuel additives in the automotive industry. A diesel fuel blended with water based Al_2O_3 nanofluid exhibits a higher combustion heat and reduction of nitrous oxide exhaust emissions. Al_2O_3 and CuO nanoparticles are frequently used in manufacturing of aluminum oxide brake nanofluid (AOBN) and copper oxide brake nanofluid (CBN). These new types of braking fluid provide enhanced thermal conductivity, higher viscosity, and boiling point which elevate the quality of the novel braking oil when compared to the conventional oil [44].

Nanofluids are used as a smart fluid in many applications and one of them is subsurface nano-sensors in the oil industries dispersing nanoparticles into oil and gas wellbores [45]. The injected nanofluid sensors will migrate in to the wellbores and out to the geological structure to deliver the specimen carried by the nanofluid convection. Data collected from the procedure will enhance oil recovery and exploration applications. A study from Cheraghian et al. [46] shows TiO_2 is extremely useful in the upstream petroleum industry. TiO_2 based nanofluid demonstrates better oil recovery in their experiment.

In pressurized-water nuclear reactors nanofluid based coolants can play a major role in reducing the temperature of overheated surfaces. Kim et al. [47] at the Nuclear Science and

engineering department of Massachusetts Institute of Technology (MIT), have studied the effect of dilute-dispersion of nanoparticles with a base fluid of water in the enhancement of critical heat flux. Dilute-dispersion of Al_2O_3 and other nanoparticle in water exhibits substantial enhancement in critical heat flux in wire heaters. The formation of alumina nano-layers on the surface of the fuel rods will increase the critical heat flux significantly by avoiding the formation of water vapor bubbles and their heat transfer reduction property. Most water based nuclear reactors have a limited critical heat flux, and this limit can be exceeded by the application of nanoparticles in to the working fluid.

The increase in demand of superior electronics and technology competition for better equipment yields a powerful electrical product with high information processing capability. The application of nanofluid in electronics is one of the major features of nanotechnology, specifically cooling of microprocessors in super computers or other electronic devices. The ultra-high heat flux dissipation from microchips requires a super conductor cooling fluid to assure the electrical equipment is working efficiently. Nguyen et al. [48] investigated the heat transfer enhancement on microprocessors using alumina nanofluid cooling through physical experimentation. In their experiment, alumina nanofluid elegantly demonstrates that the use of nanofluid has a greater advantage in dissipating more heat from the electronic devices than the conventional methods. For a volumetric concentration of 4.5% alumina nanoparticle, a heat transfer enhancement up to 23% is observed. Lin et al. [49] investigated the effect of silver nanofluid using a pulsating heat pipe which results in a significant heat transfer enhancement when compared to the conventional working medium which is water. Dash et al. [50] have studied the effect of electro-wetting on dielectrics. A promising result is observed in the reduction of the contact angle of a fluid droplet, which enhances the liquid transport performance

in microsystems and cooling microchips. This characteristics of nanofluid in minuscule amount of liquid is important in emerging micro-electro mechanical systems (MEMS). Optical devices such as miniature cameras use this type of enhanced liquid for an improved method of lens focusing.

A novel application of nanofluid in biomedical technology promises a prodigious future in cancer therapy, nano drug delivery, cryopreservation, nanocryosurgery, sensing and imaging [12]. Magnetic nanofluids are used to target a tumor cells in human body through blood streams via a guiding using magnetic field. This will help to deliver strong medication to the specific location without damaging healthy tissues [51]. In cryosurgery (eliminating unwanted tissue by freezing) application, nanoparticles made from magnetite (Fe_3O_4) and diamond demonstrate a good result in enhanced freezing and gives an encouraging future treatment of tumors [52].

The wide application of nanofluids addresses numerous engineering problems involving heat transfer in industrial processes, microelectronics, microfluidic systems, nuclear reactors, transportation, space, defense and so on. The applications of nanofluids have been also extended to the biomedical field and demonstrate an encouraging result toward challenges facing physicians. Additional research is needed to be done in the field of nanotechnology to exploit the untapped potential of these novel fluids. Studies should also look into the unexpected result from the nanofluids like agglomeration, settling, and erosion possibilities that adversely affect the performance, service life, and quality of a system.

CHAPTER 3

STATISTICAL MODELING OF NANOFLUID PROPERTIES

3.1 Experimental Evidence Review

Numerous studies have been conducted on enhancing the heat transfer capacity of a nanofluid used in heating and cooling systems. Thermophysical properties of nanofluid are also thoroughly studied in much research even though most research papers are limited to the study of the nanofluid heat transfer aspect. The most pivotal thermophysical properties of a nanofluid are the conductivity and viscosity. Those properties are determined by laboratory experimentation or by indirect measurement of a Nusselt number. For example Duan [53] in 2012 conducted an experiment for a measurement of conductivity of water based Alumina (Al_2O_3) nanofluid. The viscosity of the nanofluid is correspondingly studied. Duan [53] used a hot wire transient method to for a measurement of the relative conductivity of the fluid. A constant current is supplied to a wire to raise its temperature and the surrounding nanofluid which helps to correlate the temperature rise and thermal conductivity of the medium in which the wire is dipped. The hot wire transient method eliminates the error due to the effect of natural convection. Due to this advantage most experiments are in favor of THW method. Nguyen et al. [48] extensively studied the viscosity of some water based nanofluids. Nguyen et al. [48] studied CuO nanoparticle with a 29nm particle size and Al_2O_3 with 36nm and 47nm particle size. The temperature range in this research is from room temperature to 75°C. This study reported that the viscosity of the nanofluid highly depends on particle concentration and temperature.

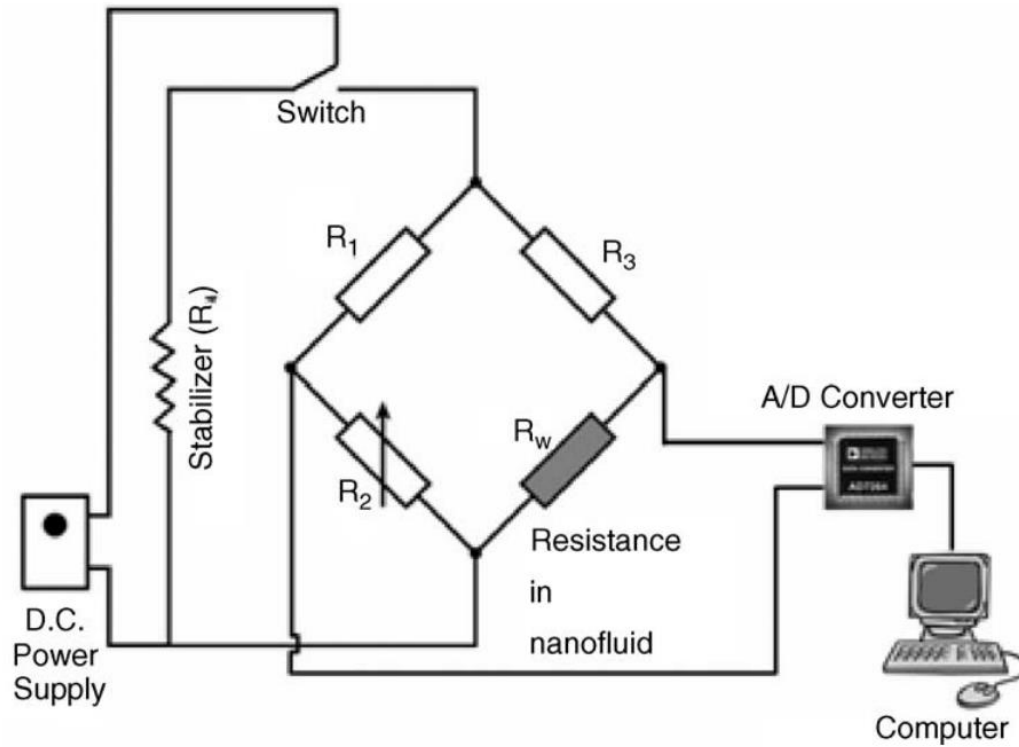


Figure 3.1 Schematics of transient hot wire experiment setup. (Source: Paul et al. [54] *Renewable and Sustainable Energy reviews*, 2010)

Wang et al. [11] investigated the conductivity and viscosity of alumina and CuO in water, engine oil, and ethylene glycol base fluid. In his research a parallel plate method is used to measure the effective conductivity of the nanofluid. Parallel plate conductivity measurement is a type of steady-state technique. In this technique a sample of nanofluid is placed between two copper plates and a glass spacer will be used to support the upper copper plate. Heat will be supplied to the copper plate in different directions. Consequently, the overall conductivity across the two copper plates, the nanofluid sample, and the supporting glass will be calculated from the one dimensional heat conduction equation.

$$k = Q\Delta x / A.\Delta T \quad (3.1)$$

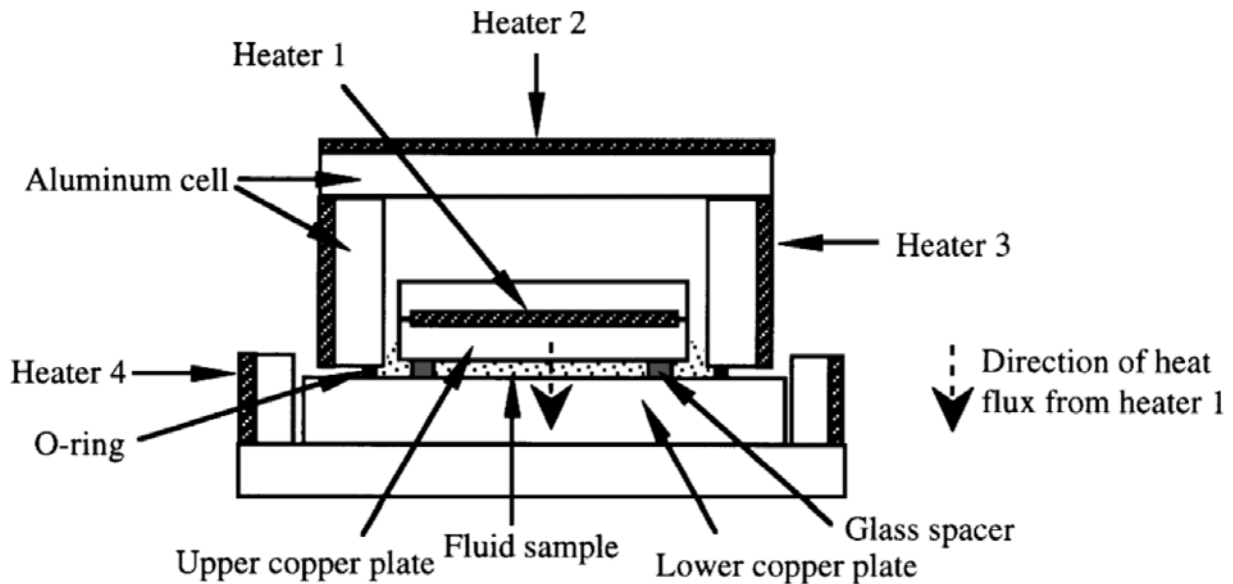


Figure 3.2 Parallel plate steady state conductivity measurement. (Source: Wang et al. [11] *Thermal Conductivity of Nanoparticle–Fluid Mixture, Purdue University, 1999*)

Wang et al. [11] concluded from the experimental and research results that the thermal conductivities of nanoparticle fluid mixtures increase relative to those of the base fluids. The experiment shows that there is a direct relationship between the thermal conductivities and the size of nanoparticle: the conductivity of the nanofluid will increase with decreasing size of nanoparticles. Wang et al. [11] also shows the dependency of the alumina and CuO water based nanofluids viscosity to the degree of dispersion. If the nanoparticles have a better dispersion, the solution will have a lower viscosity. The reports demonstrate that there will be approximately a 30% increase in viscosity at 3 vol. % when compared to water alone. Chen et al. [55] published a paper that reports the viscosity of alumina nanofluid with a base fluid of water. The experimental research shows the viscosity of alumina nanofluid has a strong interaction with the concentration of the nanoparticles. The higher the concentration the solution becomes more viscous. Eastman et al. [1] comprehensively studied the rheological properties of nanofluids and their aspect of

heat transfer augmentation. Regarding their studies, they have tried to look further by investigating the experimental factor that affects the thermo physical properties of the nanofluid. The first outlook was the nanoparticle size; hence reducing the size of the nanoparticle leads to increased heat transfer. This conclusion hypothesized the idea that the heat transfer happens around the vicinity of the nanoparticle. Although most scholars entertain the argument that smaller nanoparticle diameter increases the heat transfer rate, it is very difficult to control the nanoparticle size at certain range. An adverse effect of particle agglomeration is also discussed in this research. Poor nanoparticle dispersion into a base fluid causes the particles to cluster to each other which leads to a higher viscosity associated with higher pumping energy and lower heat transfer rate. Effect of temperature on the performance of the nanofluid is also investigated and suggests that despite the temperature being strong factor in conductivity enhancement, the research is limited to support this argument.

3.2 Data Collection and Processing

3.2.1 Experiment Observation

In this study previous research is investigated thoroughly to collect reliable data on the water based nanofluid mixtures. Despite the fact that nanofluid science has been investigated meticulously for the last couple of decades, experimental results published on the study of rheology and thermo-physical properties of nanofluids varies considerably. Given that the variation of experiment setup from study to study can cause a tolerable disparity in the result, the discrepancies between studies presented in the research field are significantly higher. This anomaly of heat transfer in the research thrusts scholars to throw a theory based hypothesis. Although a governing model is not constructed in the science of nanofluid heat transfer, researches show that there are some atomic and micro scale level theories that somehow explain

the anomaly. Additionally, the observed result from several studies demonstrates that the existing macro theories cannot explain the discrepancy [1]. Tavman et al. [56] published their findings on measurement result of diluted solution of water with alumina and silicon oxide. The report showed that the effective thermal conductivity of nanofluids increases particle concentration increases but not anomalously as indicated in the majority of the studies. Tavman et al. [56] shows the enhancement is close to the theoretical model of Hamilton-Cross studies. This research ruled out the Einstein [28] theoretical model of nanofluid properties since the effect of temperature was dominant in variation of the viscosity. As the temperature goes up, the dynamic viscosity of the nanofluid will decrease. But it will increase by increasing the concentration of nanoparticles. Wang et al. [11] obtained some data for the dynamic viscosity of alumina in both water and ethylene glycol solutions at various temperatures. Pak and Cho [35] measured the dynamic viscosity of alumina and titania in water as the base fluid. The experiment shows that the nanofluids have much higher dynamic viscosity compared to pure water.

3.2.2 Experimental Results

Published research on the rheological and thermo-physical properties of nanofluids might have significant difference between experimental results as discussed in section 3.2.1. Nanofluids data from published papers should not be taken literally. As explained above, nanofluid manufacturing process, experimental conditions, and approaches have an impact on the result of the study. Consequently, nanofluid properties data should be compared with equivalent research and also compared to theoretical models. This study surveyed a reasonable number of existing published studies and compared their experimental result. The collection of these results will improve the accuracy and precision of the mathematical model to be proposed.

The two most valuable properties that dictate the thermo-physical properties of nanofluids are the effective thermal conductivity and effective dynamic viscosity. Those properties should be investigated and estimated accurately to study the effect of nanofluids in the study of heat transfer enhancement. Most research papers focus on the enhancement of thermal conductivity to study the heat transfer augmentation rather than studies of other heat transfer properties [2]. Some literature shows that dynamic viscosity of these fluids also plays a big role in the improvement of heat transfer. Since the heat transfer coefficient is highly dependent on the Prandtl and Reynolds number, it is necessary to study the viscosity associated with concentration on the nanofluids [57]. The present work reports thermo-physical properties of oxide nanoparticles diluted in pure water with a concentration of 0 to 5 % by volume.

3.2.2.1 Effective Dynamic Viscosity of Nanofluids

One of the most important thermo-physical properties of fluids is viscosity. As discussed on the above section, the Prandtl and Reynolds number of a flowing fluid, which are the main factors that dictate a heat transfer enhancement, are a function viscosity. Extensive study of the rheology properties of diluted fluids with a nanoparticle will propel the study toward accurate mathematical modeling.

$$Pr = \frac{\mu_{nf} C_p}{\rho_{nf}} \quad (3.2)$$

$$Re = \frac{\rho_{nf} U D_h}{\mu_{nf}} \quad (3.3)$$

The inconsistency of published research on the rheological property of nanofluids inhibits scientists and engineers to come up with a standard viscosity model. This has become manifest as some researchers have published data reporting that relative viscosity of nanofluids is

independent of temperature and some authors showing a strong correlation between viscosity and temperature [40]. Although the viscous properties of water can be classified as a Newtonian fluid, adding considerable amount of nanoparticle will change this behavior. Newtonian fluids have the following properties.

- Stress is a linear function of strain rate.
- When the fluid is stationary, the stress is the thermodynamic pressure.
- The fluid is isotropic
- The average normal viscous stress is zero.

As described on the first criterion all Newtonian fluids satisfy the linear equation governing the Newtonian characteristics of a fluid which is given by,

$$\tau = \mu\gamma \quad (3.4)$$

Fluids that are not classified as Newtonian don't fulfil the first criterion. If a fluid is a mixture, slurry or a suspension of particles, it can be classified as a non-Newtonian fluid. Some types of non-Newtonian fluids are: clay suspended in water, blood, tooth paste, Ketchup, oil-well drilling fluid, and so on. Most of these types of fluids are theoretically approached as a two-phase fluid flow problem [58].

In the case of nanofluid rheology property scholars published research showing that the fluid type will be strongly dependent on the concentration of the suspended particles and temperature. Kole et al. [59] published their research on dispersed Al_2O_3 particles in a car engine coolant. They report a low loading of nanoparticles (< 0.4 vol. %) will behave like a Newtonian fluid at higher temperature. But at high loading of particles and low temperature this research

shows a nanofluid will behave like a non-Newtonian fluid. Turgut et al. [60] studied the thermophysical and rheological property of water based nanofluids. In this published report, characteristics of the viscosity of a nanofluid accurately follow the curve of pure water at 0.2 vol. % of TiO_2 . At this low concentration of nanoparticles, the solution can be explained via most theoretical viscosity models (will be discussed forward sections). At high loading of nanoparticles this property doesn't hold and the viscosity is much higher (anomalously increasing) than the expected values. Namburu et al. [61] specifically observed the rheological property of copper oxide suspended in ethylene glycol and water. Their report suggests non-Newtonian fluid flow observed for higher nanoparticle concentration. Kulkarni et al. [62] also investigated the viscosity of CuO nanoparticles dispersed in water as a base fluid and reported that CuO particles with concentration from 5-15 % by volume in water has a non-Newtonian properties specifically from 5-50°C.

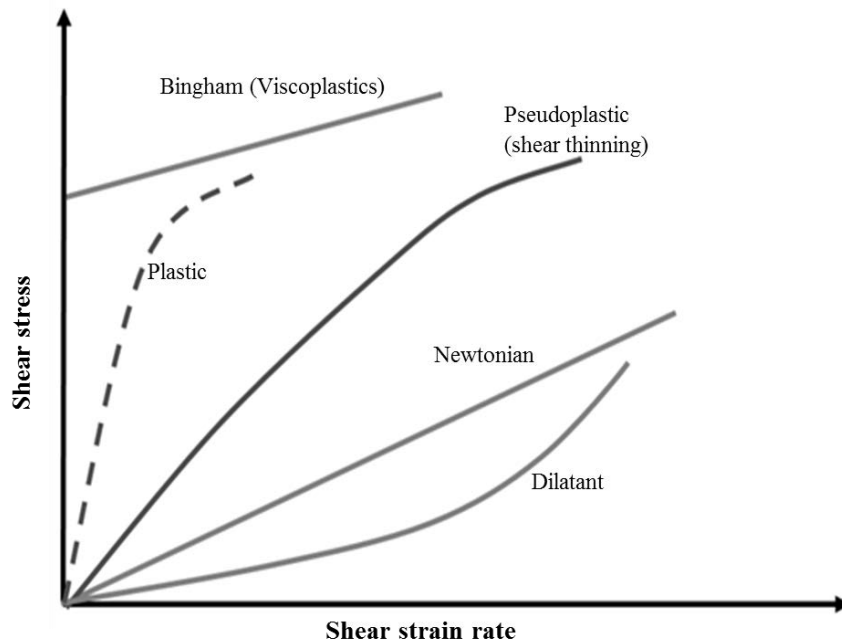


Figure 3.3 Stress - strain dependence of different classification of fluids.

However, research shows nanofluids with nanoparticles concentration below 5 % by volume using water as a base fluid retains their Newtonian fluid properties. The experiments indicate the change in strain rate does not have an effect on the nanofluid viscosity. Chandrasekar et al. [63] studied an experimental investigation of thermal conductivity and viscosity of Al_2O_3 - water nanofluids and the outcome supports the hypothesis of Newtonian fluid flow at low loading concentration. Naik et al. [64] studied the rheological property of copper oxide suspended in 60/40 water glycol mixture. The experiment was conducted at 0.025-1.2% concentration of CuO and they concluded that the shear stress and shear strain rate of the nanofluid shows a linear relationship and thus Newtonian behavior. Zhu et al. [65] studied the manufacturing process and heat transfer behavior of CaCO_3 aqueous nanofluids. Their experiment was done using a stable mixture of CaCO_3 nanoparticles dispersed in distilled water under optimal preparation condition. From their research, theoretical models that have already been developed can predict the behavior of the solution mixture. At room temperature the study observed a linear relationship between the shear stress and shear strain rate for a particle volume fraction of 0.12 - 4.11 %. This linear relationship indicates the mixture can be accurately modeled as a Newtonian fluid. Putra et al. [66] studied a natural convection of nanofluids. This study selected a water suspension of Al_2O_3 and CuO nano particles for their research. Al_2O_3 and CuO have a well-established thermal and flow properties as shown in a number of previous studies. These nanoparticles also have a good stability with water as a base fluid when compared to other properties. The experiment was done at a particle concentration of 1 - 4 % by volume and the results were collected at 20°C, 40°C and 60°C. A rotating rheometer is used to measure the nanofluid shear rate and shear stress, and the end result demonstrates both properties have a linear relationship. This confirms nanofluid mixture behaves as a Newtonian fluid.

Based on numerous research studies and conclusions on the rheology of nanofluids, this paper will focus on nanofluids that are considered as a Newtonian fluid by most scholars. This study conducted research only on nanofluids with a particle concentration up to 5% by volume maximum. This will ensure that the Newtonian mathematical model used in the computer simulation is satisfied.

Data points of nanofluids are comprehensively collected from endorsed and cited research studies using Engage Digitizer 5.1. Engage Digitizer is free software used to convert graphical data from published researches into numerical data. Consequently, collected data points are post processed on Excel sheet and presented as a graph as shown below. Thermophysical properties are gathered from different research but with the same experimental conditions. This assumption allows the consideration that all points are observed from the same population. Although the assumption creates uncertainties, statistical methods are implemented to avoid any outlier that might contaminate the collected data.

In the study of the rheological properties of Alumina nanoparticles suspended in a water base fluid, five major studies are referenced in building the mathematical model for the dynamic viscosity. Duan [53] Due to lack of accurate prediction from theoretical models, experimental results are nevertheless valuable and are used in the estimation of mixture properties. In this research alumina nanoparticles suspended in de-ionized water is used as a nanofluid. The concentration of the nanoparticles used in the experiment is from 1 -5 % by volume. It is observed that the viscosity of the alumina nanofluid is independent from the shear rate. This supports the hypothesis that a well-mixed alumina in de-ionized water as a base fluid will behave as a Newtonian fluid. The experimental research also demonstrates that the effective

viscosity ratio (μ_{nf}/μ_{bf}) increases as the volume concentration of nanoparticle increases. The study suggests that the “normal linear fluid surrounding the nanoparticles” assumption (micro fluid convection) fails to explain the result at higher particle loading rate and proclaims that linear fluid theory may no longer be applicable to the modeling of nanofluids. Nguyen et al. [48] have studied the phenomenon of water based nanofluid viscosity. 36 nm and 47 nm average particle diameters of alumina suspensions in water as a base fluid are used in the research. The objective of the experiment is to determine the viscosity property variation as a function of particle volume fraction and temperature. The particle volume fraction studied in this research is in a range of 1 to 9.4 % and the temperature range 21 to 75°C. This research also published a result for an increment of viscosity with increasing the particle volume fraction. The finding is explained as the effect due to that volume fraction of the nanoparticle directly affects the internal viscous shear stress of the fluid whereas the temperature weakens the inter-particle and intermolecular force. Nguyen et al. [48] observed a remarkable phenomenon when nanofluids are heated beyond their critical temperature, the rheological properties of the suspended particle in a base fluid is drastically altered. The study recommended considering this hysteresis effect before engaging the practical application of nanofluids for heat transfer enhancement. Wang et al. [11] presented an experimental study of alumina water mixture with an average particle diameter of 28nm. In this paper 20 to 30 % of viscosity increases is seen when compared to the base fluid water at a particle fraction of 3 % by volume. Note that the preparation of these nanofluid mixtures creates a discrepancy between studies. Chen et al. [55], presented experimental studies on alumina particles with water as a base fluid. The average particle diameter used is 36 nm. Below a graph is shown which describes the effect and magnitude of particle volume fraction on

the viscosity of nanofluids. Data points are collected from published research which are briefly discussed in this section and rearranged according to the amount of particle volume fraction.

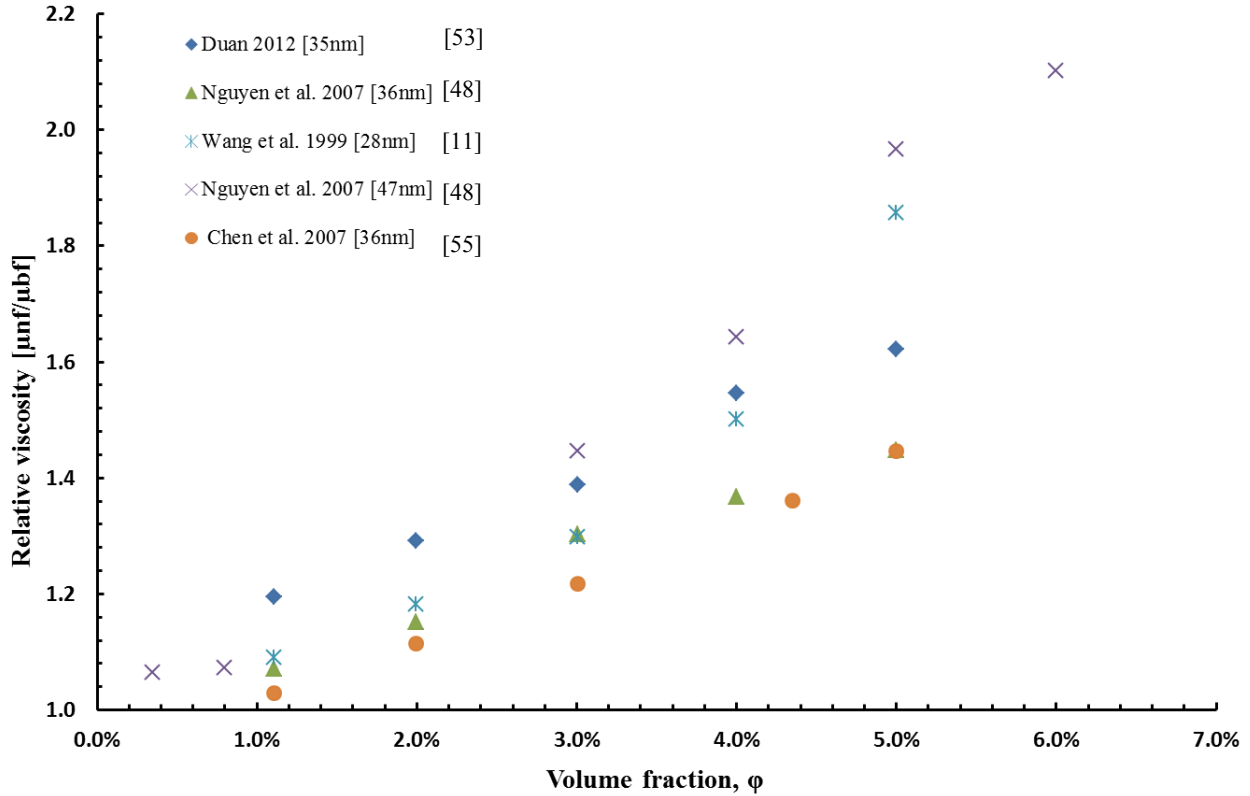


Figure 3.4 Comparison of the experimental data of relative viscosity for Al_2O_3 - water nanofluid.

Although sufficient research is presented on the viscosity study of water based copper oxide nanofluids, a few scholars conducted an extensive study on the rheological properties. Nguyen et al. [48] have studied a copper oxide nanoparticle suspended in water as a base fluid. 29nm average particle diameter is used in the research and during experimentation the nanofluid viscosity is measured for a temperature range varying from room temperature up to 75°C. The hysteresis phenomenon is observed when the fluid is heated up above its critical temperature. In this experiment a piston type viscometer is used in measuring the viscosity. Sample points from the research of Nguyen et al. [48] are collected and plotted as shown on Figure 3.5 below.

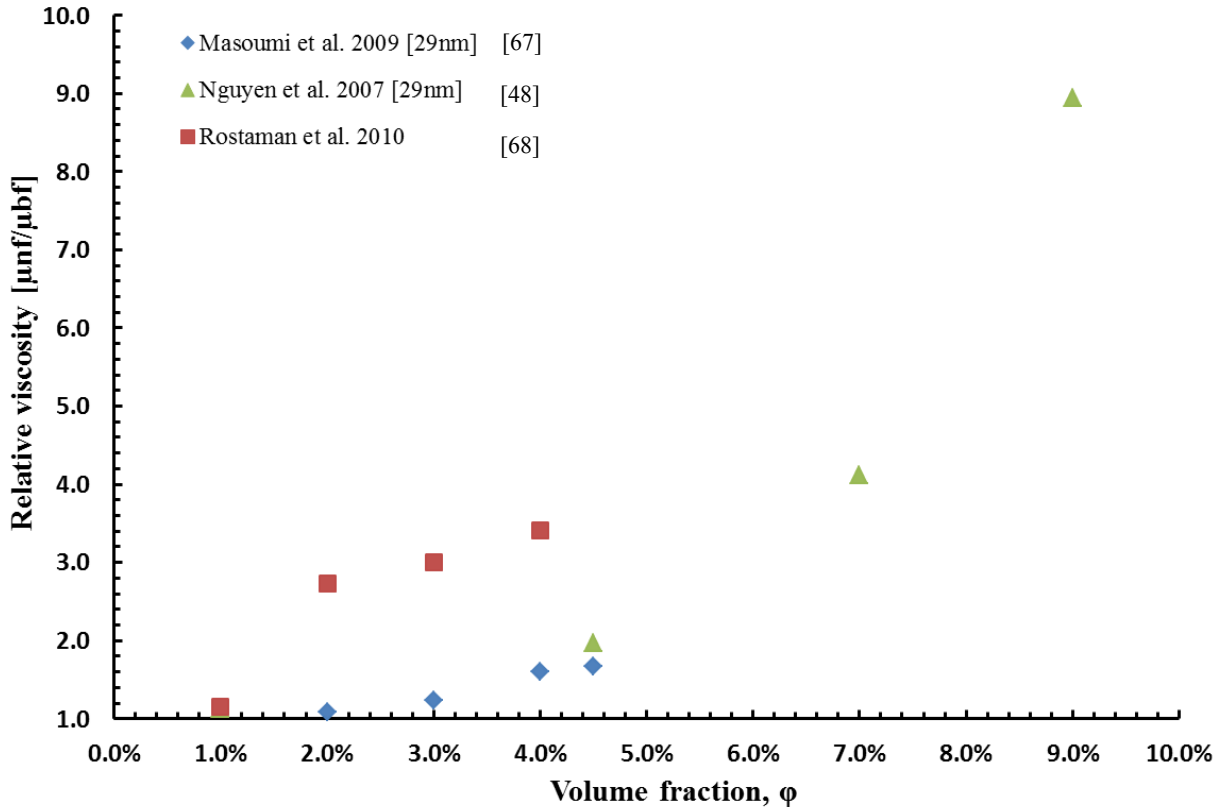


Figure 3.5 Comparison of the experimental data of relative viscosity for CuO - water nanofluid.

In the study of a water based titania (TiO_2) nanofluid, publications are well developed in reporting the rheological and thermo-physical properties. Murshed et al. [69] have studied the convective heat transfer characteristics of TiO_2 with in deionized water as a base fluid. The test was conducted under controlled laminar flow with Reynolds number ranging from 900-1700. A titania particle volume fraction of 1 – 5 % is studied in the investigation of viscosity and heat transfer enhancement. Masuda et al. [6] also published a paper on the investigation of rheological properties. In their study, water is used as a base fluid to suspend the titania particles. The relative viscosity data points are gathered and plotted on the graph below. Pak and Cho [35] comprehensively investigated the hydrodynamic and heat transfer effect of metallic oxide nanoparticles. In their studies, 1 to 5 % by volume of TiO_2 particle volume fraction is used to

determine the associated rheological and thermo-physical properties. A TiO₂ nanofluid is observed experiencing a shear thinning effect at a particle concentration of 10 % by volume.

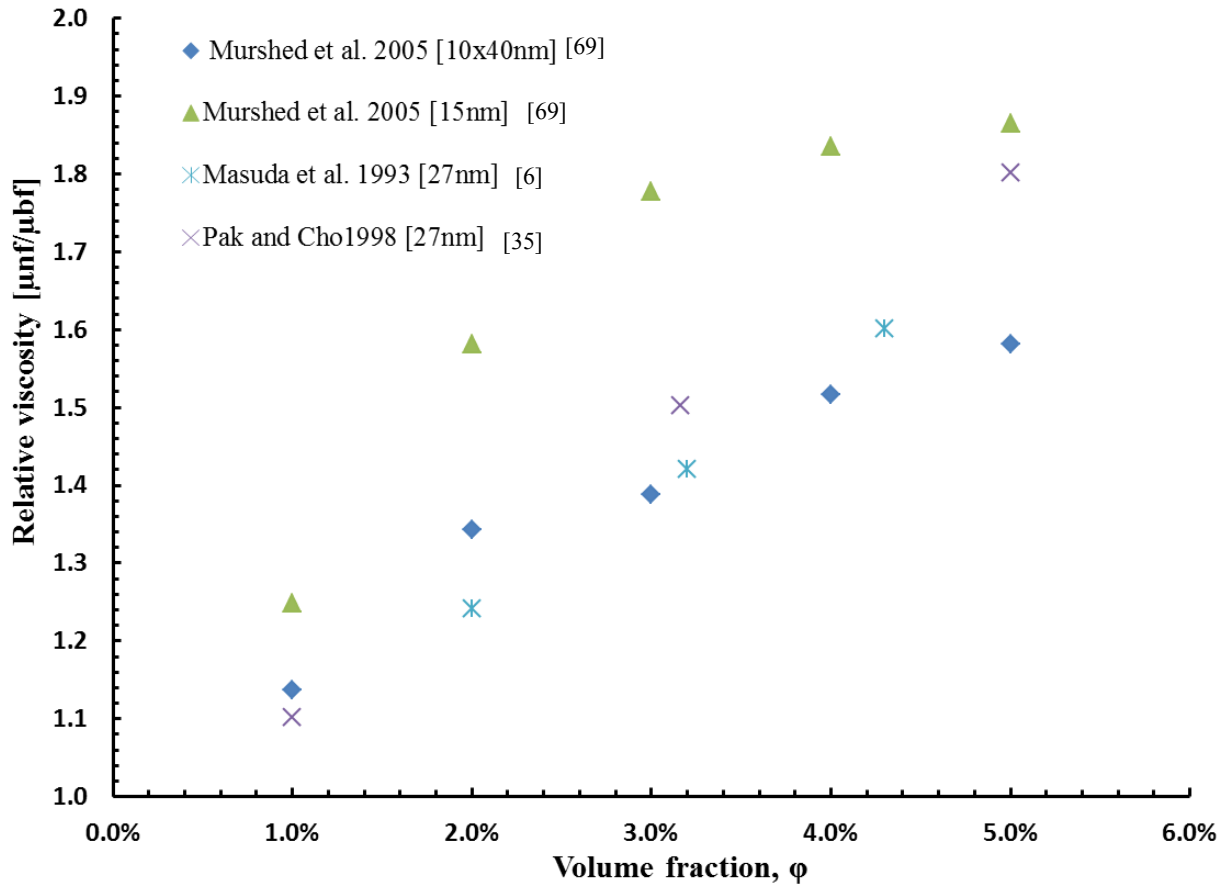


Figure 3.6 Comparison of the experimental data of relative viscosity for TiO₂ - water nanofluid.

This non-Newtonian fluid behavior is only observed at higher loading rate of particles and for lower volume fractions (< 5 % by volume). Shear stress is observed to be linear to the shear strain rate of the nanofluid.

3.2.2.2 Effective Thermal Conductivity of Nanofluids

Effective thermal conductivity of a nanofluid is the most significant thermo-physical property in heat transfer. Studies of nanofluid thermal conductivity has been more prevailing properties [70]. The effective thermal conductivity of nanofluids is different from the ordinary

fluids and complex to analyze the total effect. To the present day theoretical mathematical models doesn't explain the conductivity behavior and magnitude accurately. In late 19th century paper had been published regarding thermal conductivities of mixtures and development of effective medium theories by Mossoti, Clausius, Maxwell and Lorenz. Effective medium theories are not limited to nanofluids but thoroughly investigated and applied in many fields of science and engineering. Most published researches meticulously investigated the thermal conductivity of nanofluids with a constituent of metals, metallic oxides, nonmetallic oxides and carbide nanoparticles. Eastman et al. [1] reported nanofluid consisting metallic nanoparticles where found to exhibit higher effective thermal conductivity than nanofluid with the same volume fraction of oxides. In this study, Cu nanoparticles in ethylene glycol as a base fluid shows 40% conductivity enhancement at a concentration of 0.3 vol. %. Patel et al. [71] also reports a thermal conductivity enhancement up to 21%. The experiment used gold and silver nanoparticle dispersed in the water. Moreover, Patel et al. [71] observed intriguing results on conductivity enhancement with a volume fraction as low as 0.011 vol. %. Previous researches also reported that only enhancing the thermal conductivity of the mixture will increase the heat transfer in the system. The Thermal conductivity of nanofluids has dominated the publications in the past decades [13].

Table 3.1 Thermal conductivity comparison of solids and liquids at room temperature (*Source: Eastman et al. [1], Thermal Transport in nanofluids, March 17, 2004*)

Material		Room temperature thermal conductivity [W/mK]
Metallic solid	Silver	429
	Copper	401
	Aluminum	237
Nonmetallic solids	Diamond	3300
	Carbon nanotubes	3000
	Silicon	148
	*Alumina (Al ₂ O ₃)	45
	*Copper Oxide (CuO)	18
	*Titania (TiO ₂)	11.7
Metallic liquids	Sodium at 644 K	72.3
Nonmetallic liquids	Water	0.613
	Ethylene glycol	0.253
	Engine oil	0.145

In this study, data points are gathered from different researches on heat transfer enhancement using nanofluids. Based on the experiment setup, equipment variation, personal skill variation and other factors that affect the observation, results might appear different from study to study. In this section, data collection and organization regarding thermal conductivity behavior of nanofluids is discussed briefly.

Duan [53] published a paper on thermal property measurement on Al₂O₃ – water nanofluids. Up to 5% volume fraction of alumina nanoparticle (with average size of 25nm) suspended in a water is measured its conductivity using a transient hot wire method. Thermal conductive of a nanofluid is strongly a function of temperature and the effect is investigated from 15°C to 55°C. In their study, the THW setup was calibrated by measuring the thermal conductivity if deionized water. The procedure of measurement was identical to measuring the nanofluid. Published data points in this study have an accuracy of ±2% of the measured thermal

conductivity values. Eastman et al. [72] have also studied the thermal conductivity behavior of alumina nanofluid with an average particle size of 33nm. And their experimental result is plotted as shown below.

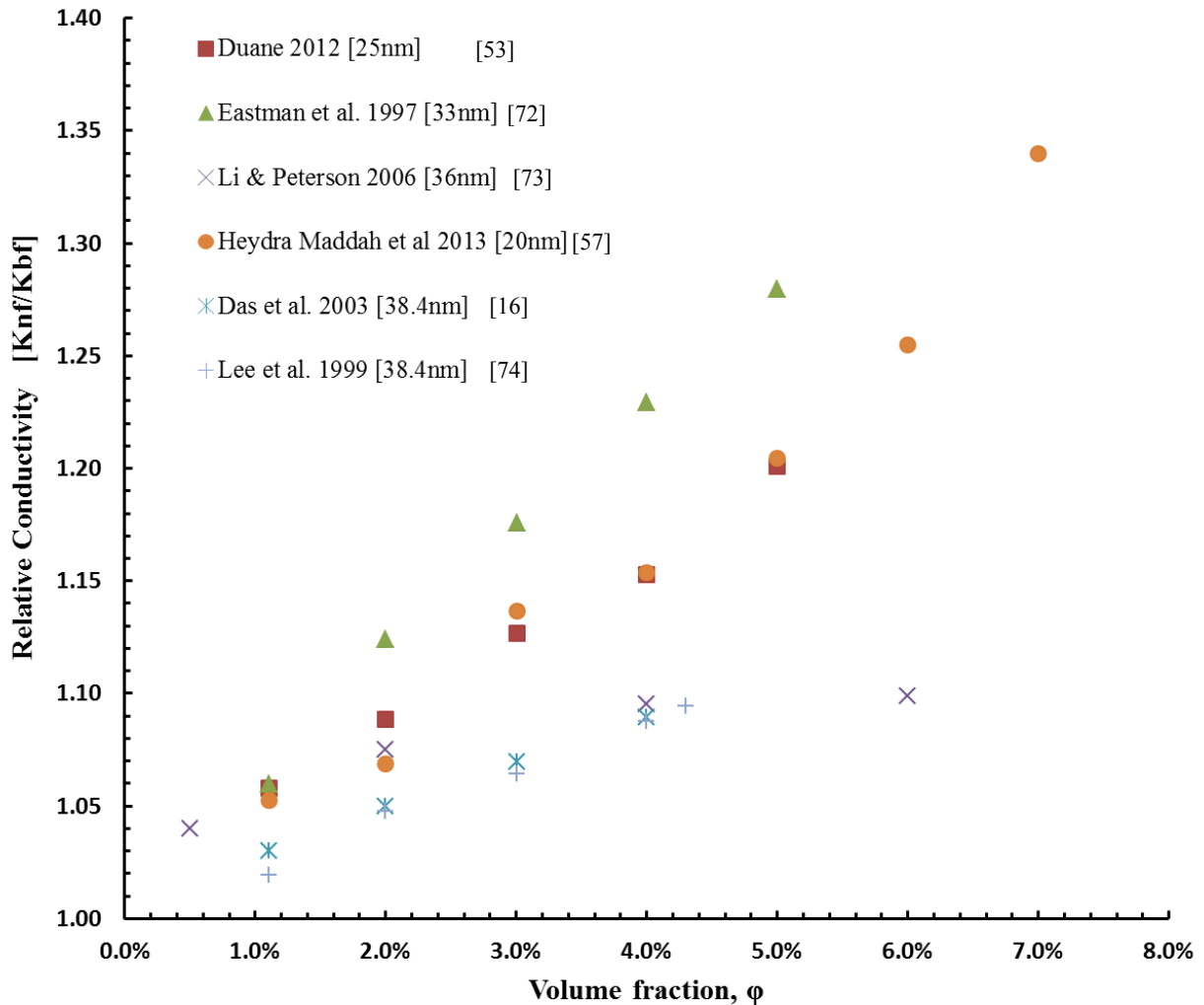


Figure 3.7 Comparison of relative conductivity of experimental data for Al_2O_3 - water nanofluid.

Maddah et al. [57] published a research on thermo-physical properties of Al_2O_3 and Ag nanoparticles suspended on distilled water. 20 to 40nm of nominal particle diameter at a concentration of 0.25 vol. % to 5 vol. % with a temperature of 15°C investigated in the experiment. In their studies thermal conductivity of alumina nanofluid significantly increases

linearly with increasing particle volume fraction. Das et al. [16] investigated the effective thermal conductivity of alumina and copper oxide nanoparticles suspended in the water. A nanoparticle fraction from 1 vol. % to 4 vol. % is experimented under variable temperature. At a room temperature with 1 vol. % concentration of alumina show a 2% enhancement of heat transfer. Nevertheless, this study also shows 10.8% enhancement can be achieved at the same nanoparticle loading but at mixture temperature of 51°C.

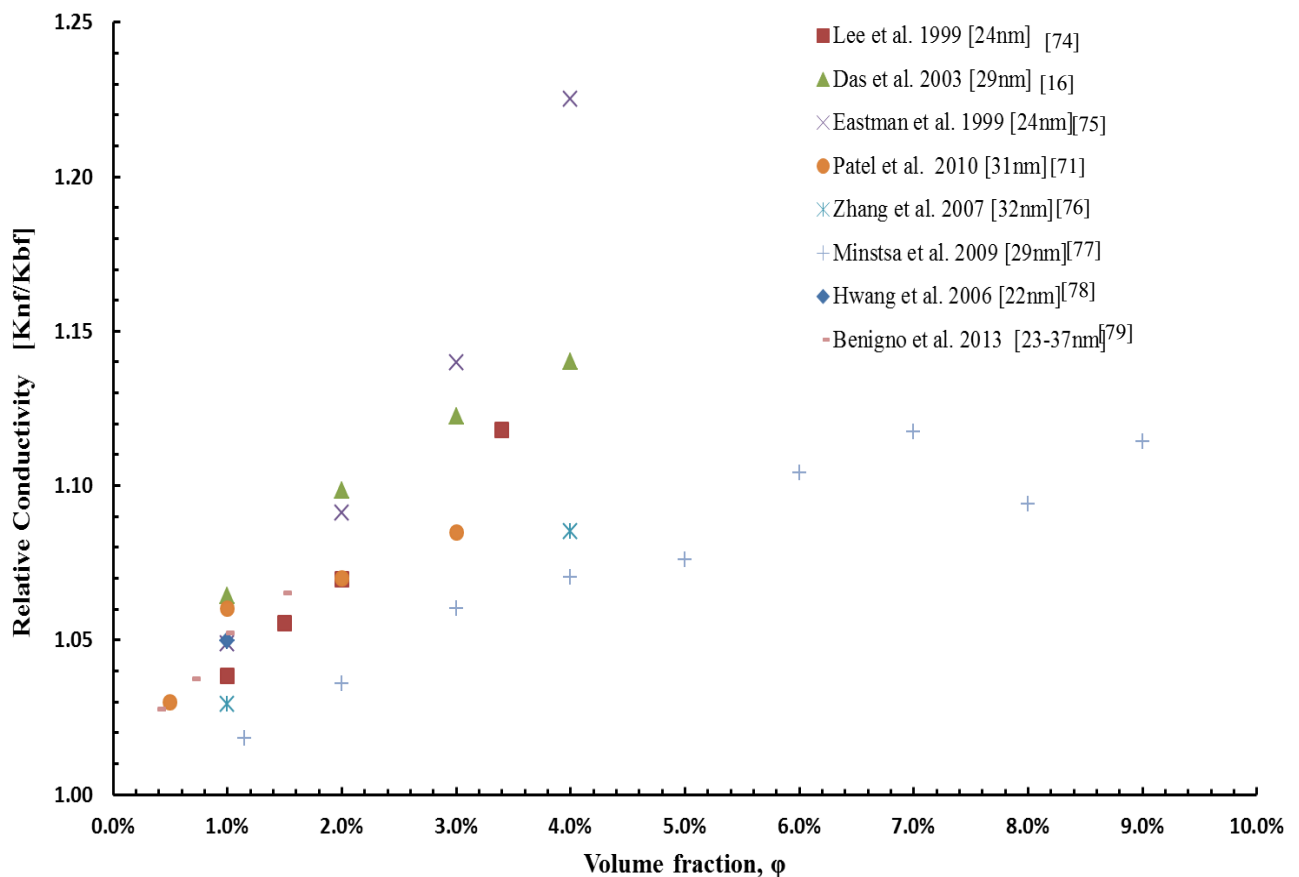


Figure 3.8 Comparison of relative conductivity of experimental data for CuO - water nanofluid.

Das et al. [16] also shows a 4 vol. % concentration can enhance the heat transfer up to 9.4% at room temperature and at a working temperature of nanofluid reaches 51°C, the heat transfer enhancement goes from 9.4 to 24.3%.

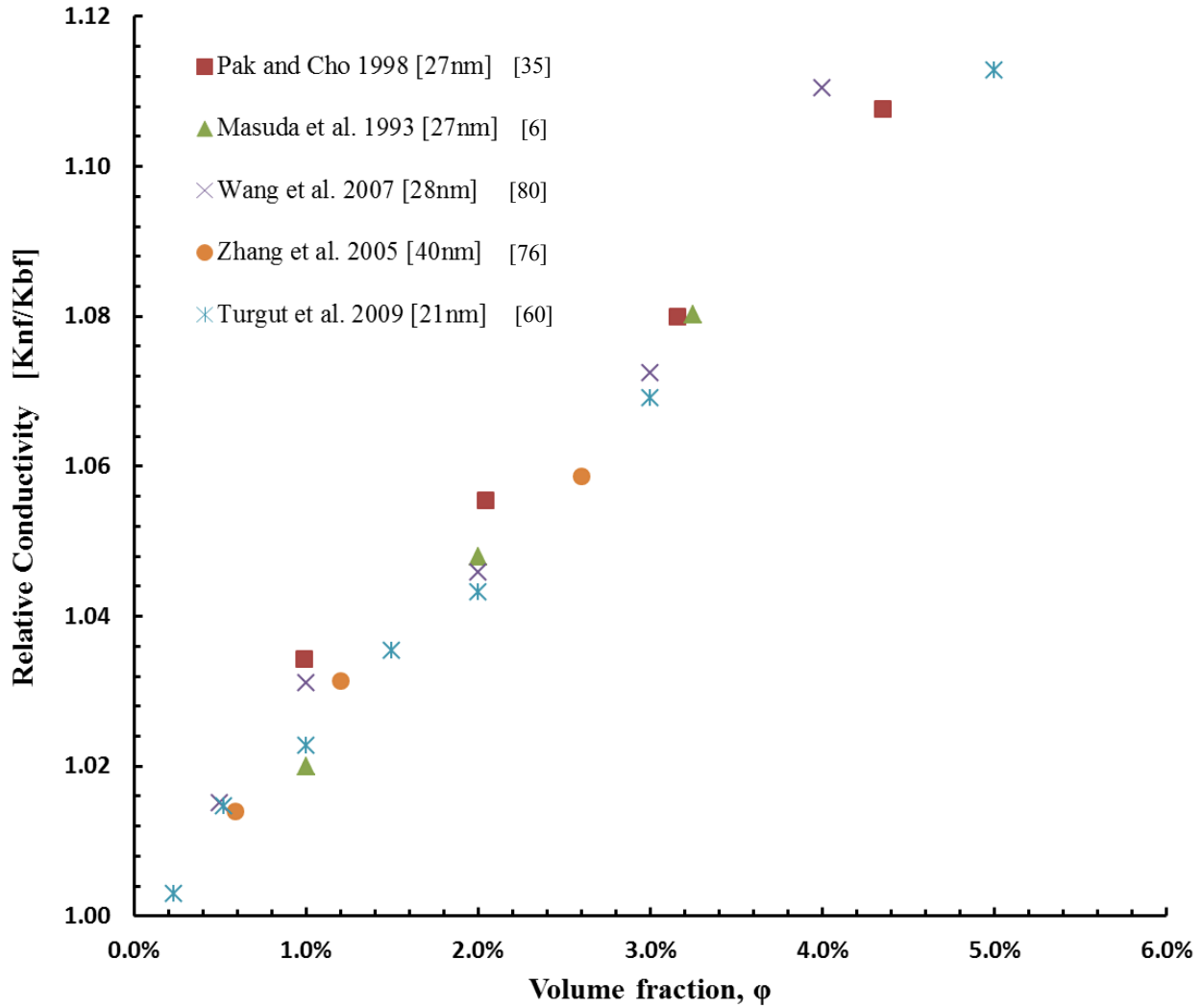


Figure 3.9 Comparison of relative conductivity of experimental data for TiO₂ - water nanofluid.

Pak and Cho [35] investigated the hydrodynamic and heat transfer of metallic oxides. In their studies alumina and titania nanoparticle suspension in base fluid water at particle mean diameter of 13 and 27nm, respectively, were used. Also a concentration of nanoparticles fraction from 1.3 to 4.3 % by volume is considered in the experiment. This study reports a heat transfer enhancement observed at higher concentration of nanoparticles.

3.2.3 Data Process Summary

Literature on nanofluid researches are highly dependent on the outcome of repeated experiments. Most researches provide their conclusion on the heat transfer enhancement or deterioration based on their observation. Since there is no available developed theoretical law that governs the thermo fluid properties on nanofluids, all conclusions are very much relied on the accuracy and precision of the experiment. Yulong et al. [13] suggests that, although there are abundant published studies and valuable progress are made on the effect of nanofluids on heat transfer, the fundamental working principles are not quite understood. As discussed above this new thriving science without a concrete theoretical foundation reflects a significant disagreement between published data and leading to unconvincing arguments. Eastman et al. [1] points out the weak theoretical foundation and understanding of this new class of heat transfer of fluids. He also suggested that in-depth study on atomic scale of nanofluids and understanding the mechanics of heat transfer between solid-liquid molecular particle interactions will pave a way to unlock the potential of these new generation fluids. Despite a numerous number of experimental publications in nanofluid, due to preparation, calibration and human errors result might get contaminated which leads to a wrong conclusion. So, it is very significant to compare and contrast between research publications. In this study, we have selected studies that are cited, reviewed and recommended throughout the nanofluid research community. A number of data collection criterions have been used in this study to assure that collected points have similar behaviors and to reproduce meaningful results. Some of the criterions are experiment objective, type of nanoparticles and base fluid used, experiment repeatability, experiment equipment used, nanofluid preparation, experiment publication year and general acceptance with the research community.

3.3 Statistical Modeling

Statistical analysis is the most essential mathematical tool in engineering during interpretation numerical data in to a meaningful and useful statistical model. After the collection of data points, a systematic statistical analysis is implemented to build the statistical model of the nanofluid thermo-physical properties. A nonlinear relationship between the dependent variables (viscosity and conductivity) and independent variable (particle volume fraction) is observed in previous and this present study. In order to address the nonlinear relationship a polynomial regression modeling is used to fit a second order polynomial line through collected data points. In this study, relative viscosity and conductivity are estimated with a single volume fraction factor.

3.3.1 Regression Modeling of Al₂O₃ Nanofluid Properties

On section 3.2.2.1 and 3.2.2.2 the thermo-physical properties of nanofluids have been briefly discussed and data points gathered from previous researches are plotted against the main factor concentration. As explained on previous chapters, this study will focus the research on the effect of nanoparticle concentration. And nanofluid thermo physical characteristics are modeled only as a function of nanoparticle concentration.

A quadratic model is proposed to fit an equation line through the data points. The equation of the model can be simply expressed as

$$Y = a_0 + a_1x + a_2x^2 + \varepsilon \quad (3.5)$$

Where, Y is the regressed dependent variable,

a_0 , a_1 and a_2 are the partial regression coefficient, in which a_1 measures the expected change of Y in per unit change of x and a_2 measures the expected change of y in per unit change of x^2 . The independent factor of the experiment is represented by the variable x . Al_2O_3 nanofluid viscosity data points from Figure 3.4 are regressed using a least square curve fitting. The curve fitting is at 95% confidence of interval with 30 sample observations.

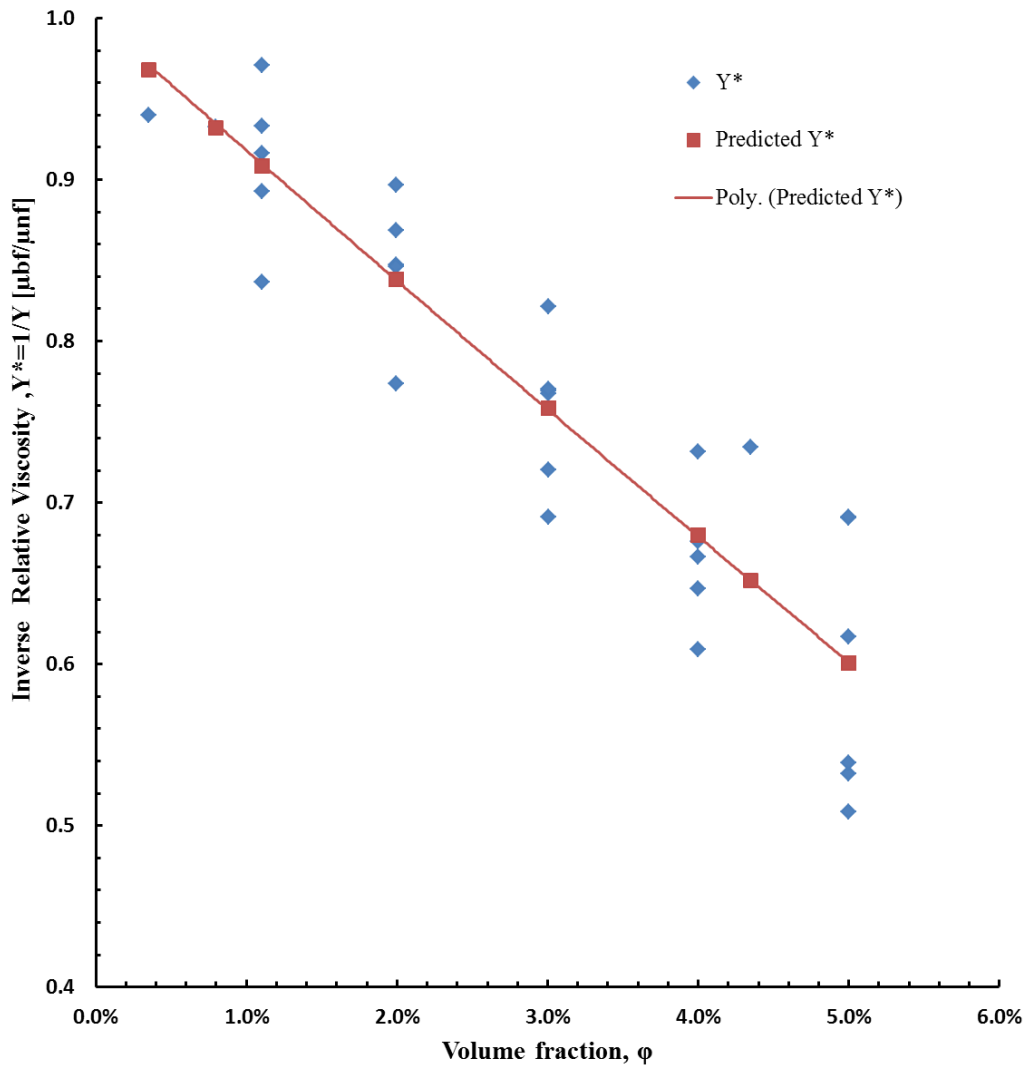


Figure 3.10 Regressed viscosity model plot for Al_2O_3 - water nanofluid.

The regression statistics shows that an adjusted R squared (R^2) of 83%. This can be expressed as 83% of the data can be explained by the new predicting points. From the regression report, a good agreement is observed between the sample point taken and the predicted relative viscosity values. Based on the research and presented experiment data of Duan [53], Nguyen et al. [48], Wang et al. [11], and Chen et al. [55]. The new regressed equation for the effective viscosity of water based alumina nanofluid can be written as

$$\mu_{nf} = \frac{(\mu_{bf})}{(5\varphi^2 - 8.22\varphi + 1)} \quad (3.6)$$

An inverse transformation is used to stabilize the error pattern, $Y^* = 1/Y$. After the transformation, there is no observable pattern of residuals as the independent factor (nanoparticle concentration) increase or decrease in amount. The higher F value shown on the ANOVA table gives more confidence on the validity of the viscosity regressed model.

Table 3.2 ANOVA table of Al₂O₃ nanofluid effective viscosity

	DF	SS	MS	F	Significance F
Regression	1	0.409	0.409	144.8428	1.39E-12
Residual	28	0.079	0.003		
Total	29	0.488			

Alumina is the most common used nanofluid when it comes to industry and also in the research community. The abundance of the particles, cost and good thermal conductivity behavior makes alumina the preferable nanoparticle. A stability of nanoparticles as a suspension is the most significant properties of nanofluids. The diluted alumina particles in the water have an appreciable stability property when compared to other type of nanoparticles. This property shows a level sedimentation and separation of nanoparticles from the base fluid due aggregation and

gravity. Based on some researches alumina nanoparticles have conductivity up to 45 W/m. K. The water based nanofluid of alumina particles similarly has a higher conductivity as reported on the researches. The thermal conductive regression model for alumina nanofluid also has been developed using the least square method as described above. A 95% confidence of interval is used to estimate the regression model of the thermal conductivity. A number of sample observations are taken from studies of Duan [53], Eastman et al. [72], and Maddah et al. [57].

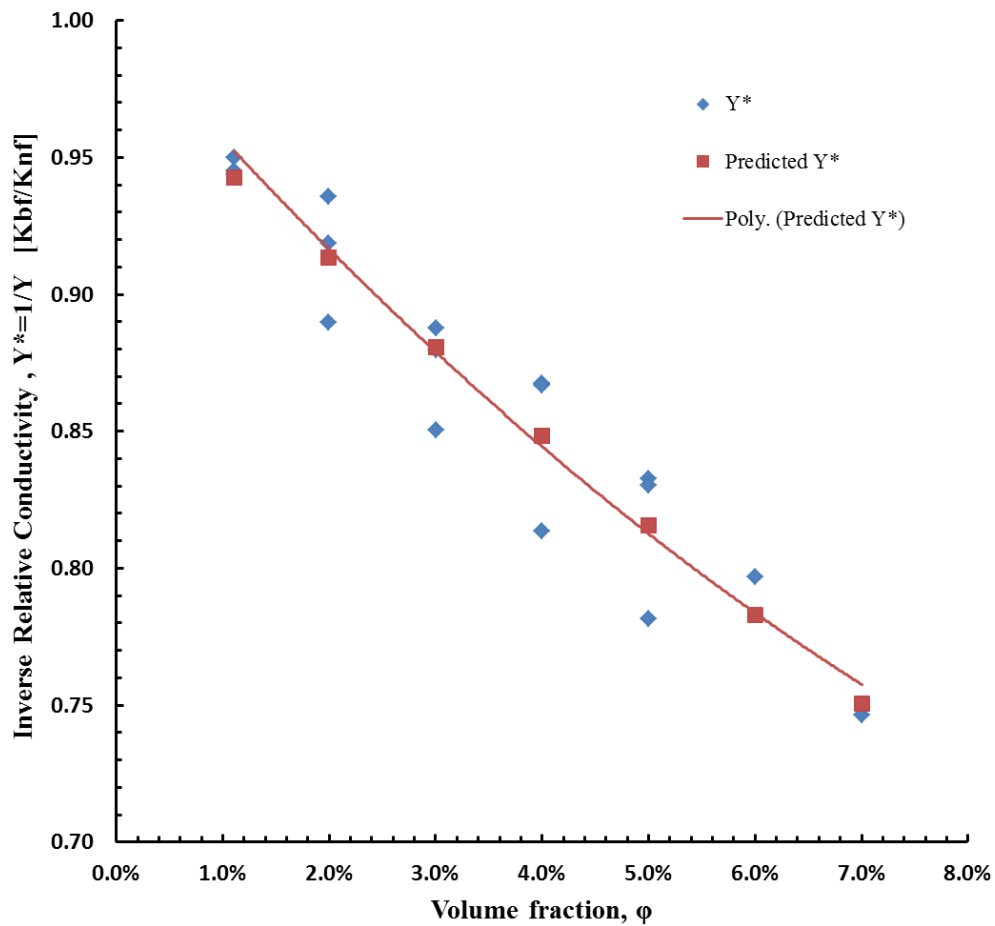


Figure 3.11 Regressed conductivity model plot for Al_2O_3 - water nanofluid.

The new regressed equation of the thermal conductivity model has an adjusted R squared (adj. R^2) value of 89%. This shows a good agreement between the sample data and the proposed

model of the effective thermal conductivity. Precisely, 89% of the collected data can be modeled by the new equation at 95% of confidence interval.

$$K_{nf} = \frac{(K_{bf})}{(14.28\varphi^2 - 4.46\varphi + 1)} \quad (3.7)$$

The residual of the predicted value in the statistical modeling is calculated and a transformation of the responses is used to avoid pattern of errors. An inverse transformation is found to be a suitable approach to stabilize the residuals, $Y^*=1/Y$.

Table 3.3 ANOVA table of Al₂O₃ nanofluid effective conductivity

	DF	SS	MS	F	Significance F
Regression	1	0.0538	0.0538	136.99	6.07E-09
Residual	15	0.0059	0.000393		
Total	16	0.0597			

3.3.2 Regression Modeling of CuO Nanofluid Properties

Copper oxide nanoparticles are also the most common constituent on nanofluids in industries and research community. Despite its common availability the rheological studies provided in the literature are extremely limited. A rheological experiment on water based copper oxide nanofluid was done in 2007 by Nguyen et al. [48] on their study of “Hysteresis Phenomenon on Water Based nanofluid Viscosity”. On their studies, the viscosity of CuO nanofluid concisely reported at wide range of nanoparticle concentration. Putra et al. [66] also have studied the viscosity behavior of CuO nanoparticles suspended in a water base fluid. The amount of nanoparticle concentration used was 0.1 to 1.2 % by volume. A viscosity increment was observed by Putra et al. [66] as the volume concentration of the CuO nanoparticle increased.

Based on valid experimental data points collected from the literature, the regression model is developed using a second order polynomial curve fit. A 95% confidence of interval is used to estimate the effective viscosity model of the copper oxide water mixture.

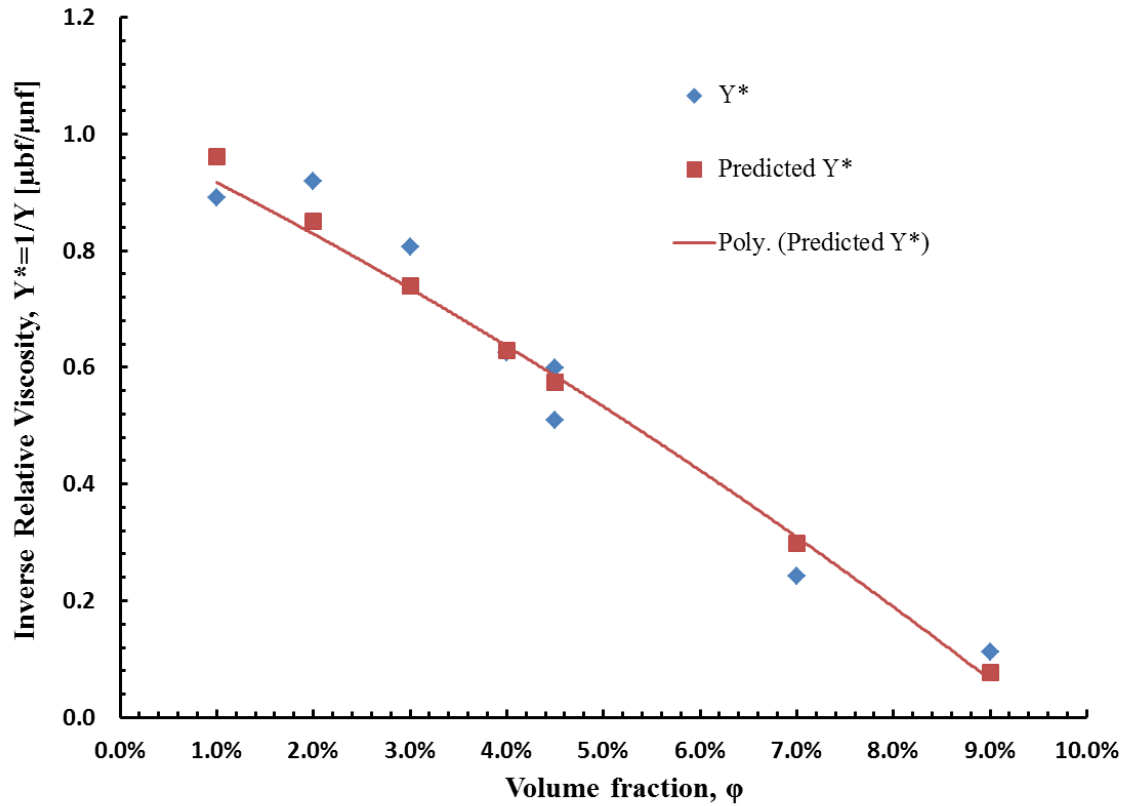


Figure 3.12 Regressed Viscosity model plot for CuO - water nanofluid.

In this study, the regressed viscosity model equation for the water based CuO nanofluid can be written as,

$$\mu_{nf} = \frac{(\mu_{bf})}{(-26.20\varphi^2 - 8.03\varphi + 1)} \quad (3.8)$$

The adjusted R squared (R^2) value from the statistical analysis is 95.5%. A 95.5% agreement between the sample data collected and the predicted model is an excellent prediction in statistics.

The response is transformed with a transformation equation $Y^*=1/Y$ to stabilize the error pattern against the independent variable particle concentration.

Table 3.4 ANOVA table of CuO nanofluid effective viscosity

	DF	SS	MS	F	Significance F
Regression	1	0.580	0.580	151.85	1.74E-05
Residual	6	0.0230	0.004		
Total	7	0.603			

Effective thermal conductivity of CuO nanofluid is comprehensively discussed on many literature. Lee et al. [74] have studied the conductivity of copper oxide particles suspended in water. Their experiment was conducted using a transient hot wire method under room temperature condition. In their report water based CuO oxide nanofluids significantly enhanced thermal conductivity when compared to the base fluid with 0% of nanoparticle concentration. Lee also summarized that the thermal conductivity enhancement of the nanofluid mixture solution is dependent on both the nanoparticle and the base fluid thermal conductivity. Das et al. [16] on their literature of studying the thermo physical properties of water based CuO nanofluid, the thermal conductivity enhancement rate is lower than alumina nanofluids. The increment of conductivity is linear with the concentration of CuO nanoparticles.

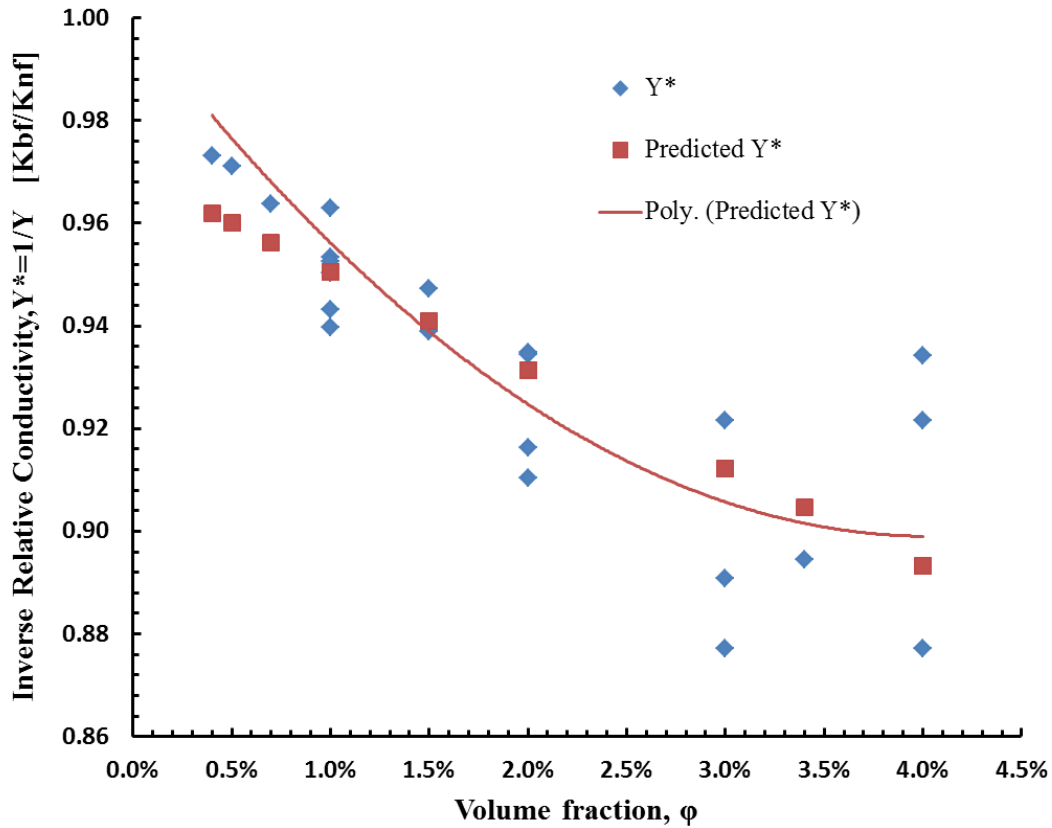


Figure 3.13 Regressed conductivity model plot for CuO - water nanofluid.

The statistical study of thermal conductivity is conducted based on experiments collected from literature. For the present study the effective thermal conductivity data points are collected from Lee et al. [74], Das et al. [16], Eastman et al. [75], Patel et al. [71], Hwang et al. [78] and Benigno et al. [79]. 21 sample points are considered to develop the regression model at 95% confidence of interval.

The predicted regression model for the conductivity of the CuO nanofluid can be stated as

$$K_{nf} = \frac{(K_{bf})}{(61.84\varphi^2 - 4.99\varphi + 1)} \quad (3.9)$$

62% adjusted regression coefficient is reported from the statistical analysis, which can be clarified as only 62% percent of the data collected is explained by the new predicted effective thermal conductivity model. Although the R^2 value is much lower when it is compared to other preceding studies, a 62% agreement between the sample data collected and the predicted model is a good prediction based on an engineering judgment.

Table 3.5 ANOVA table of CuO nanofluid effective conductivity

	DF	SS	MS	F	Significance F
Regression	1	0.0109	0.0109	36.29	6.86E-06
Residual	20	0.0060	0.0003		
Total	21	0.0169			

3.3.3 Regression Modeling for TiO₂ nanofluid properties

Titanium dioxide (TiO₂) or Titania nanoparticles are frequently used in the heat transfer enhancement and related technology. It is also the ninth most abundant oxide nanoparticle in its category. Murshed et al. [69] have studied the property of TiO₂ suspended in deionized water. They have used a TiO₂ nanoparticle concentration up to 5.0 % by volume. In their findings the effective viscosity of the nanofluid mixture is highly dependent on the amount of concentration. A linear relation between them is observed from the experiment. Pak and Cho [35] have conducted an extensive study on the TiO₂ nanoparticle suspended on water. They have reported that a 10 vol. % of TiO₂ oxide will increase the viscosity of the mixture 3 times when compared to the base fluid water. This finding also has higher value than the prediction of the classical theory of nanoparticles suspension rheology.

As shown on Figure 3.6, rheology properties of TiO₂ nanofluid are collected from some major studies found on the literature. This study used measured effective viscosities from Murshed et al. [69], Masuda et al. [6], and Pak and Cho [35].

The statistical modeling of the rheology property of TiO₂ nanofluid is done at 95% confidence of interval. The predicted models and regression are shown on Figure 3.14 below.

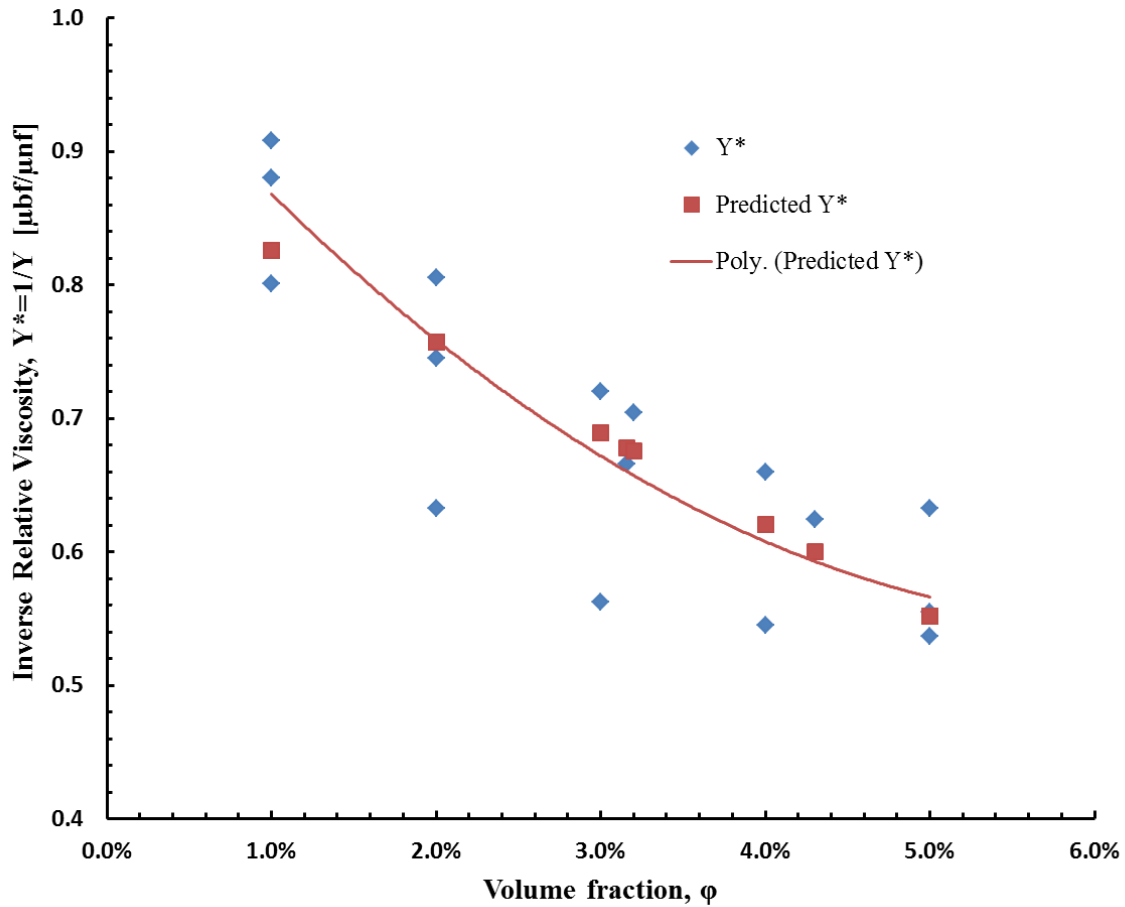


Figure 3.14 Regressed Viscosity model plot for TiO₂ - water nanofluid.

The statistical analysis reported an adjusted R squared value of 68% for the predicted model. This shows that 68% of the data can be accurately modeled by the predictor, which can be

concluded as a good experiment-model agreement. The regressed model for the effective viscosity of TiO₂ nanofluid is

$$\mu_{nf} = \frac{(\mu_{bf})}{(112.98\varphi^2 - 14.33\varphi + 1)} \quad (3.10)$$

Table 3.6 ANOVA table of TiO₂ nanofluid effective viscosity

	DF	SS	MS	F	Significance F
Regression	1	0.1438	0.1438	33.1	5.01E-05
Residual	14	0.0608	0.0043		
Total	15	0.2046			

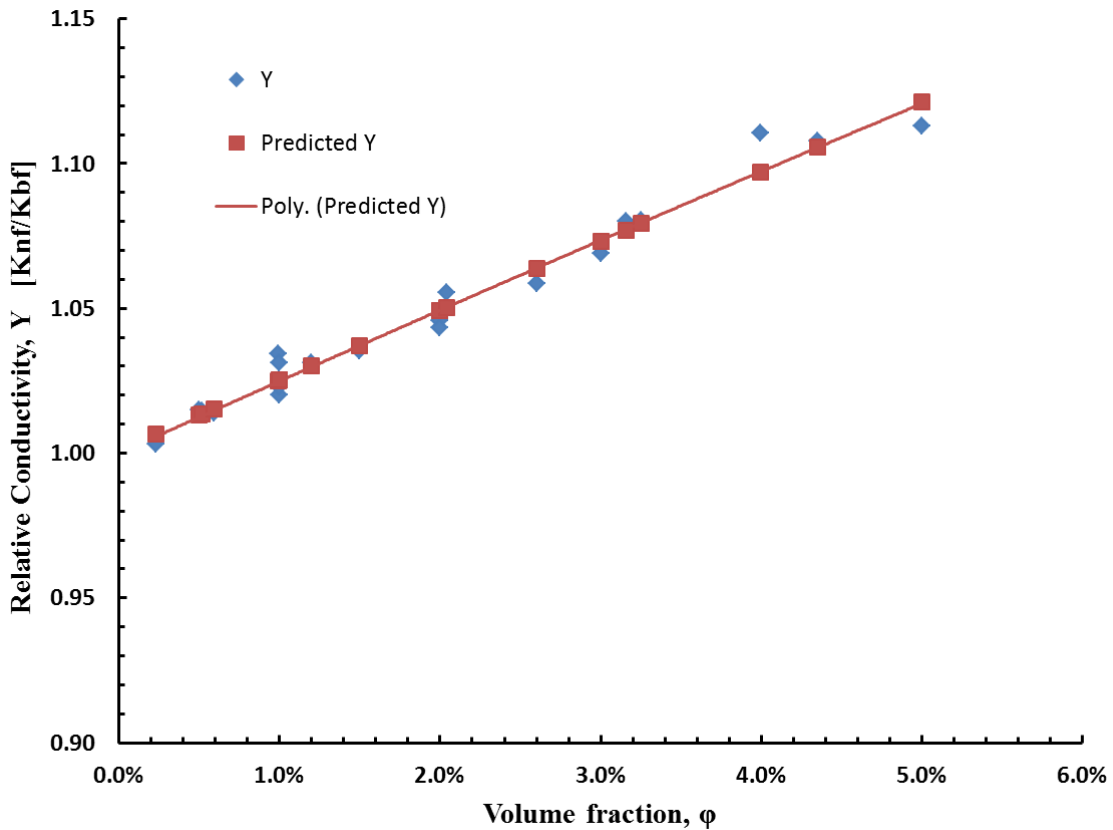


Figure 3.15 Regressed conductivity model plot for TiO₂ - water nanofluid.

The thermal conductivity of TiO₂ nanofluid is studied in different literature and it is one of the abundant nanofluids in the technology. As per the research reported by Pak and Cho [65], the Anatase type of TiO₂ nanoparticle has a thermal conductivity of 8.4 W/m.K. But in this study, the most recent data for the thermal conductivity of TiO₂ nanoparticle which is 11.7 W/m.K is picked.

On Figure 3.15 shown above, the statistical modeling is developed using experiment data from Pak and Cho [35], Masuda et al. [6], Wang et al. [80], Zhang et al. [76], and Turgut et al. [60]. The predicted statistical model of the thermal conductivity at 95% confidence of interval will be,

$$K_{nf} = K_{bf}(-1.852\phi^2 + 2.51\phi + 1) \quad (3.11)$$

This predicted model of the effective thermal conductivity has a 97.4% agreement with the collected data points from the literature. A model with an adjusted R squared value of 97.4% more or less explains all the experiment result.

Table 3.7 ANOVA table of TiO₂ nanofluid effective conductivity

	df	SS	MS	F	Significance F
Regression	1	0.0220	0.0220	786.68	1.56E-17
Residual	20	0.0006	2.8E-05		
Total	21	0.0226			

CHAPTER 4

FINITE ELEMENT MODELING AND GRID VALIDATION

4.1 Computational Fluid Dynamics

In the processes of studying a fluid flow system, it is a recognized fact that the analytical solutions of an equation are inadequate. This can be due to complex boundary condition, irregular fluid flow path, fluid channel shape, or other factors. Experimental fluid mechanics is another methodology to study the dynamics of fluids. This approach of studying fluid dynamics faces many difficulties when it comes to implementation. Due to variable fluid behavior or geometry for various problems, cost of building the physical setup and time consumption, experimental studies of fluid will be limited to a particular situation. A numerical study of fluids is the key engineering solution which solves all the problems that has been asked. Numerical studies of fluid started from many years back, nevertheless, the present development of computer technology benefits the implementation of fluid dynamics computation. Using high speed super computers, complex fluid systems can be solved with an improved accuracy and computing time. Some of the complex fluid flows scenarios that demands a numerical tool are, supersonic flows, turbulent flows, two phase fluid flows and so on. The fundamental approach of computational fluid dynamics is an approximation. The nature of governing equations (Navier-Stokes equation, mass and energy conservation equation) for fluid flow and heat transfer are partial differential equation. Mathematical approximations are used to reduce these partial differential equations in to algebraic expression with insignificant error. The algebraic expression developed from the governing equation approximation will be solved numerically with the aid of a computer. The numerical studies conducted are not taken as final solution for a fluid problem,

the result has to be compared with an experimental study for validation. Once it is confirmed that the numerical solution is in a tolerable error range when compared to the experiment, the numerical program can be used for various fluid problems with in the limit imposed by the assumption it is based on.

In the present study, a numerical tool (FloEFD V13.0) is used to estimate the effect of nanoparticles concentration suspended in pure water on a heat transfer enhancement. A Homogenous single phase model is deployed to execute the numerical study. This type of model is widely used in the literature [22, 90] and effective thermophysical properties of the nanofluid are estimated from statistical regression of experimental results and will be used in the single phase model.

A FloEFD V13.0 computer program which is developed by Mentor Graphics mechanical analysis division is used to do the numerical analysis regarding the nanofluid research in this study. The FloEFD is fully embedded into CATIA V5, which makes the CFD study can be done in conjunction with any CAD modification. This will avoid all the complexity that comes with a 3D file exchange between CAD and CFD. The program also makes it easier to change the design as per the numerical feedback and start the loop process until the required CFD result is obtained.

4.1.1 Domain Discretization Methods

In conducting a CFD study, discretization plays the main role on achieving the accuracy of the result. Selecting the right type of discretization is based on the fluid problem type, complexity and computation resource [81]. The three type of discretization method being used are finite difference methods (FD), finite volume methods (FV), finite element methods (FE).

Finite difference methods are mainly used with structured grid. The domain is discretized in space and in time and the computed solution is interpolated across each grid points. The error is estimated by comparing the numerical solution and exact solution. This error is a truncated error caused by the Taylor series approximation which ignores the higher order terms in the process. Finite volume methods are the most standard scheme in fluid mechanics. Timothy et al. [82] studied finite volume methods and explain that, FV methods are extensively used in fluid mechanics, meteorology, electromagnetics, semiconductor device simulation, biological processes that have integral control form from a governing conservative system. FV methods are used in conjunction with unstructured grids and those methods are numerically robust in extension of discrete maximum or minimum principles. Finite element methods are another type discretization schemes that are being used in the field of computational fluid dynamics. FE methods are broadly used in structural analysis of solids rather than in fluid mechanics. Dick [83] concluded that FEM is superior to FVM when complex higher order terms are used in the formulation. With a FEM, complex geometries, complex grid cells, and unstructured grids can be easily executed. The most beneficial property of FEM is the problem solving approach, instead of finding the solution of the partial differential equation, FEM looks for more general integral form of the PDE which helps for ease of achieving high order accuracy.

In this study, the discretization is prepared using FloEFD which uses a full 3D finite volume method. For solution accuracy, the grid properties are adjusted by manipulating the solid/fluid interface refinement, cell refinement, and narrow channel refinement criteria.

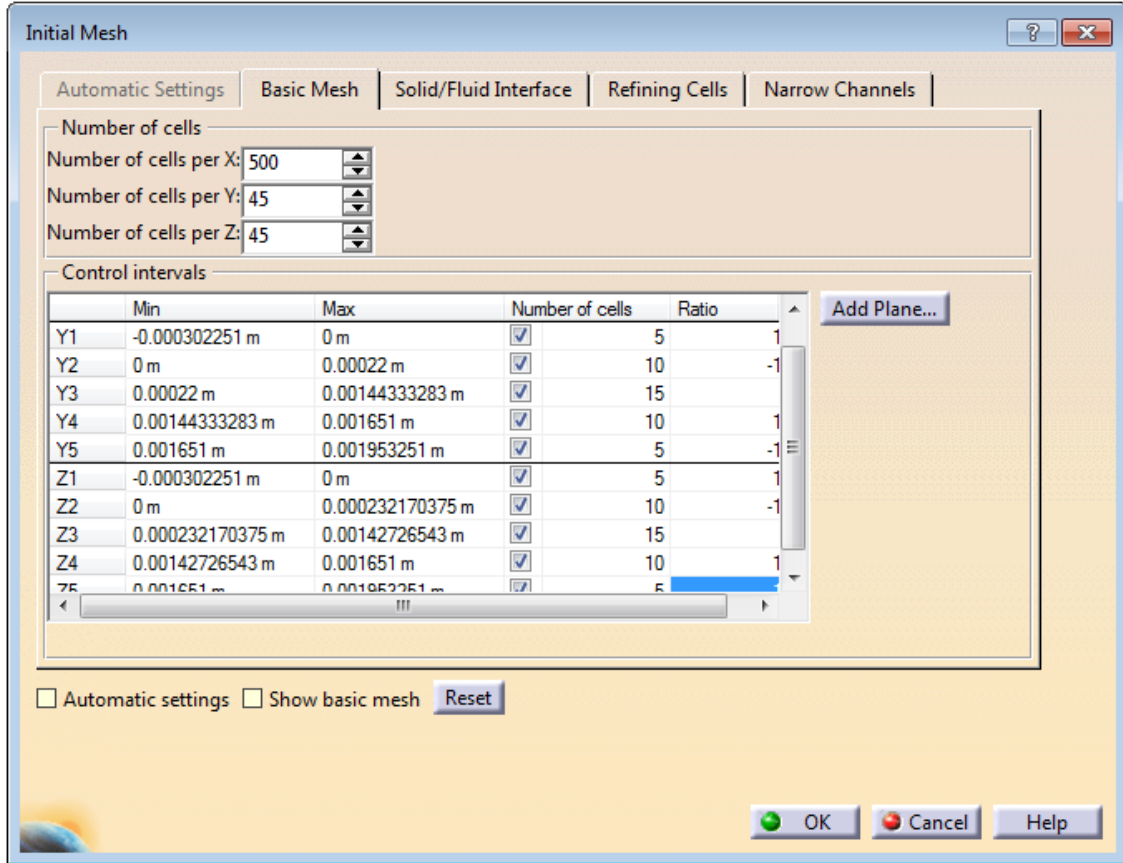


Figure 4.1 FloEFD V13.0 manual mesh setup window

4.2 Grid Selection and Validation

Grid selection is the main and prior task that has to be clinically approached in computational fluid dynamics. Selecting the right type of grid for a given problem is always a matter of iteration. Grid selection and optimization can be related to many factors that affect the simulation result. Although there is no available grid (mesh) that results 100% accurate, engineers always look forward in mitigation of the errors in to a tolerable range. Grid size, number and type are the main parameters in generating a mesh for a numerical simulation and significantly dependent on the fluid flow problem and geometry of the system. For example, grids near to the solid wall should be small enough in size and sufficient in quantity to capture the effect of boundary layer on the fluid flow dynamics and heat transfer of the system.

4.2.1 Domain Size and Specification

The fluid flow problem in this study is designed to exploit the maximum result accuracy from the structured grid of a finite volume discretization scheme without compromising the fluid flow dynamics and heat transfer effectiveness. A millimeter scale size rectangular copper tube (1.651mm x 1.651mm x 200mm) is considered to characterize the property of the nanofluid and study the heat transfer enhancement achieved. The flow cross section geometry of the copper tube is a square channel which considerably improves the structured mesh quality around the vicinity of fluid and tube interface when compared to different channel geometry. Comparison of different channel geometry regarding structured mesh quality is discussed as show below on Figure 4.2.

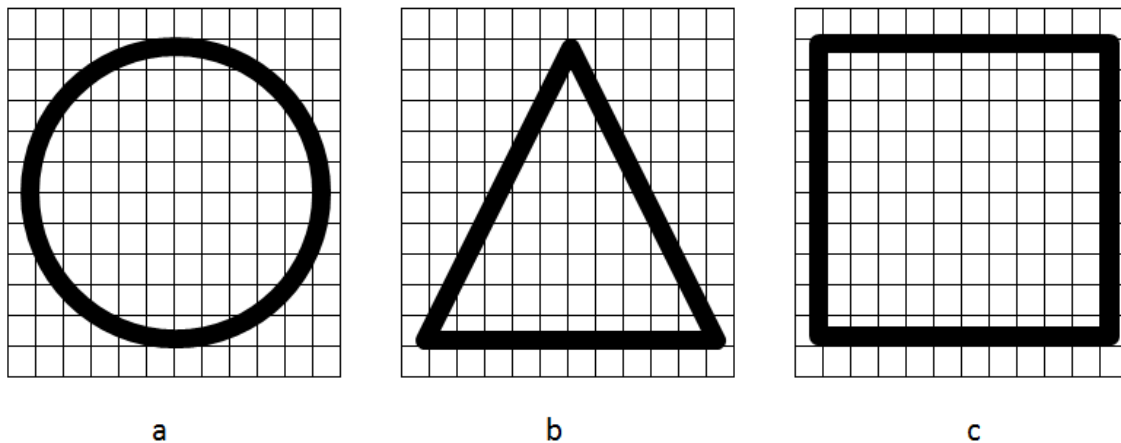


Figure 4.2 (a) Circular flow cross section tube in a structured grid domain (b) Triangular flow cross section channel in a structured grid domain (a) Square flow cross section channel in a structured grid domain

As it is clearly shown on Figure 4.2, a structured 3D finite volume discretization scheme can be fully exploited using the right type of channel geometry. Regarding Figure 4.2(a) a circular channel is discretized with structured rectangular mesh, however during cell refinement, around

the inner wall of the tube, the symmetry and quality of elements will degrade which significantly compromise the final result. On Figure 4.2(b) element refinement near to the solid/fluid interface will not be good enough to capture the fluid behavior on the solid wall. Figure 4.2(c) provides an ideal grid quality during mesh refinement and optimization due to the edge of the channel is aligned in parallel with the computational domain which contributes on the symmetry and quality of the elements along the inside four walls.

Optimized final grid for the fluid medium is shown below. Grid cells near to the wall channel are made fine and symmetric purposely. The boundary layer effect, wall shear viscosity and the Nusselt number are calculated based on the fluid and heat transfer property on the solid/fluid interface.

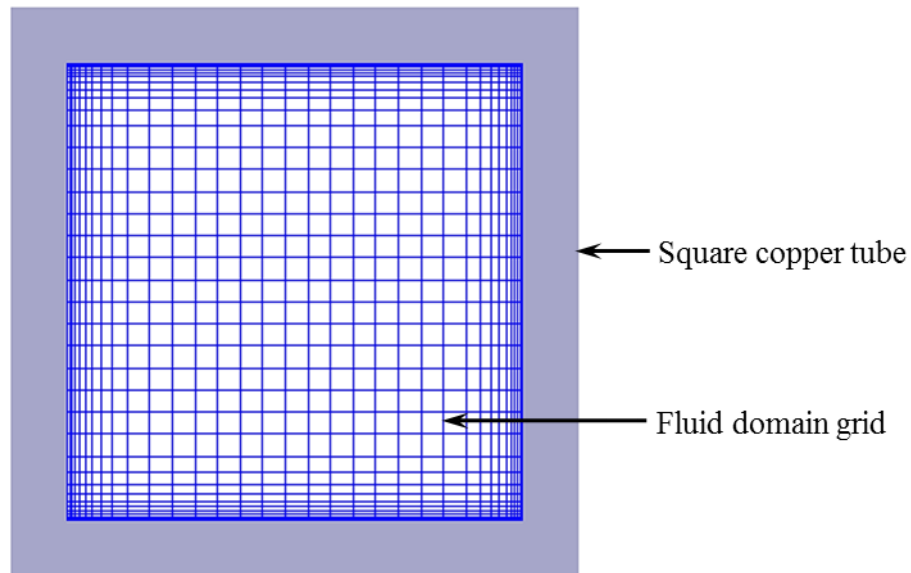


Figure 4.3 Optimized grid of fluid flow cross section in square channel.

The mesh quality, and number around the fluid/solid wall affect the result accuracy of all significant properties listed above. On Figure 4.3, the final grid dimension selected based on the

iteration conducted using pure water with the empirical equation of Nusselt number for short tubes, discussed on the next chapter.

4.2.2 Grid Validation

Iteration of different grid types and size is conducted during selecting the grid model for a better result. Grid testing experiment is affected by different factors. The boundary conditions applied, computer processing capability and available RAM, and numerical solver schemes are some of the main factors that play a major role on the grid selection. The grid also has a significant impact on CPU time required, solution rate of convergence, and solution accuracy. In computational fluid dynamics study a decent grid quality will lead toward a good result and this depends on mainly grid density, grid cell aspect ratio, boundary layer mesh, and mesh refinement through adaption.

Pure water flowing in a laminar flow regime is used as a medium to validate the grid quality by comparing an estimated value of Nusselt number. The water entering to the channel is modeled to have a hydro-dynamical fully developed and thermally developing flow. For this internal flow in a short pipe condition, a familiar theoretical correlation of Nusselt number is used from Sellars et al. [84] which approximates the local Nusselt number.

$$Nu = 1.30 \left[RePr \frac{D}{x} \right]^{1/3} \quad (4.1)$$

A constant heat flux of 91 kW/m² is applied on the surface of the copper tube which has 1.64E-3 m² surface area. The water inlet temperature is kept at 293°K and flowing with a velocity of 0.5m/s which is equivalent to a Reynolds of ~1200. A grid with a dimension of 45 X45 X 500 shows a better result which yields an error less than 5% when compared to the Sellars

et al. [84] Nusselt approximation. As show on the the Table 4.1, the numerical result is plotted for average fluid and thermal proprties at eleven axial locations.

Table 4.1 Grid 1 CFD result data of different thermo-physical properties

x [mm]	L [mm]	X/L	Hydraulic diameter [μm]	HTC [$\text{w}/\text{m}^2\text{k}$]	K [w/mk]	Pr	ρ [kg/m^3]	μ_b [Pa.s]	μ_s [Pa.s]
2	200	0.01	1651	7812.4	0.609	6.05	995.7	8.79E-04	5.15E-04
20	200	0.10	1651	4349.8	0.625	5.00	991.9	7.40E-04	4.42E-04
40	200	0.20	1651	3494.1	0.631	4.75	989.0	6.94E-04	3.99E-04
60	200	0.30	1651	3047.3	0.632	4.53	986.4	6.65E-04	3.68E-04
80	200	0.40	1651	2760.5	0.637	4.33	984.8	6.46E-04	3.44E-04
100	200	0.50	1651	2553.5	0.639	4.37	982.9	6.44E-04	3.25E-04
120	200	0.60	1651	2393.3	0.638	4.27	980.8	6.28E-04	3.08E-04
140	200	0.70	1651	2262.1	0.640	4.30	978.8	6.12E-04	2.94E-04
160	200	0.80	1651	2152.1	0.643	4.26	978.6	6.10E-04	2.81E-04
180	200	0.90	1651	2058.9	0.645	4.10	976.7	6.14E-04	6.73E-04
200	200	1.00	1651	1995.2	0.643	4.00	975.1	5.93E-04	2.71E-04
AVERAGE				3170.8	0.63	4.5	983.7	6.66E-04	3.84E-04

Different sizes of grids are also tested under the same requirement and compared to each other. Size of the grid cells in the fixed computational domain is used as a variable factor between the proposed meshes. The percentage error results for some different type of grids are published on Table 4.2.

Table 4.2 Error comparison between different grids

Gird Size (w x h x l)	CFD Nusselt number	Theoretical Nusselt number	Percentage error
45 x 45 x 500 (1)	8.118	7.751	4.756%
40 x 40 x 500 (2)	8.319	7.785	6.859%
55 x 55 x 400 (3)	8.648	7.758	11.473%
40 x 40 x 600 (4)	8.285	7.791	6.336%

The Nusselt number is plotted against the dimensionless length of the copper channel for the grid that has the lower error percentage. Figure 4.4 shows that the result from the Grid size 45 x 45 x 500 has a good agreement with the theoretical model provided.

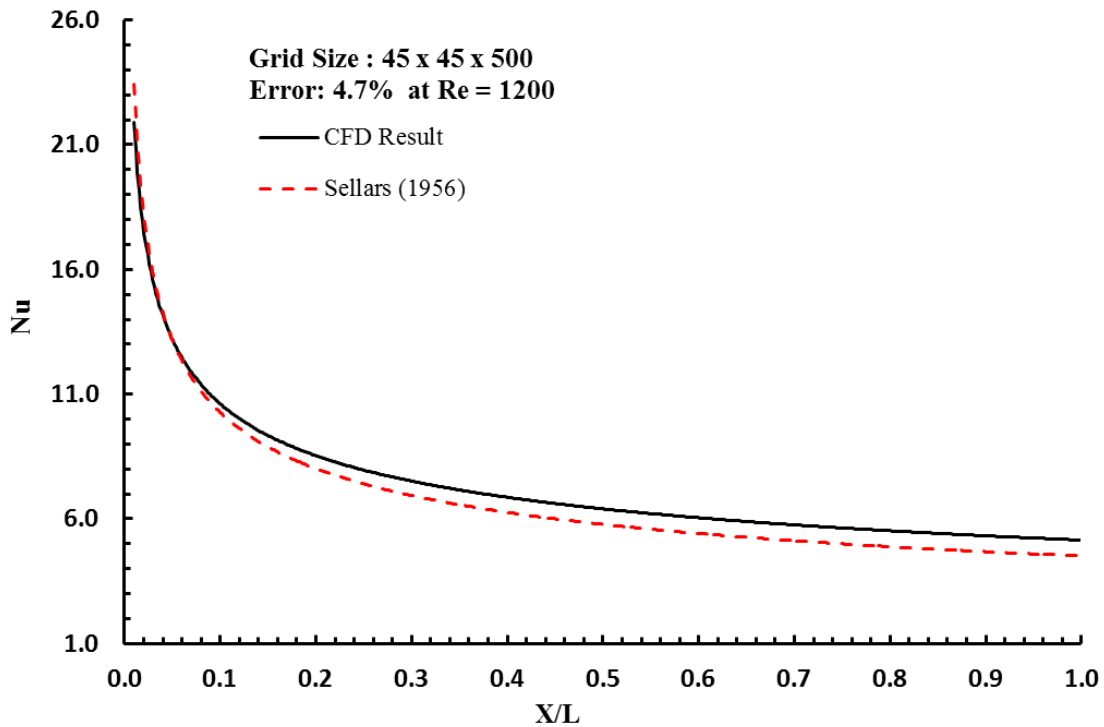


Figure 4.4 CFD result comparison with a theoretical Nusselt number correlation.

It is quite possible to increase the accuracy of the result or reduce the error by increasing the number of grid cells and the refinement level. But this procedure will escalate the computational

time required to converge. In numerical studies, results that has a 5% error or below when compared to an experiment can be suggested as a good agreement.

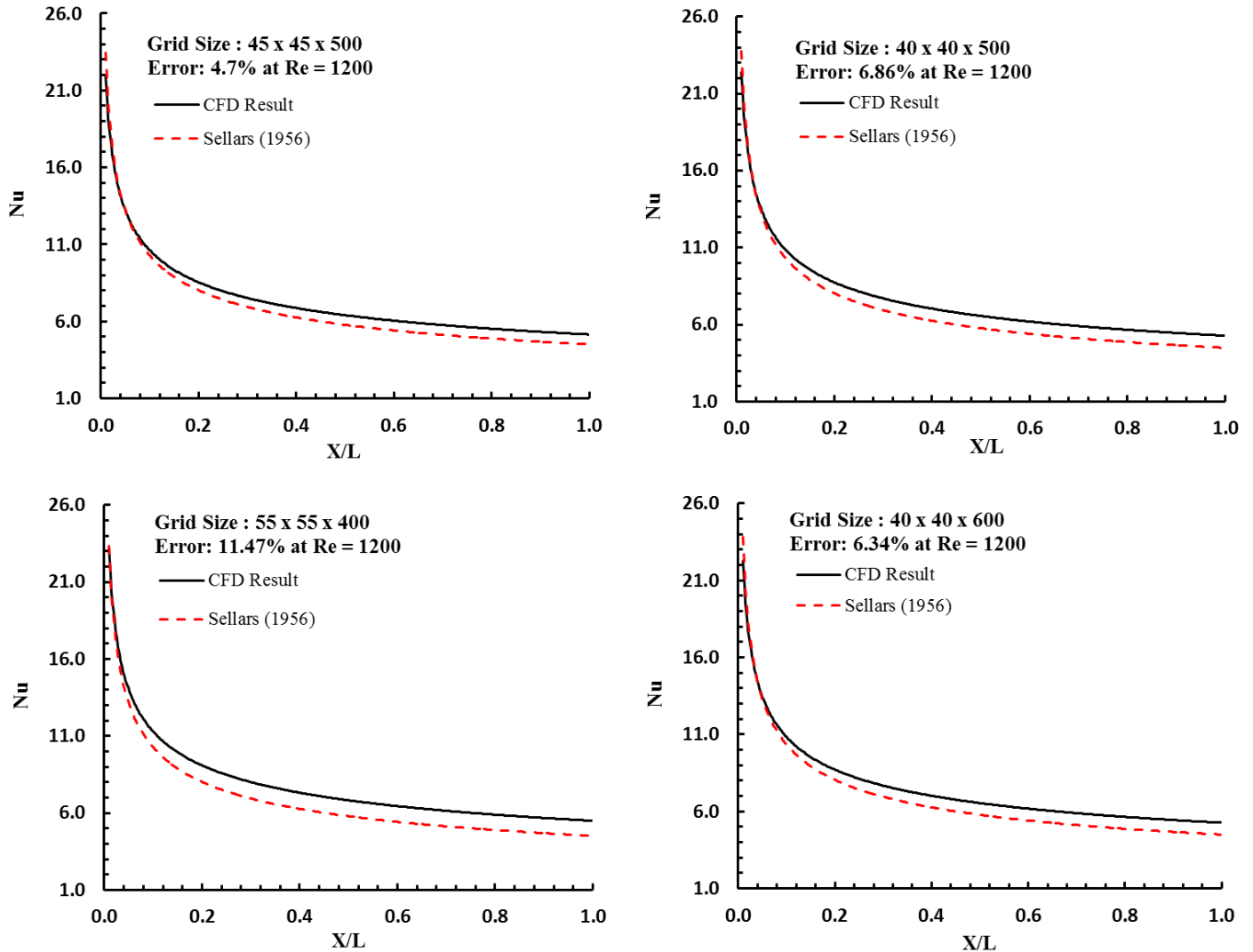


Figure 4.5 Error comparison with different grids.

The grid validation with numerical computation iteration approach yields a success result with a small percentage error at a reasonable computation time which allows us to use the current grid properties for further studies of nanofluids under the limits imposed by the assumption on which it was based.

4.3 Mathematical Modeling

Computational fluid dynamics study of a nanofluid should be studied carefully in order to match the numerical result to an experiment. The lack of understanding of the heat transfer in the nano scale level hinders the ability to come up with a comprehensive model that serves all type of categories of nanofluids. The mathematical modeling of a nanofluid can be approached in different perspective according to literature. Mojarrad et al. [85] studies main two models for hydro-dynamically fully developed and steady thermal fluid flow. Their studies were focused on comparing the accuracy of those models.

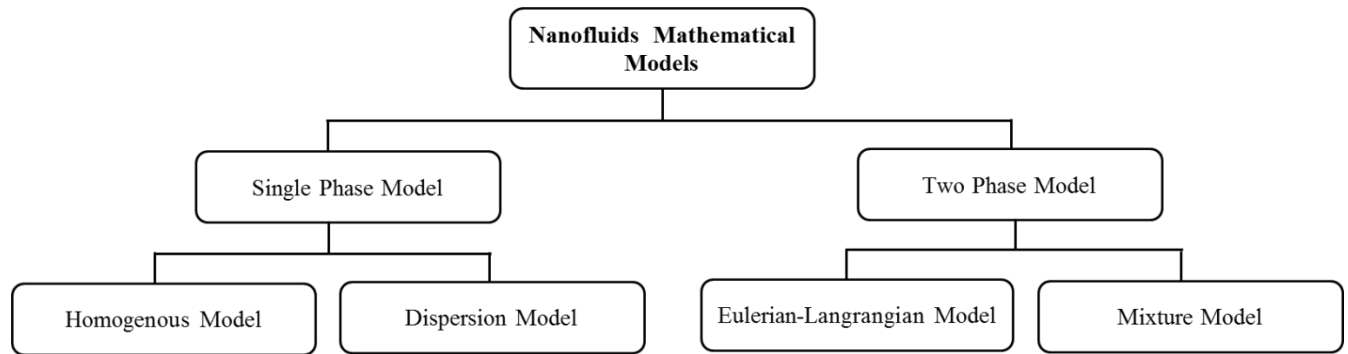


Figure 4.6 Applicable mathematical models for solid-fluid mixture

Homogenous single phase model of a nanofluid is based on the classical fluid transport equations which are the conservation of mass equation, momentum equation and the energy equation. The thermo-physical properties of the mixture are calculated as an effective property from the solid nanoparticle and the base fluid. The two phase solution will be reduced to a single phase mathematical model with effective mixture property assumption.

Continuity equation

$$\nabla \cdot (\rho \vec{V}) = 0 \quad (4.2)$$

Momentum equation

$$\nabla \cdot (\rho \vec{V} \vec{V}) = -\nabla p + \nabla(\mu \cdot \nabla \vec{V}) + \rho g \quad (4.3)$$

Energy equation

$$\nabla \cdot (\rho \vec{V} C_p T) = \nabla \cdot (K \nabla T) \quad (4.4)$$

The Homogenous model is improved by the Dispersion single phase model. Xuan² et al. [21] published a research based on the assumption that nanofluids properties are more similar to pure fluid rather than solid-fluid mixtures. This is due to a nano size particles can be perfectly diluted on the base fluid and behaves as a single phase fluid. In their findings the random chaotic movement of nanoparticles, which is understood to be the Brownian motion of particles, will increase the energy exchange rate in the fluid. That is the thermal dispersion effect will be significant in the fluid flow. This effect will augment the heat transfer between the nanofluid and the wall of the container. Koblinski et al. [2] studies on mechanisms of heat flow in suspension of nanoparticles, propose and explain a Brownian motion is significantly accountable for in increasing the thermal conductivity of the nanofluid and backs the thermal dispersion phenomenon proposed by Xuan et al. [21]. Mojarrad et al. [85] state that the thermal dispersion property is highly dependent of the flow pattern, nanoparticle shape, size and their volume concentration suspended in the base fluid. They have suggested a new thermal conductivity correlation due to the thermal dispersion effect. The radial dispersed thermal conductivity is given as,

$$K_d = C(\rho C_p)_{nf} \frac{R\varphi}{d_p} \left(\frac{\partial T}{\partial r} \right) \quad (4.5)$$

The dispersed single phase model has an identical continuity and momentum equation with the homogenous single phase model. But on the energy equation, the conductivity will be substituted with a new effective parameter that considers the effect of Brownian motion of nanoparticles on the thermal dispersion.

$$K_{eff} = K_{nf} + K_d \quad (4.6)$$

The improved thermal energy equation can be written for a single phase dispersion model as,

$$\nabla \cdot (\rho \vec{V} C_p T) = \nabla \cdot (K \nabla T) \quad (4.7)$$

Two phase models also proposed in literature to accurately compute the heat transfer between nanoparticles and base fluids. In this approach the effect of base fluid and nanoparticles on each other is also studied and accounted in to the model [85]. The basic two approaches suggested for modeling two phase flow are the Eulerian-Lagrangian for low volume fraction of nanofluids and Eulerian Eulerian (mixture) approach for relatively higher volume fraction. In the Eulerian-Lagrangian model a Newton's third law of motion is comprised to couple the Navier-Stokes equation with the solid phase of the nanofluids. In the Eulerian Eulerian (Mixture) model approach, it is possible that the two phases to have different velocity and allows the phase to be interpenetrating.

4.3.1 Governing Equation

In this study the governing equation is written based on the homogenous single phase model of nanoparticle suspensions in water base fluid. All major effective thermo-physical properties are statistically estimated from experiments found on the literature and a classical

fluid transport equation to solve the heat transfer problem. In the numerical computation, FloEFD V13.0 uses a Navier-Stokes equation for a forced convective laminar flow of nanofluids.

$$\frac{\partial \rho}{\partial t} + \frac{\partial(\rho u_i)}{\partial x_i} = 0 \quad (4.8)$$

$$\frac{\partial(\rho u_i)}{\partial t} + \frac{\partial(\rho u_i u_j)}{\partial x_i} + \frac{\partial p}{\partial x_i} = \frac{\partial}{\partial x_i} (\tau_{ij} + \tau_{ij}^R) + s_i \quad (4.9)$$

$$\frac{\partial(\rho H)}{\partial t} + \frac{\partial(\rho u_i H)}{\partial x_i} = \frac{\partial}{\partial x_i} (u_j (\tau_{ij} + \tau_{ij}^R) + q_i) + \frac{\partial p}{\partial t} - \tau_{ij}^R \frac{\partial u_i}{\partial x_j} + \rho \varepsilon + s_i u_i + Q_H \quad (4.10)$$

where; $H = h + \frac{u^2}{2}$

4.3.2 Effective Nanofluid Viscosity Model

The effective dynamic viscosity of a nanofluid is studied and new correlation provided on chapter three. The new developed correlation for Al₂O₃, CuO, and TiO₂ nanoparticles suspended in water is used to estimate the effective values. For nanoparticles suspended in water base fluid, the effective dynamic viscosity is modeled using the equations summarized on Table 4.3 below.

Table 4.3 New effective dynamic viscosity models of nanofluids

Nanofluid	Developed Correlation
Al ₂ O ₃ - Water	$\mu_{nf} = \frac{(\mu_{bf})}{(5\varphi^2 - 8.22\varphi + 1)}$
CuO - Water	$\mu_{nf} = \frac{(\mu_{bf})}{(-26.20\varphi^2 - 8.03\varphi + 1)}$
TiO ₂ - Water	$\mu_{nf} = \frac{(\mu_{bf})}{(112.98\varphi^2 - 14.33\varphi + 1)}$

4.3.3 Effective Nanofluid Thermal Conductivity Model

Currently available theoretical models in the literature for nanofluids are not accurate in predicting the right property of the thermal conductivity. Those theoretical models ignore the nano scale level heat transfer mechanism and only reliable for micro and millimeter sized particle mixture. In this study, experimental data on nanoparticles are collected from literature and the thermal conductivity property is derived statistically from collected data.

Table 4.4 New effective thermal conductivity models of nanofluids

Nanofluid	Developed Correlation
Al ₂ O ₃ - Water	$K_{nf} = \frac{(K_{bf})}{(14.28\varphi^2 - 4.46\varphi + 1)}$
CuO - Water	$K_{nf} = \frac{(K_{bf})}{(61.84\varphi^2 - 4.99\varphi + 1)}$
TiO ₂ - Water	$K_{nf} = K_{bf}(-1.852\varphi^2 + 2.51\varphi + 1)$

4.3.4 Effective Nanofluid Density Model

Effective density of a nanofluid is significantly dependent on the density of the base fluid and the nanoparticle used. It is also variable under different temperature but since the change in density of the oxide nanoparticles is insignificant, it is mainly driven by the change in density of the base fluid.

In this present work, density of nanofluids is estimated using the assumption of mass conservation during mixing of nanoparticle in to the base fluid. As concisely described on section 2.4, the effective viscosity of any solid-fluid mixture is theoretically given by equation (2.11)

4.3.5 Effective Specific Heat Capacity Model

One of the basic thermo-physical properties of a nanofluid is specific heat capacity. From the theoretical mixing theory models provided in the literature [15,22,90], the effective specific heat capacity can be modeled as a function of nanoparticle and base fluid specific heat capacity, nanoparticle and base fluid density, nanofluid mixture density and volume fraction of the nanoparticle. Harry et al. [86] reports a measurement of nanofluid specific heat capacity using heat-flux-type differential scanning calorimeter and results of specific heat were presented at 35°C, 45°C, and 55°C. They have reported that the experimental studies conducted are in a good agreement with the theoretical model for all type of nanofluid tested at each temperature.

In this study, a theoretical model for the heat capacity is used to estimate for nanofluids used in the numerical computation. All the parameter shown in the formula will be substituted based on the type of nanofluid used in the simulation. The effective specific heat of any solid-fluid mixture is given by equation (2.12).

4.4 Boundary Conditions

The governing equation used in the numerical study should be satisfied by providing boundary conditions (initial conditions) to pledge the partial differential equation computation. A boundary condition is the basic requirement in the numerical study that the dependent variable or its derivatives must satisfy on the boundaries of a domain [81]. Most boundary conditions are grouped in to these four main types of boundary conditions, DBC, NBC, RBC, and MBC.

4.4.1 Inlet and Outlet Boundary Conditions

A laminar flow of nanofluids on the effect of heat transfer is studied in the present work. The inlet condition of the nanofluid in to the channel is taken to be hydro-dynamically fully

developed and thermally developing. For inlet condition a velocity is prescribed over the inlet boundary for a Reynolds number ranging from 500-2300. The inlet temperature of the nanofluid is fixed at 293°K (20°C).

The outlet boundary condition of the flow is prescribed as a pressure opening. A zero gauge pressure (Ambient pressure) is set to the outflowing fluid.

4.4.2 Thermal Load Condition

As per the brief discussion on the executive summary of this study regarding applicable areas, a constant load of 150 watt heat is imposed on the outside walls of the channel. The equivalent constant heat flux of the load has a value of 91419 W/m².

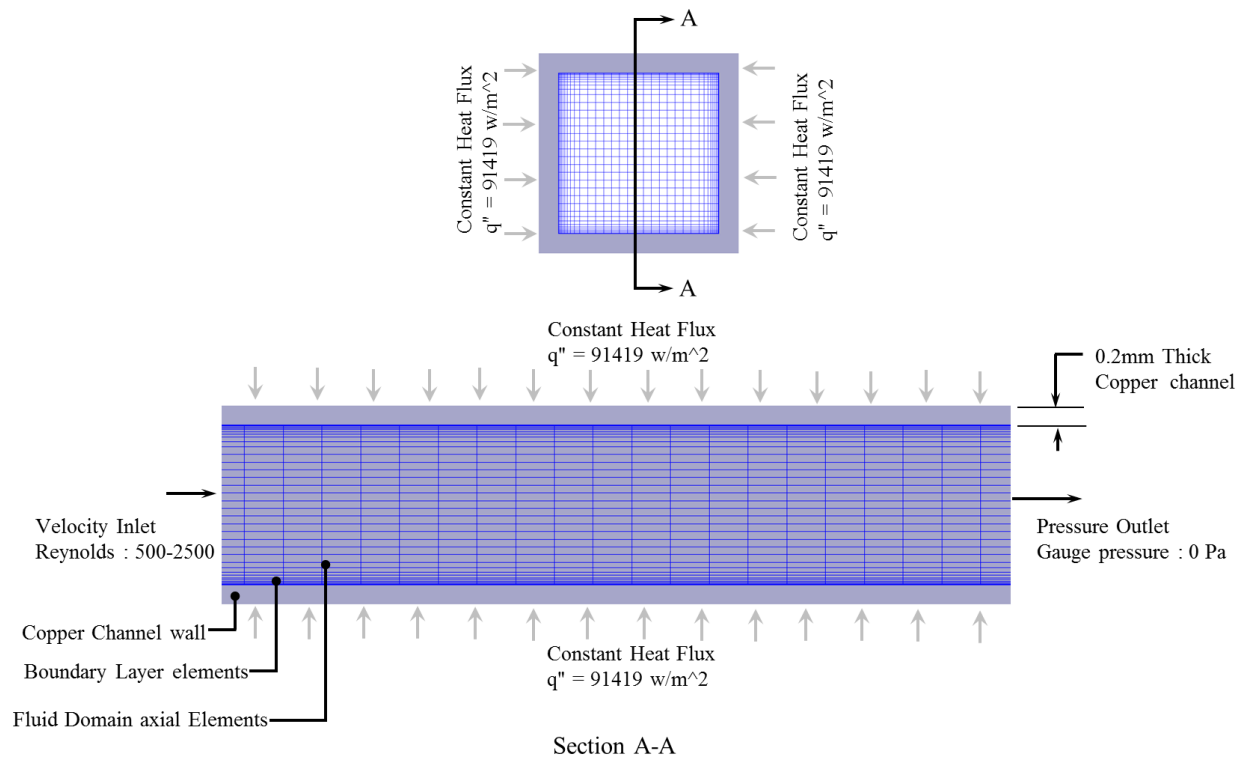


Figure 4.7 Geometrical configuration of 3D numerical analysis setup.

4.5 Computation Goals Convergence and Goals Criteria

Parametric goals are used to control the numerical simulation accuracy and computation time. By controlling the precision of these numerical goals using insignificantly small errors between consecutive iterations, an accurate numerical result can be achieved. The running simulation will terminate automatically once the progress of the goals is fully satisfied (converged) with a given criterion value. The parameters used as goal in this study are the outlet temperature of the nanofluid, the inlet-outlet mass flow rate and inlet-outlet velocity.

Table 4.5 Numerical analysis goal convergence criterion

Parameters	Converging Criterion value
Inlet mass flow rate	1E-05 Kg/s
Inlet velocity	0.001 m/s
Outlet mass flow rate	1E-05 kg/s
Outlet velocity	0.001 m/s
Outlet fluid temperature	0.01 °K

CHAPTER 5

NUMERICAL ANALYSIS RESULT

In this chapter, the numerical results from the simulation conducted published for each independent variable used, which are nanofluid types, concentration of nanoparticles and corresponding Reynolds number. The results are post processed from the numerical simulation output data and compared against the independent variables. The numerical simulation result mainly focus on the heat transfer parameter, Nusselt number (Nu), heat transfer coefficient and temperature profile. Those are the primarily heat transfer parameters used on the comparison plots. The surface heat transfer coefficient is measured on the solid-fluid boundary wall, which is directly reported by the numerical solver. The temperature profiles are captured from the flow cross section of the pipe at different sections.

The convective and the conductive heat transfer of the nanofluid are related using the Nusselt number. The local Nusselt number is calculated at different section of the pipe and integrated over the length of the channel in order to estimate for the equivalent Nusselt number of the heat transfer system. The local Nusselt number is calculated from the ratio of conductive thermal resistance to the convective thermal resistance, which the familiar formulation is given by:

$$Nu_x = \frac{h_x D_h}{K} \quad (5.1)$$

After estimating the local Nusselt value at each section of the pipe (11 evenly spaced points in this particular study) the average Nusselt number is approximated for an equivalent value in a single numerical study.

$$\overline{Nu} = \frac{1}{N} \sum_{x=1}^N Nu_x \quad (5.2)$$

Where ‘N’ is the number of sample points

Although the Nusselt number is estimated for each nanofluid investigated in this study, the objective is to propose a correlation that accurately models the heat transfer enhancement of a nanofluid under stated conditions.

5.1 Numerical Simulation Matrix

Combinations of independent variables are used to develop the matrix for the numerical simulation. Each nanofluid is analyzed at 5 different nanoparticle concentrations and 5 range of inlet fluid velocity in the laminar regime. The combination of the independent variables numerical simulation table is as below.

Table 5.1 Numerical analysis result matrix table

Nanofluid	Inlet Velocity [m/s]	Nanoparticle Concentration by volume, ϕ				
		1%	2%	3%	4%	5%
Al ₂ O ₃ - Water	0.19					
	0.38					
	0.57					
	0.76					
	0.95					
CuO - Water	0.19					
	0.38					
	0.57					
	0.76					
	0.95					
TiO ₂ - Water	0.19					
	0.38					
	0.57					
	0.76					
	0.95					

5.2 Numerical Results and Discussion

5.2.1 Numerical Results of Al₂O₃ Nanofluid

Result data from the numerical analysis are post processed after the calculated numbers are extracted from the simulation and exported to an excel sheet. Average results are collected at 11 equally spaced points along the length of the channel. Those average value of the fluid property of basic thermo-physical properties are tabulated as shown below.

Table 5.2 Numerical result for 1% concentration of Al₂O₃ nanofluids at Re=540

x [mm]	L [mm]	X/L	Hydraulic diameter [m]	ρ [kg/m ³]	μ_{bulk} [Pa.s]	HTC [w/m ²]	K [w/mk]	Pr	CFD Nu
2	200	0.01	1.651E-03	1023.7	0.00086327	6021.6	0.641	5.4	15.5
20	200	0.10	1.651E-03	1020.1	0.00074542	3228.8	0.655	4.7	8.1
40	200	0.20	1.651E-03	1016.1	0.00072455	2577.0	0.662	4.5	6.4
60	200	0.30	1.651E-03	1014.1	0.00069295	2231.3	0.667	4.4	5.5
80	200	0.40	1.651E-03	1010.4	0.00066165	1999.8	0.671	4.1	4.9
100	200	0.50	1.651E-03	1006.8	0.00061216	1827.2	0.677	3.8	4.5
120	200	0.60	1.651E-03	1003.7	0.00056247	1690.1	0.681	3.4	4.1
140	200	0.70	1.651E-03	999.9	0.00053152	1577.2	0.684	3.2	3.8
160	200	0.80	1.651E-03	996.7	0.00048794	1481.2	0.691	2.9	3.5
180	200	0.90	1.651E-03	993.4	0.00045565	1398.3	0.692	2.7	3.3
200	200	1.00	1.651E-03	989.7	0.00041470	1323.9	0.696	2.5	3.1
AVERAGE				1006.8	0.000614	2305.1	0.674	3.788	5.7

Table 5.3 Numerical result for 5% concentration of Al₂O₃ nanofluids at Re=645

x [mm]	L [mm]	X/L	Hydraulic diameter [m]	ρ [kg/m ³]	μ_{bulk} [Pa.s]	HTC [w/m ² k]	K [w/mk]	Pr	CFD Nu
2	200	0.010	1.651E-03	1143.7	0.0014084	8328.5	0.751	6.7	18.3
20	200	0.100	1.651E-03	1141.4	0.0012453	4492.0	0.762	5.9	9.7
40	200	0.200	1.651E-03	1139.2	0.0012116	3594.8	0.766	5.7	7.7
60	200	0.300	1.651E-03	1137.6	0.0011598	3136.4	0.772	5.5	6.7
80	200	0.400	1.651E-03	1135.8	0.0011409	2836.9	0.774	5.3	6.1
100	200	0.500	1.651E-03	1135.9	0.0011061	2617.1	0.780	5.2	5.5
120	200	0.600	1.651E-03	1134.3	0.001073	2444.1	0.781	5.1	5.2
140	200	0.700	1.651E-03	1132.2	0.0010325	2302.1	0.786	4.9	4.8
160	200	0.800	1.651E-03	1130.6	0.0009879	2181.9	0.789	4.7	4.6
180	200	0.900	1.651E-03	1129.4	0.000961	2078.0	0.794	4.5	4.3
200	200	1.000	1.651E-03	1128.6	0.0009366	2008.2	0.797	4.4	4.2
AVERAGE				1135.3	0.00111	3274.5	0.777	5.3	7.0

As it is mentioned on the numerical analysis matrix, the CFD set-up is tested at 5 different Reynolds numbers. Apart from the data tabulated on table 6-2, other runs at higher Reynolds number are plotted on the next page. Below as shown on Figure 5.1 a graph is plotted for the heat transfer coefficient variation along the length of the tube. The boundary condition setup for different nanoparticle concentration is done based on equal inlet velocity. It is demonstrated that the addition of nanoparticle affects the viscosity of the nanofluid. Even though the inlet velocity

is kept similar for different nanoparticle concentration analysis, the Reynolds numbers tends to drop for higher nanoparticle loading due to viscous effect.

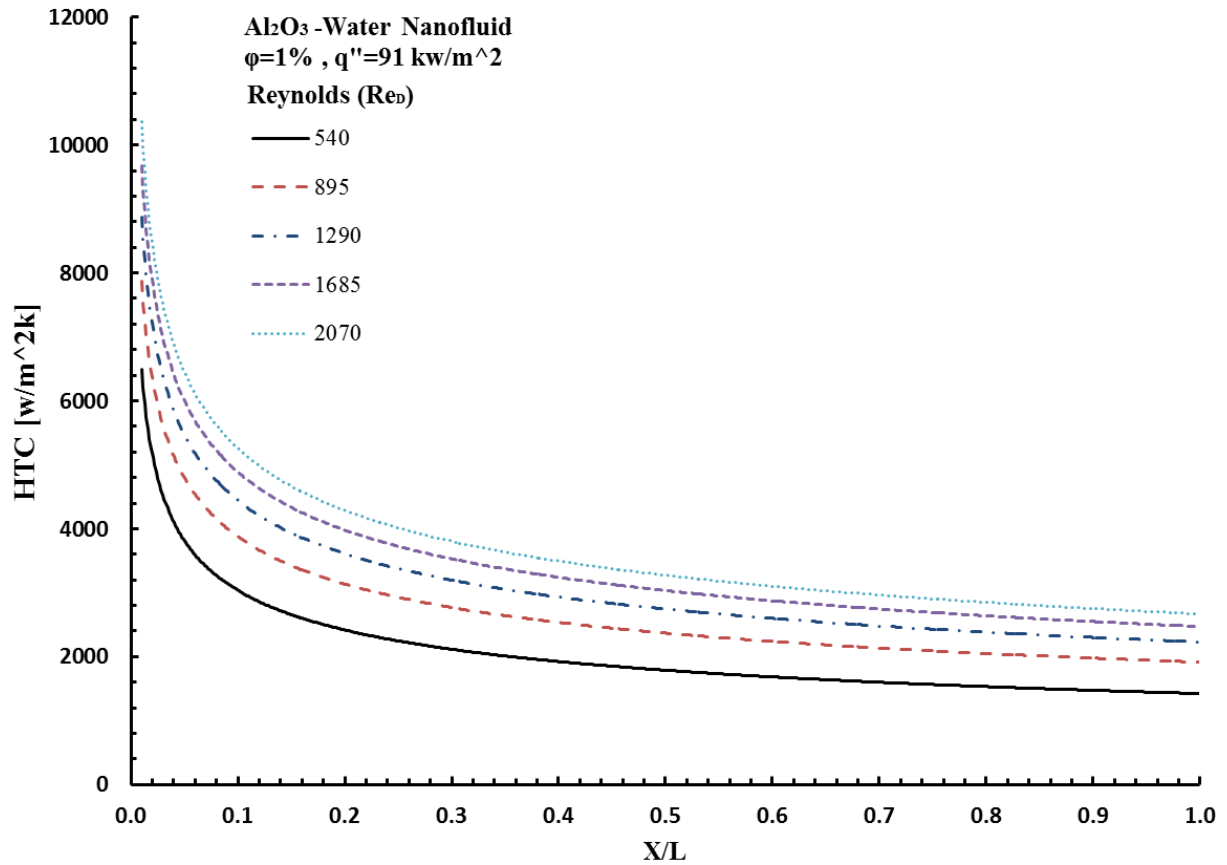


Figure 5.1 Heat transfer variation along the channel length at 1% concentration of Al₂O₃.

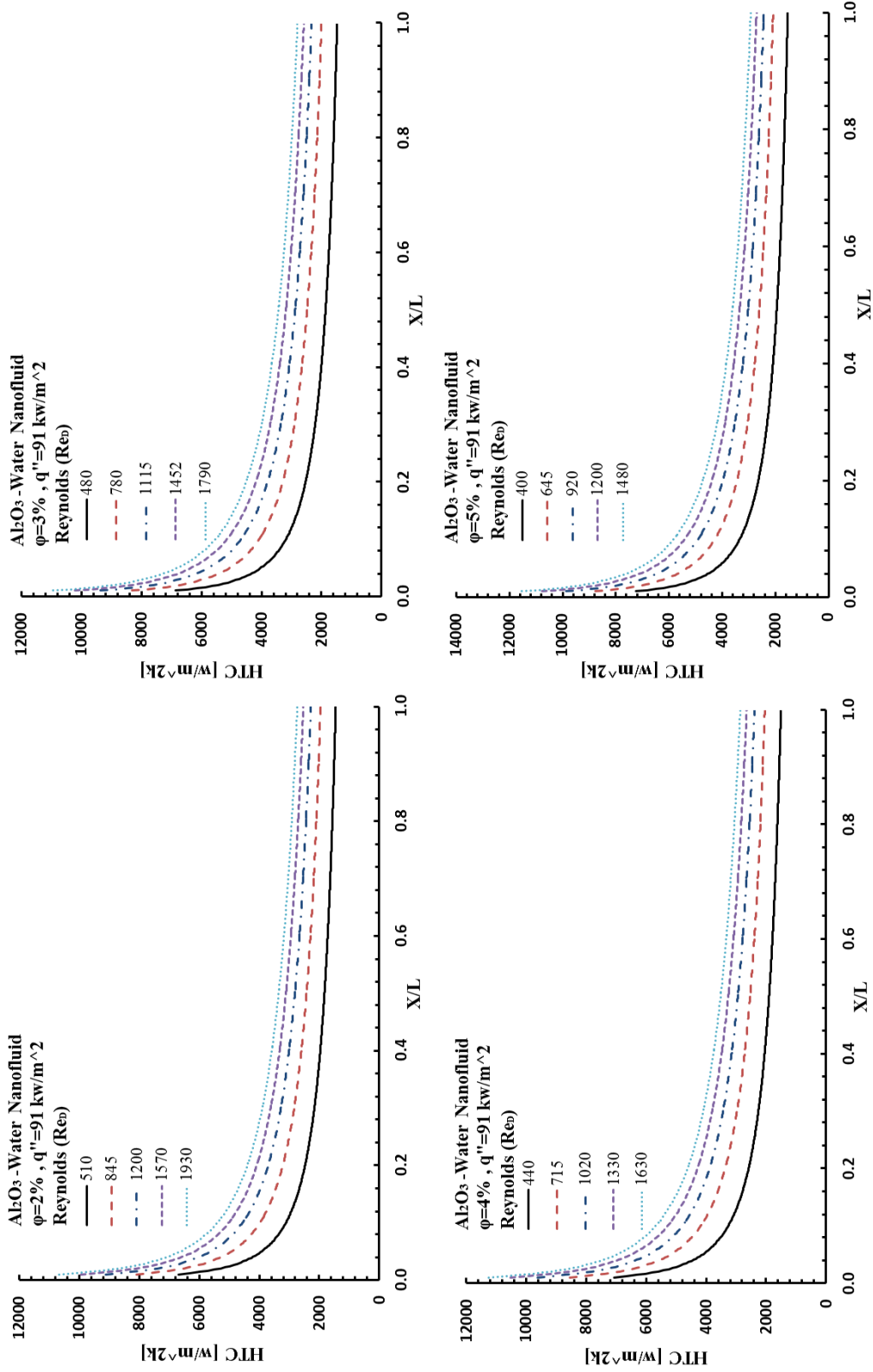


Figure 5.2 Heat transfer variation along the channel length for different concentration of Al₂O₃

Reynolds number reduced at constant inlet velocity when comparing 1% to 5% volumetric fraction of alumina nanoparticle, due to the viscosity augmentation along with the increment of nanoparticle concentration. At 1% by volume concentration of alumina particle the viscosity of the nanofluid is increased approximately twice in average when compared to the base fluid water.

Due to the flow regime of the numerical experiment conducted and the trend observed on the results collected from the finite element analysis, the heat transfer properties can be extrapolated to some extent. With the assumption of a laminar flow condition, heat transfer effect is estimated up to Reynolds of 2500.

5.2.1.1 Heat Transfer Enhancement of Al₂O₃ Nanofluid

Intensification of a heat transfer coefficient is a desirable property of nanofluids. Based on the numerical research conducted on comparing the thermal performance of nanofluid with different nanoparticle volume concentration and with pure water using the new correlation developed for the viscosity and conductivity, a significant enhancement is observed. The comparison of the average heat transfer coefficient developing along the length of the channel with different Reynolds (inlet velocity) for different amount of loading particle is plotted on Figure 5.3. As seen on the numerical result plot below increasing the amount of nanoparticle concentration will clearly enhance the heat transfer. As discussed on chapter four, however, increment of nanoparticle concentration beyond 5% by volume will drastically change the fluid viscous properties which considerably affect the thermal management of a system.

The thermal performance observed for Al₂O₃ nanoparticles dispersed in pure water for a volume fraction of 1% by volume shows a 4.97% HTC enhancement on average when

compared to the base fluid. Accordingly, the average HTC enhancement for a nanoparticle volumetric concentration of 2%, 3%, 4% and 5% is estimated to be 10.5%, 16.6%, 23.4% and 31.2% respectively.

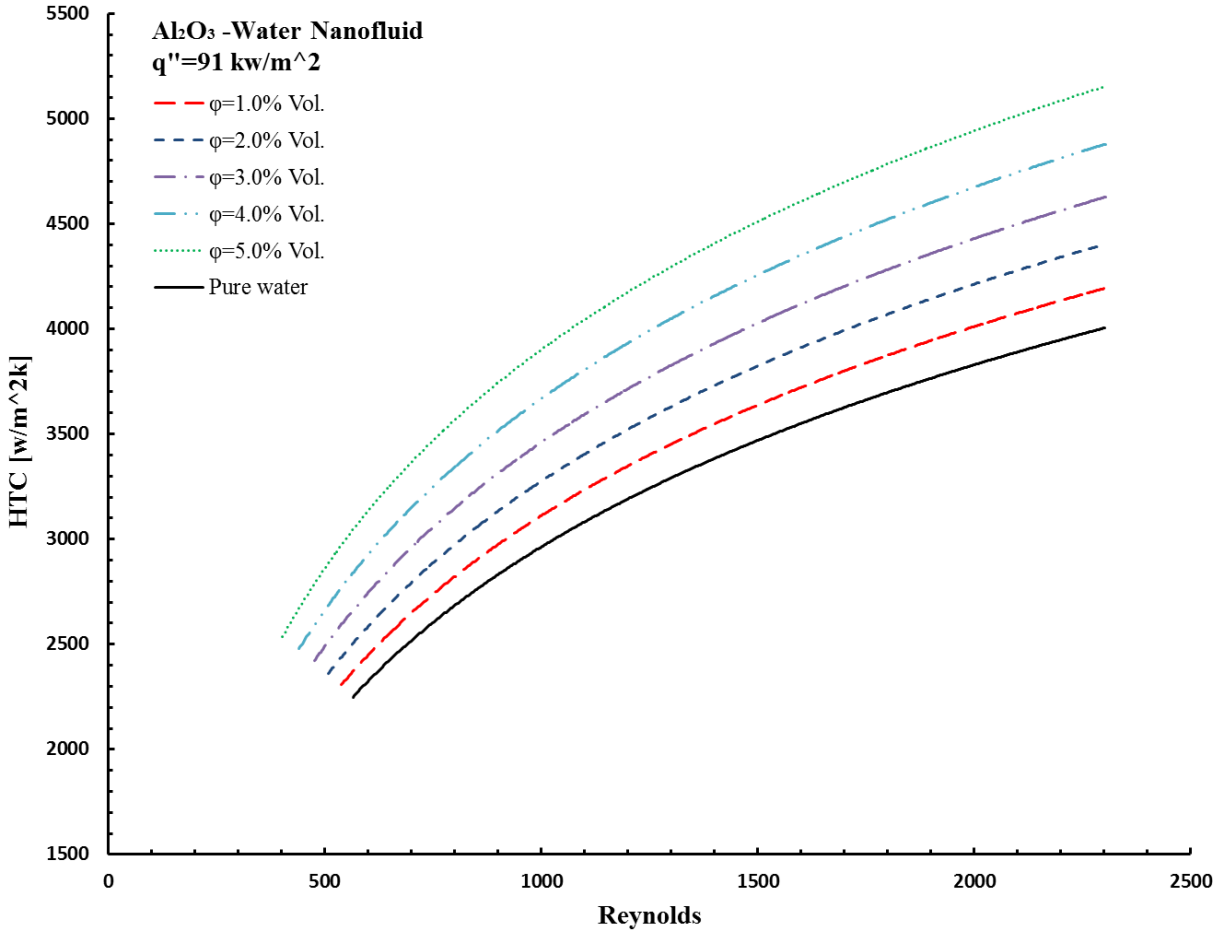


Figure 5.3 Heat transfer coefficient of Al₂O₃ nanofluid at different volume fraction and Reynolds number.

As show on Figure 5.3, for a laminar regime of a nanofluid flow, the slop of the HTC line drops as the Reynolds value increases. Comparing the thermal performance of the nanofluid for a given nanoparticle concentration with the base fluid water, the HTC enhancement decreases slightly as the Reynolds number increases. For example, the HTC enhancement of a 2% by volume

concentration of Al₂O₃ nanofluid at Re 2500 is 14.5% lower than the HTC enhancement at Re 500.

5.2.2 Numerical Result of CuO Nanofluid

A steady state convective heat transfer study of the CuO nanofluid flow in a copper channel is conducted for a nanoparticle volume fraction ranging from 1% to 5%. For the ease of comparison, all the boundary conditions are kept identical to the alumina and titania nanofluids numerical study. Data points are collected from the numerical analysis in the same fashion as described in section 5.2.1.

Table 5.4 Numerical result for 1% concentration of CuO nanofluids at Re=525

x [mm]	L [mm]	X/L	Hydraulic diameter [m]	ρ [kg/m ³]	μ_{bulk} [Pa.s]	HTC [w/m ² k]	K [w/mk]	Pr	CFD Nu
2	200	0.010	1.651E-03	1102.2	0.0009518	6156.1105	0.663	5.4	15.3
20	200	0.100	1.651E-03	1098.7	0.0008282	3295.0550	0.678	4.6	8.0
40	200	0.200	1.651E-03	1094.8	0.0008042	2628.5335	0.682	4.5	6.4
60	200	0.300	1.651E-03	1093.3	0.0007584	2274.7236	0.690	4.2	5.4
80	200	0.400	1.651E-03	1089.3	0.0007324	2037.6117	0.694	4.1	4.8
100	200	0.500	1.651E-03	1086.3	0.0006779	1860.5314	0.700	3.8	4.4
120	200	0.600	1.651E-03	1083.5	0.00063	1720.1435	0.705	3.5	4.0
140	200	0.700	1.651E-03	1080.5	0.0005809	1604.2034	0.707	3.2	3.7
160	200	0.800	1.651E-03	1076.5	0.0005382	1505.8771	0.712	2.9	3.5
180	200	0.900	1.651E-03	1072.5	0.0004928	1420.6786	0.718	2.7	3.3
200	200	1.000	1.651E-03	1070.0	0.0004644	1344.6678	0.720	2.4	3.1
AVERAGE				1086.1	0.00068	2349.8	0.697	3.747	5.6

Table 5.5 Numerical result for 5% concentration of CuO nanofluids at Re=645

x [mm]	L [mm]	X/L	Hydraulic diameter [m]	ρ [kg/m ³]	μ_{bulk} [Pa.s]	HTC [w/m ² k]	K [w/mk]	Pr	CFD Nu
2	200	0.010	1.651E-03	1265.4	0.0015645	7789.8	0.675	7.6	19.1
20	200	0.100	1.651E-03	1263.2	0.0013968	4218.3	0.685	6.7	10.2
40	200	0.200	1.651E-03	1260.8	0.0012945	3380.1	0.692	6.1	8.1
60	200	0.300	1.651E-03	1259.2	0.0012842	2951.3	0.696	6.1	7.0
80	200	0.400	1.651E-03	1257.3	0.0012537	2671.6	0.697	6.0	6.3
100	200	0.500	1.651E-03	1256.7	0.001197	2466.7	0.701	5.8	5.8
120	200	0.600	1.651E-03	1255.3	0.0011808	2305.8	0.705	5.6	5.4
140	200	0.700	1.651E-03	1254.2	0.0011444	2174.1	0.707	5.5	5.1
160	200	0.800	1.651E-03	1251.9	0.0011198	2062.6	0.710	5.4	4.8
180	200	0.900	1.651E-03	1250.9	0.0010947	1966.3	0.713	5.2	4.6
200	200	1.000	1.651E-03	1249.8	0.001054	1900.8	0.715	5.0	4.4
AVERAGE				1256.8	0.00123	3080.7	0.700	5.9	7.3

Fluid and heat transfer parameters that are estimated from the numerical analysis and statistical modeling are tabulated on Table 5.4 and Table 5.5.

A heat transfer coefficient distribution of a CuO nanofluid along the length of the channel is plotted for a different Reynold number in a laminar flow region as shown on Figure 5.4 and Figure 5.5. A higher heat transfer coefficient is observed at the entry of the channel due to the thermally developing model at the inlet, which is the difference between the wall temperature of the channel and bulk temperature of the nanofluid is higher Muzychka et al. [87]. And once the

thermal boundary becomes fully developed along the length of the channel, the HTC and Nusselt will converge to a constant value.

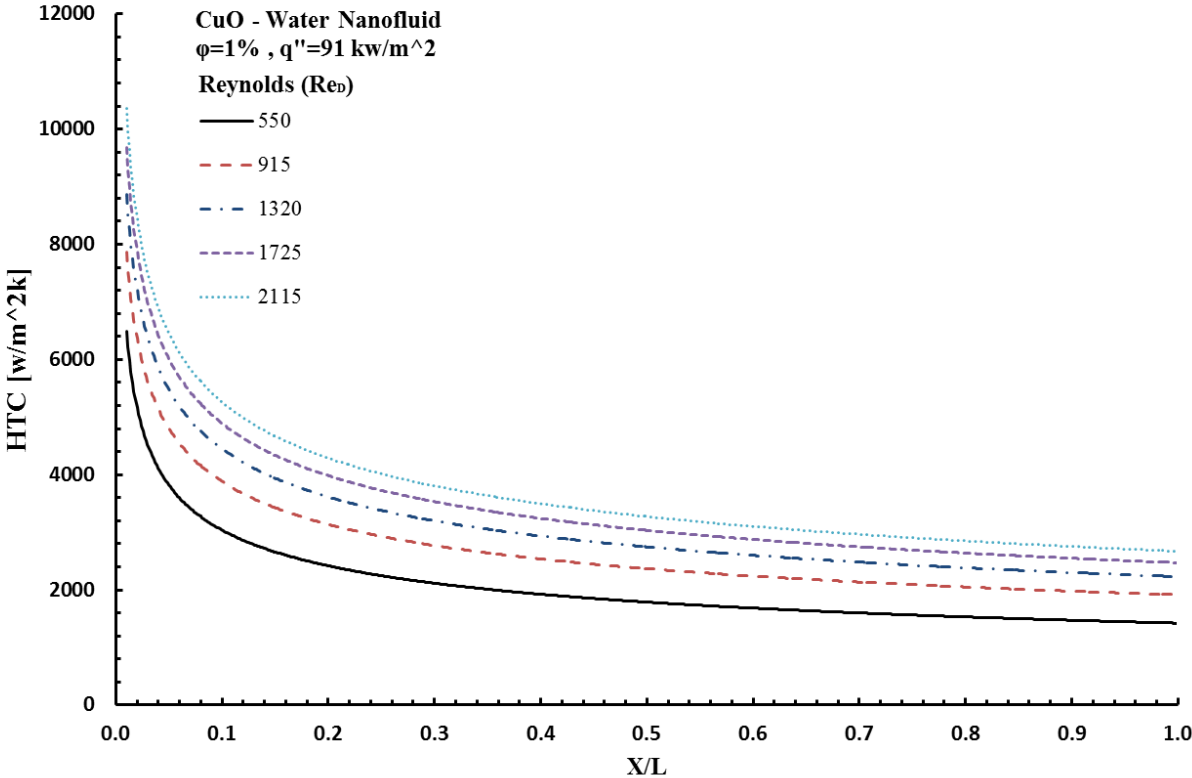


Figure 5.4 Heat transfer variation along the channel length at 1% concentration of CuO.

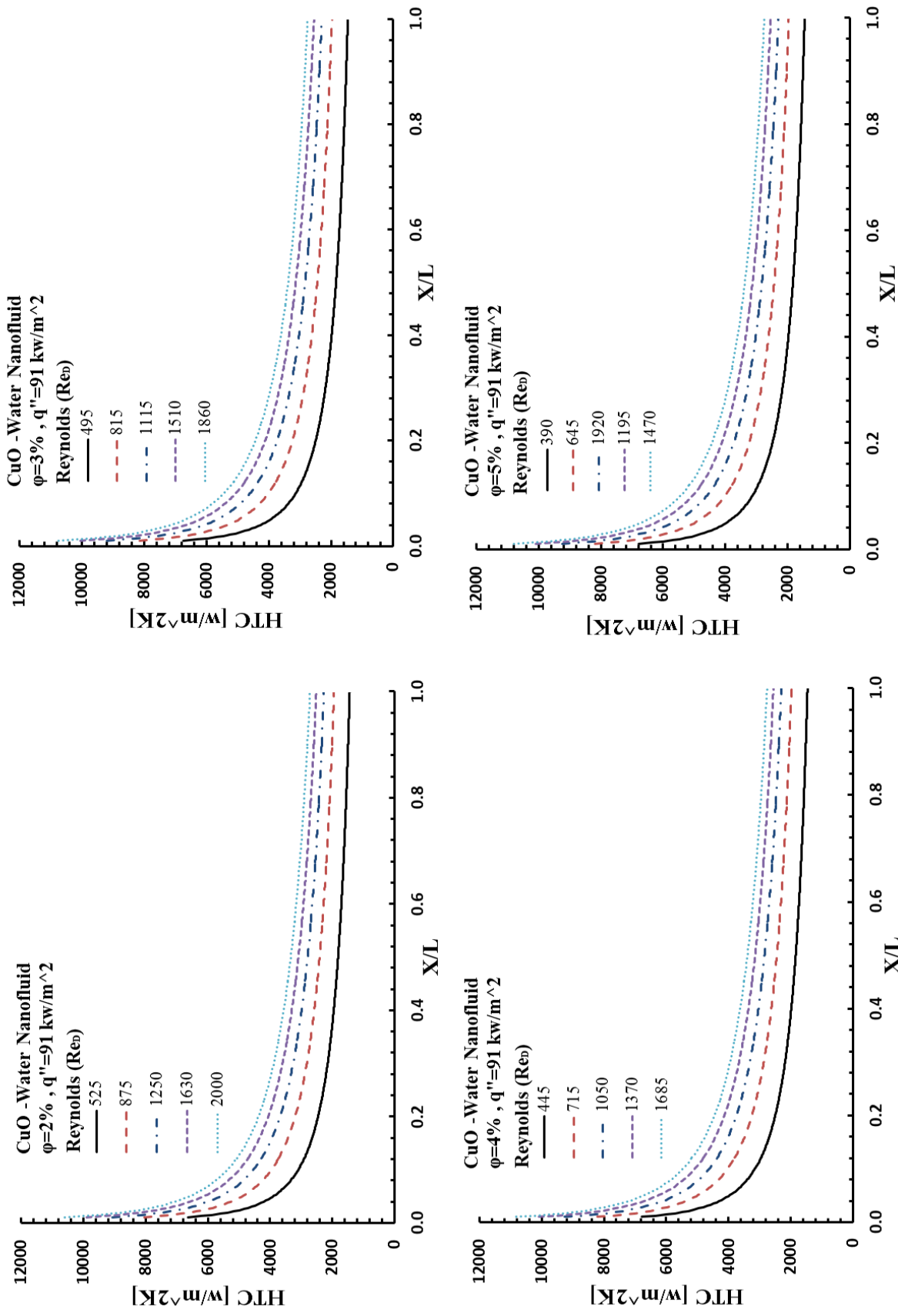


Figure 5.5 Heat transfer variation along the channel length for different concentration of CuO

5.2.2.1 Heat Transfer Enhancement of CuO Nanofluid

As per the brief discussion on heat transfer enhancement of alumina nanofluids on section 5.2.1.1, HTC is can be also intensified significantly by dispersing CuO nanoparticles in to the base fluid water. The result collected from the numerical simulation of CuO nanofluid cooling at a 150 watt heat load with a constant heat flux over a copper channel is shown on Figure 5.4 and Figure 5.5. The CuO nanofluid numerical analysis is prepared and conducted for different volumetric concentration of particles ranging from 1-5%.

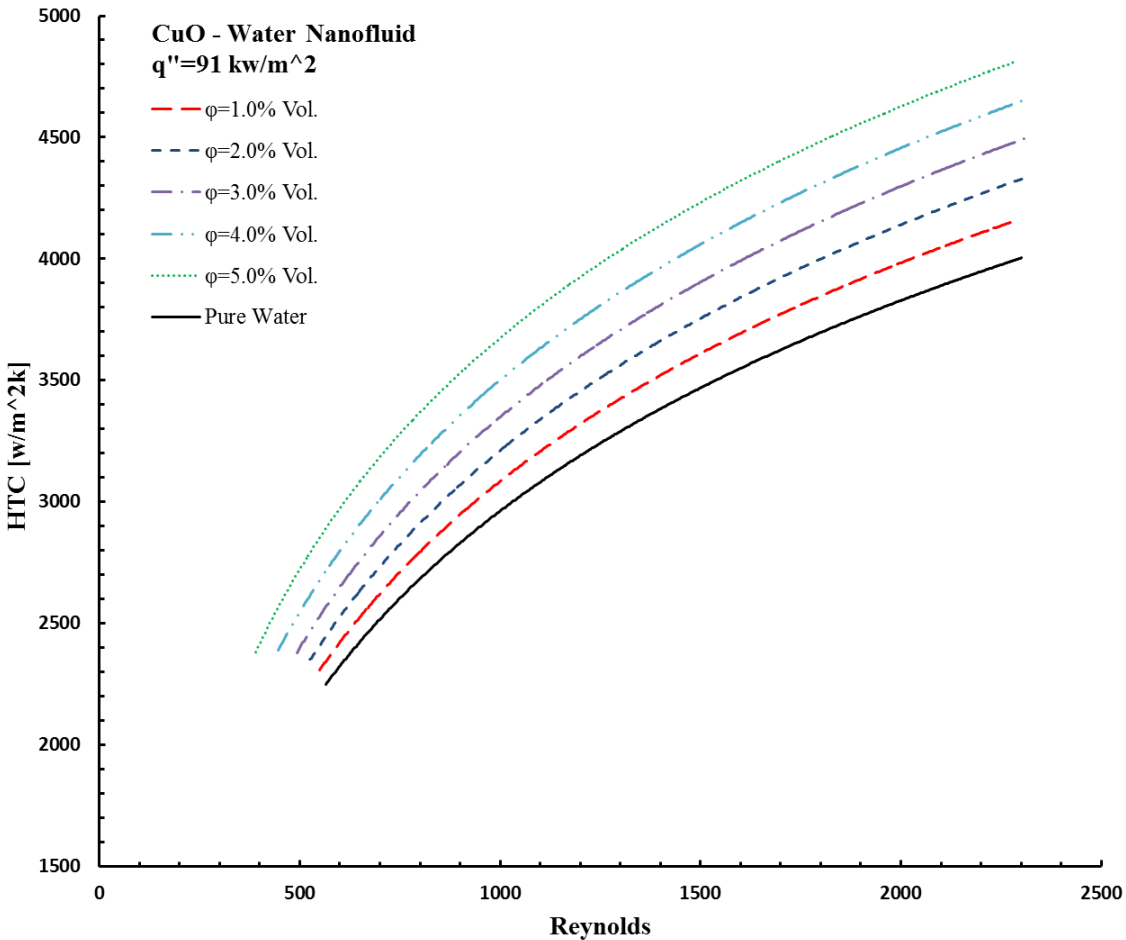


Figure 5.6 Heat transfer coefficient of CuO nanofluid at different volume fraction and Reynold number.

The inlet boundary condition is based on the fluid velocity varies from 0.19 -0.96 m/s. HTC result for higher Reynold number is approximated from the collected data points in the laminar region. Despite a similar inlet boundary condition is kept for each different particle concentration of CuO nanofluid, the Reynolds number drops significantly as the nanoparticle loading amount increases.

The heat transfer enhancement observed for CuO nanofluid is shown on Figure 5.6, in comparison with the base fluid. On average, the heat transfer enhancement of the CuO nanofluid at 1% by volume nanoparticle concentration shows 4.1% increment of HTC when compared to the base fluid. It is clearly observed that the enhancement will escalate linearly as the concentration of the dispersed CuO nanoparticles increases. From the simulation result, the thermal performance observed from a volumetric concentration of 2%, 3%, 4% and 5% CuO nanofluid is predicted to have an HTC increment by 8.4%, 12.9%, 17.8% and 23.4% respectively. On the entrance region of the channel, the heat transfer enhancement is significantly higher than the one at the outlet of the channel due to the developing thermal boundary layer, and this phenomenon is averaged along the length of the channel. The reported averaged percentages of HTC enhancement represents for the overall fluid domain of the system.

5.2.3 Numerical Result of TiO₂ Nanofluid

The heat transfer performance of titania nanoparticles suspended in the base fluid of water studied in the this paper under a convective heat transfer in a laminar flow regime. All the basic process in the numerical analysis setup for alumina and copper oxide nanofluids is also repeated for titania nanofluid. In the post analysis data points of fluid properties are exported to excel sheet for further statistical study. As it is shown on the table below, the thermo physical

properties and parameter results are averaged and tabulated. The tabulated results are collected at 11 equal distant points along the channel length and labeled as 'X' in millimeter.

Table 5.6 Numerical result for 1% concentration of TiO₂ nanofluids at Re=510

x [mm]	L [mm]	X/L	Hydraulic diameter [m]	ρ [kg/m³]	μ_{bulk} [Pa.s]	HTC [w/m²k]	K [w/mk]	Pr	CFD Nu
2	200	0.010	1.651E-03	1026.5	0.0009119	5960.2	0.629	5.9	15.7
20	200	0.100	1.651E-03	1022.4	0.0007874	3192.0	0.643	5.1	8.2
40	200	0.200	1.651E-03	1018.7	0.0007658	2548.2	0.650	4.9	6.5
60	200	0.300	1.651E-03	1016.1	0.0007328	2206.6	0.655	4.7	5.6
80	200	0.400	1.651E-03	1013.0	0.0007002	1978.2	0.658	4.4	5.0
100	200	0.500	1.651E-03	1009.3	0.0006483	1807.9	0.663	4.1	4.5
120	200	0.600	1.651E-03	1006.2	0.0006028	1672.7	0.667	3.7	4.1
140	200	0.700	1.651E-03	1002.4	0.000565	1561.3	0.670	3.4	3.8
160	200	0.800	1.651E-03	999.2	0.0005179	1466.8	0.676	3.2	3.6
180	200	0.900	1.651E-03	995.9	0.0004746	1384.9	0.679	2.9	3.4
200	200	1.000	1.651E-03	992.1	0.000447	1311.2	0.682	2.7	3.2
AVERAGE				1009.3	0.00065	2280.9	0.661	4.081	5.8

Table 5.7 Numerical result for 5% concentration of TiO₂ nanofluids at Re=625

x [mm]	L [mm]	X/L	Hydraulic diameter [m]	ρ [kg/m ³]	μ_{bulk} [Pa.s]	h [w/m ² k]	K [w/mk]	Pr	CFD Nu
2	200	0.010	1.651E-03	1156.9	0.0014732	7848.8	0.684	7.6	18.9
20	200	0.100	1.651E-03	1154.7	0.0013148	4245.4	0.696	6.7	10.1
40	200	0.200	1.651E-03	1152.6	0.0012185	3400.9	0.701	6.3	8.0
60	200	0.300	1.651E-03	1151.1	0.0012115	2968.8	0.706	6.2	6.9
80	200	0.400	1.651E-03	1148.9	0.0011792	2687.1	0.707	6.0	6.3
100	200	0.500	1.651E-03	1148.2	0.0011255	2480.5	0.711	5.8	5.8
120	200	0.600	1.651E-03	1147.3	0.0011099	2318.2	0.713	5.7	5.4
140	200	0.700	1.651E-03	1145.1	0.0010751	2185.3	0.717	5.6	5.0
160	200	0.800	1.651E-03	1143.5	0.0010514	2072.9	0.720	5.4	4.8
180	200	0.900	1.651E-03	1141.7	0.0010271	1975.7	0.723	5.2	4.5
200	200	1.000	1.651E-03	1140.7	0.0009896	1909.2	0.726	5.0	4.3
AVERAGE				1148.3	0.00116	3099.3	0.709	5.9	7.3

The heat transfer coefficient distribution result is compared along the length of the channel as shown on Figure 5.7 below. Due to the boundary layer effect at the Inlet, a higher HTC value is observed when compared to other location of the channel. As it is shown on graph for 1% by volume concentration of TiO₂ dispersed in the base fluid, a higher heat transfer coefficient is observed as the Reynold number increases. However, as it is seen on the plot below, the gap between different Reynold points at a single location starts to close down as the Reynolds number increases. This demonstrates that HTC enhancement has a negative slop as the Reynold increases.

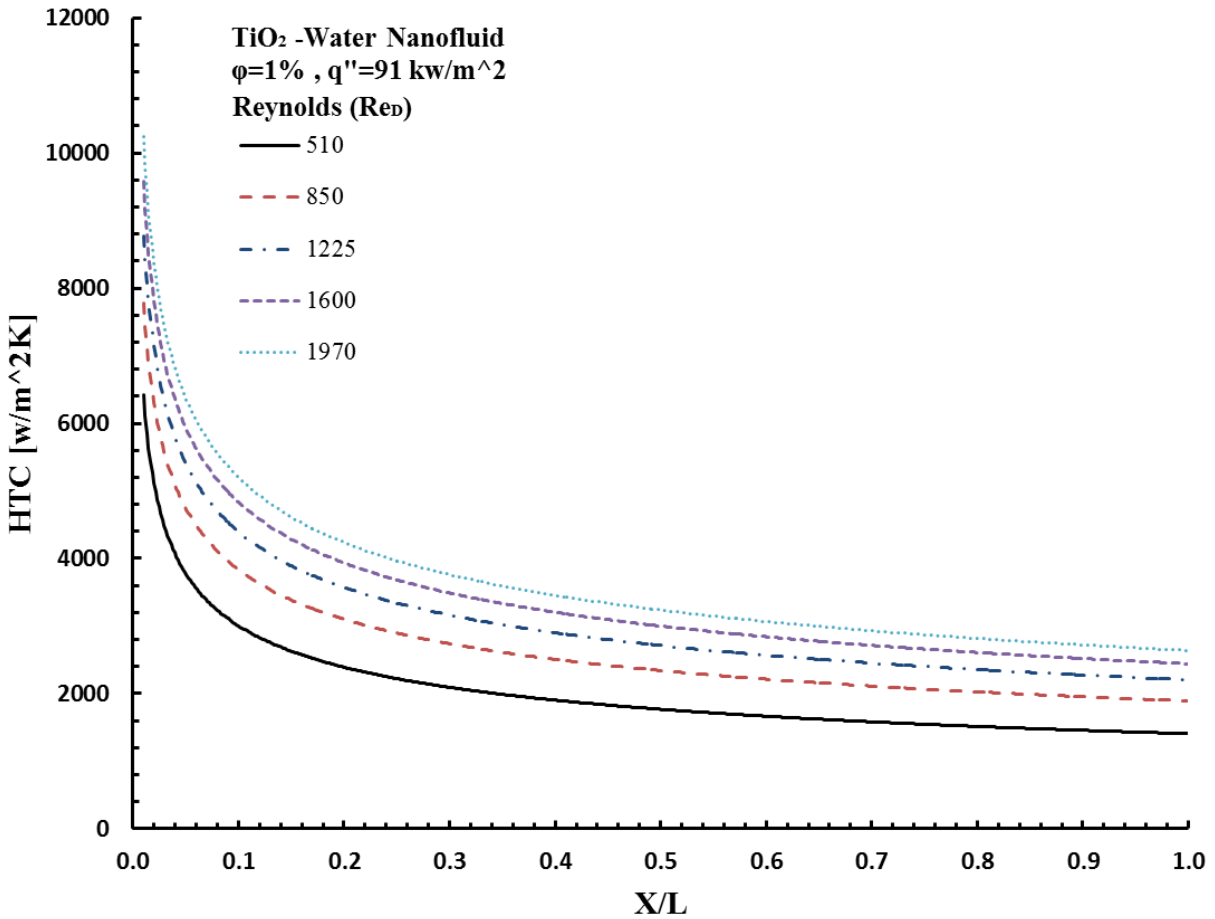


Figure 5.7 Heat transfer variation along the channel length at 1% concentration of TiO₂.

The numerical study output result is only presented for 1% by volume concentration of TiO₂ in water base fluid in this section. As it is discussed previously, the study also considers different amount of concentration of particles in estimating the heat transfer enhancement.

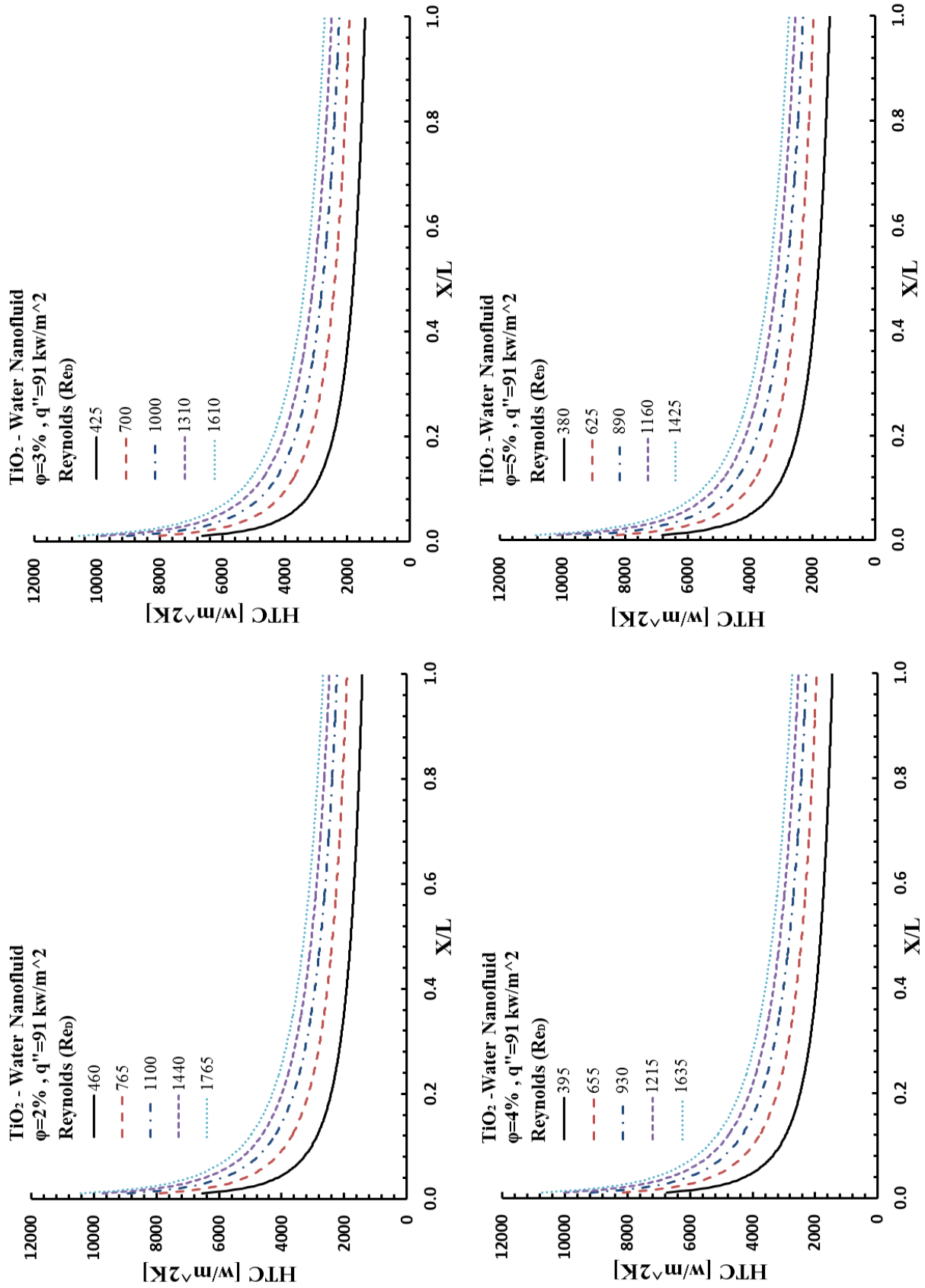


Figure 5.8 Heat transfer variation along the channel length for different concentration of TiO₂.

5.2.3.1 Heat Transfer Enhancement of TiO₂ Nanofluid

The heat transfer performance of titanium dioxide nanofluid on a constant heat flux thermal load is analyzed numerically and results are plotted as shown below. The performance of TiO₂ nanoparticles dispersed in the base fluid on heat transfer enhancement studied for particle loading range from 1-5% by volume. All the results regarding the TiO₂ nanofluid thermal properties and estimated fluidic parameters are published on the appendix chapter.

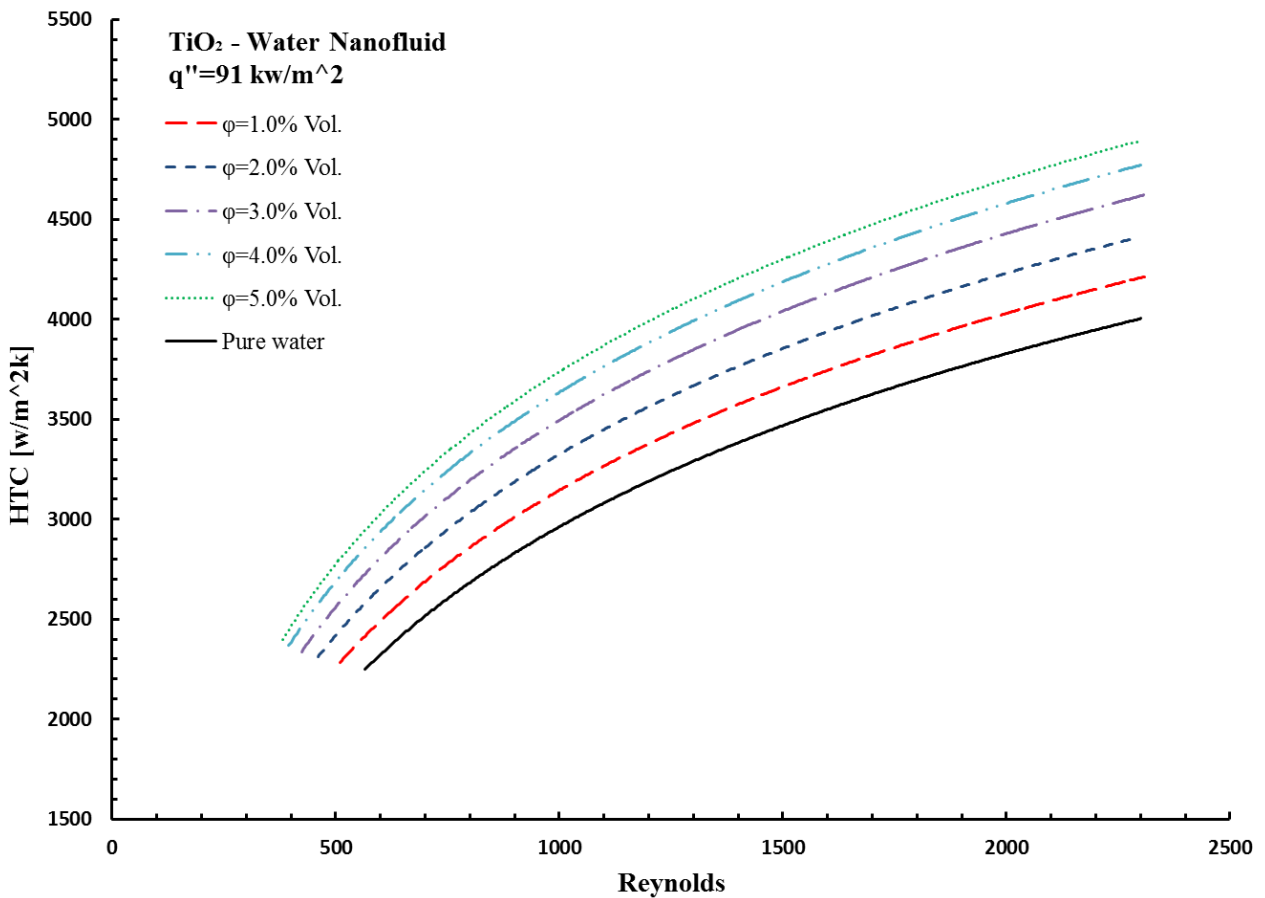


Figure 5.9 Heat transfer coefficient of TiO₂ nanofluid at different volume fraction and Reynold number.

Addition of TiO₂ nanoparticles in to the base fluid to a certain limit enhances the thermal performance of the system. In this study, a concentration up to 5% by volume is analyzed for its heat transfer enhancement by comparing the HTC value against the base fluid. The heat transfer

coefficient enhancement is estimated on average for a laminar flow regime. At a 1% by volume concentration of TiO₂ nanoparticles, a 6% of HTC enhancement is observed from the numerical study conducted. In the same way for other volume fraction of nanoparticles the enhancement significantly rises with increasing concentration of TiO₂ nanoparticles. For a volumetric concentration of 2%, 3%, 4% and 5% of nanoparticles dispersion demonstrates a HTC enhancement of 11.9%, 17.5%, 22.1% and 25.5% respectively when compared to the base fluid. The results of HTC enhancement reported here represent for the whole fluid domain of the channel (from inlet to outlet boundary) and for all ranges of Reynold number in the laminar regime.

5.2.4 Heat Transfer Enhancement Summary

According to the numerical study conducted in this paper, the additions of nanoparticles in to a base fluid will significantly enhance the heat transfer coefficient up to 32% in the laminar flow regime. The altered thermo physical properties of the nanofluid greatly affect the heat transfer intensification process. However, thermal conductivity of the fluid mixture enhancement is directly proportional to the HTC intensification and plays the major role in the procedure. It is challenging to realize how the thermal conductivity enhancement is achieved in nanofluid only by observing the numerical experiment using a single phase homogenous mathematical model since this model treats the solid-liquid composite material as a single phase and it uses an effective conductivity and other thermo physical properties to the solve the Navier-Stokes equation. Nevertheless, published literature from scientists and engineers throw strong arguments and hypothesis in the mechanics of heat transfer improvement. Although a complete theoretical and quantitative explanations are provided in the literature since 19th century studies on fluid effective medium theory, those theories do not provide or model the exact properties of this

composite fluid due to the lack of accounting the atomic scale behavior possessed by the nanofluids. Improved concepts are introduced to model the properties of a nanofluid fluid under different circumstances in advanced manure. Those models are based on the various theories that explain the mechanics of heat transfer at a micro scale level. Major mechanisms of heat transfer or conductivity enhancement are thoroughly discussed section 2.3.

The enhancement of thermal performance of nanofluids in this report is summarized for each nanoparticle type as shown on Figure 5.10 below. The percentage of enhancements is estimated by comparing the numerical heat transfer coefficient result with the base fluid heat transfer capacity. The HTC enhancement in the laminar flow region has a decreasing trend despite the fact that the Reynolds value is increasing. However, the variation in HTC percentage enhancement is considerably small compared to the enhancement itself, and an average value is recommended across the flow regime. The percentage enhancement is given by

$$E = \left[\frac{(HTC_{bf} - HTC_{nf})}{HTC_{bf}} \right] \times 100\% \quad (5.3)$$

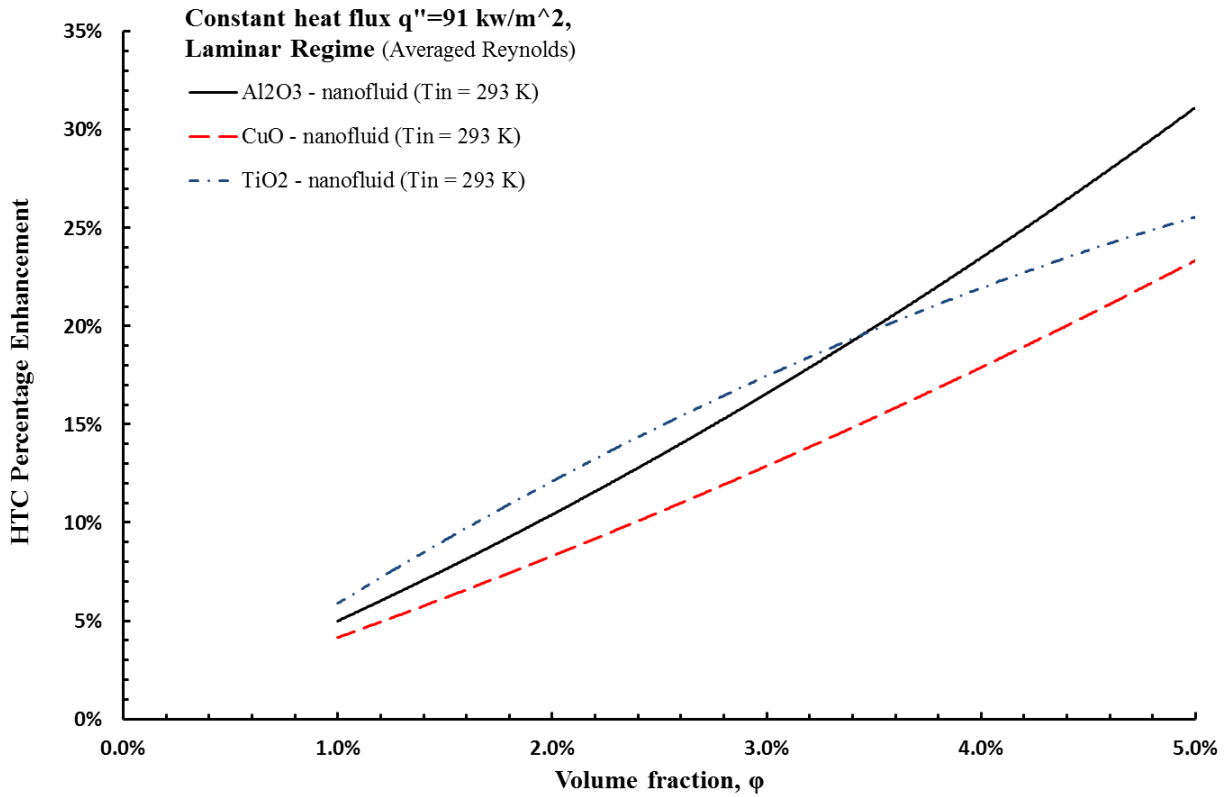


Figure 5.10 Heat transfer enhancement comparison per nanoparticle volume fraction.

Although it is challenging to compare and contrast the heat transfer enhancement between those nanofluids based on collected data, statistical model and numerical simulation, due to nuisances factors introduced in every process, the overall result of the HTC enhancement shows an increasing trend line with a proportional relation with the volume fraction of nanoparticles. All nanofluid types considered in this study have similar slope on the graph shown above and yields a closer HTC results to each other in a laminar flow regime with 1-5% by volume concentration. It seems that at higher concentration of nanoparticle, the alumina nanofluid performs better than the rest of the nanofluids, but this result will weaken at low nanoparticle loading volume.

CHAPTER 6

HEAT TRANSFER ENHANCEMENT COMPARISON

The enhancement of heat transfer due to the dispersion of nanoparticle in the liquid is investigated in many literature. On chapter 5, this study reported the numerical result on the enhancement achieved by using Al_2O_3 , CuO and TiO_2 nanoparticles suspended in base fluid water. The comparison of these oxide nanoparticles is also provided on Figure 5.10. Evaluation of different studies based on the investigated heat transfer enhancement will provide an insight to the difference and similarity between nanoparticles, nanofluid types, preparation of nanofluids, etc. This will give an ideology toward further studies.

On this chapter a comparison between the heat transfer enhancements achieved using three different types of nanoparticle suspensions of fluid in this study with different heat transfer enhancements reported in the literature. Although different researches have their own different experiment goal, setup and specifications comparison between results can be easily done by comparing heat transfer parameters that reports the performance of the cooling liquid. Nusselt number of a fluid is the most common and widely used heat transfer parameter in the study of heat transfer and performance comparison between studies. Nusselt number strongly associates the convective heat transfer of the fluid to its conductive heat transfer property. All conductive and convective heat transfer parameters that significantly affect the heat transfer performance are brought together as an independent variable to give a new Nusselt correlation which precisely models the entire fluid and heat flow in the system.

6.1 Previous Studies and Developed Correlations

Most literature reported a significant heat transfer enhancement via dispersion of nanoparticles in the base fluid. According to those researches the heat transfer enhancement is related to factors attributed from the base fluid and nanoparticle type. The major factors that affect the heat transfer enhancement are particle volume fraction, shape of particle, Particle size, thermo-physical property of the particle and nanofluid. In the experiment by varying those independent variables an optimum heat transfer enhancement can be achieved. Pak and Cho [35] have investigated a heat transfer enhancement by dispersing Al_2O_3 and TiO_2 nanoparticles into water as a base fluid. In their experiment a turbulent flow is used with a Reynolds number varies from 10^4 - 10^5 . However, at low concentration their experiment shows a deterioration of heat transfer by 12% when compared to pure water. From the experiment conducted they have provided a new correlation of Nusselt number on the convective heat transfer enhancement for oxide nanoparticles dispersed in water and given by the following equation.

$$Nu = 0.021Re^{0.8}Pr^{0.5} \quad (6.1)$$

Maiga et al. [88] suggested a new correlation after an investigation of heat transfer enhancement by dispersion of alumina nanoparticle in to water and ethylene glycol base fluids. A significant heat transfer is reported on their study and a correlation is developed for the numerical result conducted. The new Nusselt number correlation is given by,

$$Nu = 0.085Re^{0.71}Pr^{0.35} \quad (6.2)$$

Xuan et al. [89] studied a single phase of nanofluid and its related heat transfer performance enhancement. A Copper - water mixture is used on their experiment under a constant heat flux boundary condition which is supplied from a DC power. A new correlation is recommended

based on main factors that significantly affect the heat transfer, such as micro convection and micro diffusion of suspended nanoparticles for both laminar and turbulent.

$$Nu = 0.4328(1.0 + 11.285\varphi^{0.754}Pe^{0.218})Re^{0.333}Pr^{0.4} \text{ For laminar flow} \quad (6.3)$$

$$Nu = 0.0059(1.0 + 7.6286\varphi^{0.6886}Pe^{0.001})Re^{0.9238}Pr^{0.4} \text{ For turbulent flow} \quad (6.4)$$

Asirvatham et al. [90] reported an experimental study on forced convective heat transfer with low volume fraction of CuO – water nanofluid in the laminar flow regime. In their work de-ionized water with a low fraction with amount of 0.3% of CuO is used as a nanofluid that flows through a short copper tube. The performance of heat transfer is improved by 8% when compared to pure water. A new correlation is recommended in this study as given on equation (6.5)

$$Nu = 0.155Re^{0.59}Pr^{0.35} \left(\frac{D}{x} \right)^{0.38} \quad (6.5)$$

6.2 Developing Nusselt Number Correlation

A Nusselt number of a cooling nanofluid is a function of thermo physical properties of nanoparticle, shape of particle, volumetric concentration, thermophysical properties of base fluid, Reynold number and Prandtl number of nanofluid [90]. And this can be expressed as,

$$Nu = f \left(Re, Pr, K_{nf}, \varphi, D_h/x, D_p \right) \quad (6.6)$$

As it is reported in previous studies, most correlation developed for the Nusselt number gives an average value of the system, despite the fact that the Nusselt value varies significantly across the length of a channel. This variation of Nusselt number between the inlet and outlet of a channel become more substantial when short heat transfer channels are used. Due to the developing thermal boundary of the nanofluid at the inlet of the channel, the thin thermal

boundary layer thickness results a higher heat transfer rate when compared to the other section of the tube.

$$HTC \propto \frac{K_{nf}}{\delta_t} \quad (6.7)$$

Table 5.3 shows a numerical result of 5% by volume concentration of Al₂O₃ nanoparticles with base fluid water at a Reynolds number of 645. The numerical result shows the heat transfer coefficient at the inlet is 315% higher than the HTC measured at the outlet of the channel. Most correlation reported in literature disregard the effect of length in the formulation and reports the averaged heat transfer parameter across the channel. Bringing the length of the channel in to the equation of a heat transfer parameter as an independent factor will give an insight toward the heat transfer distribution.

In this study, a new correlation of Nusselt number is developed from the numerical results and compared to some other experimental and numerical based correlations found in literature. In this formulation the Nusselt number is expressed only as a function of Reynolds, Prandtl, and the axial distance along the length of the channel. Mathematically expressed as

$$Nu = f \left(Re, Pr, D/x \right) \quad (6.8)$$

The Reynolds number address the all the viscous properties of the nanofluid and the thermal properties will be handled by the Prandtl number provided. The last term reports the significant variation of the Nusselt number along the length of the channel.

From the numerical analysis, the data result for Reynolds, Prandtl, dimensionless length and Nusselt number is collected for each volume fraction of nanofluid at different inlet fluid

velocity during the regression. The statistical modeling approach is briefly discussed on the next section.

6.2.1 Data Correlation Methodology

The statistical modeling uses 275 observations from the numerical analysis result for each nanofluid type at a volume fraction range of 1-5% by volume a multi variable linear regression is used to develop the correlation between the heat transfer parameter. A Nusselt number correlation from previous literature takes a form of exponential formulation and the mathematical model setup is given as shown below.

$$Nu(x) = aRe^bPr^c \left(\frac{D_h}{x} \right)^d \quad (6.9)$$

Where the constants provided a, b, c and d are determined from the multi variable linear regression. In order to proceed with the regression analysis the above multivariable exponential equation is transformed in to a linear logarithmic equation. The transformation helps to quickly estimate the unknown constants from a linear regression. The logarithmic form of the equation is written as,

$$\ln(Nu(x)) = \ln(aRe^bPr^c \left(\frac{D_h}{x} \right)^d) \quad \text{This can be further expanded as,}$$

$$\ln(Nu(x)) = \ln(a) + b \ln(Re) + c \ln(Pr) + d \ln \left(\frac{D_h}{x} \right)$$

Form the above expanded logarithmic formulation the new linear equation will take the form of

$$Y = \beta_0 + \beta_1 x_1 + \beta_2 x_2 + \beta_3 x_3 + \varepsilon \quad (6.10)$$

Where, $Y = \ln(Nu(x))$, $\beta_0 = \ln(a)$, $\beta_1 = b$, $\beta_2 = c$, $\beta_3 = d$ and $\varepsilon = \text{error}$

A 95% confidence interval is set for the regression, and the coefficients are estimated with an R squared (R^2) value of 99% for Al_2O_3 , CuO and TiO_2 nanofluid. The new correlation developed for estimating the heat transfer performance ($Nu(x)$) in the laminar flow region is listed as shown below.

Table 6.1 New Developed Nusselt number correlation based on Numerical analysis result

Nanofluid Type	New Developed Correlation	Volume Fraction, ϕ	Flow Regime
Al_2O_3 - Water	$Nu = 0.792Re^{0.341}Pr^{0.589}\left(\frac{D_h}{x}\right)^{0.294}$	1 – 5%	Laminar
CuO - Water	$Nu = 0.848Re^{0.357}Pr^{0.496}\left(\frac{D_h}{x}\right)^{0.304}$	1 – 5%	Laminar
TiO_2 - Water	$Nu = 0.806Re^{0.349}Pr^{0.541}\left(\frac{D_h}{x}\right)^{0.299}$	1 – 5%	Laminar

The new developed correlations from the numerical analysis shows an insignificant variation between predicted Nusselt values under multiple volume fraction, in a laminar flow region. As shown on Figure 6.1, the predicted Nusselt number comparison between Al_2O_3 , CuO and TiO_2 nanofluids is done based on 90% confidence interval to test whether the variation of the heat transfer enhancement between the nanofluids is substantial. From the plot shown below the TiO_2 – water nanofluid has a higher Nusselt when compared to the other type of nanofluid. However, from the base of the statistical analysis there is no significant difference between the predicted values since all the three means at an arbitrary location of the channel falls within the 90% confidence interval to which it is being compared.

Even though nanoparticle properties are broadly diverse in their nature of thermophysical properties and their heat transfer performance after blended with the base fluid, oxide nanofluids which are investigated in this study yields a heat transfer performance nearly indistinguishable between them. From this stand point of view we can suggest a grand correlation for the Nusselt number that can be exploited by any type of nanofluid with similar thermophysical and rheological properties.

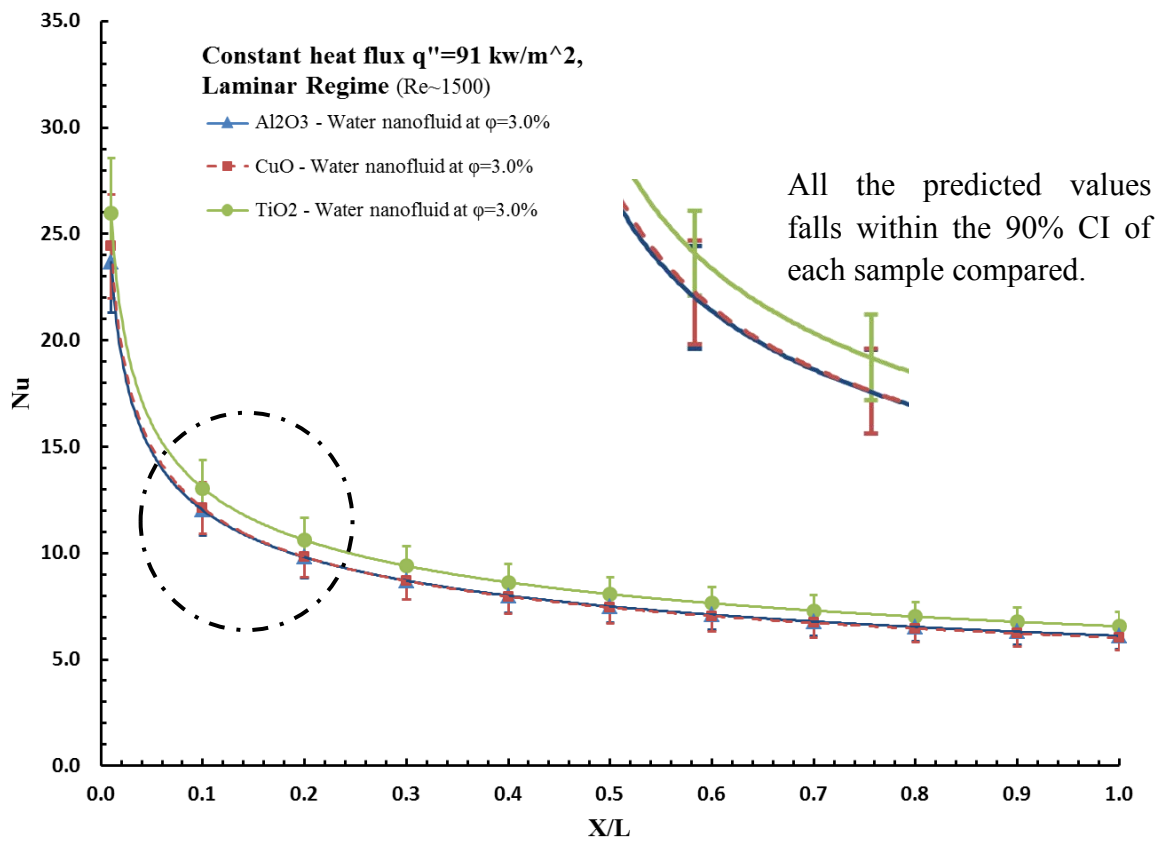


Figure 6.1 Heat transfer performance comparison between studied nanofluid types.

The overall correlation for the nanofluids investigated in this study under the obligatory fluid and thermal condition specified earlier is given by a single equation as shown below,

$$Nu = 0.812Re^{0.35}Pr^{0.54}\left(\frac{D_h}{x}\right)^{0.30} \quad (6.11)$$

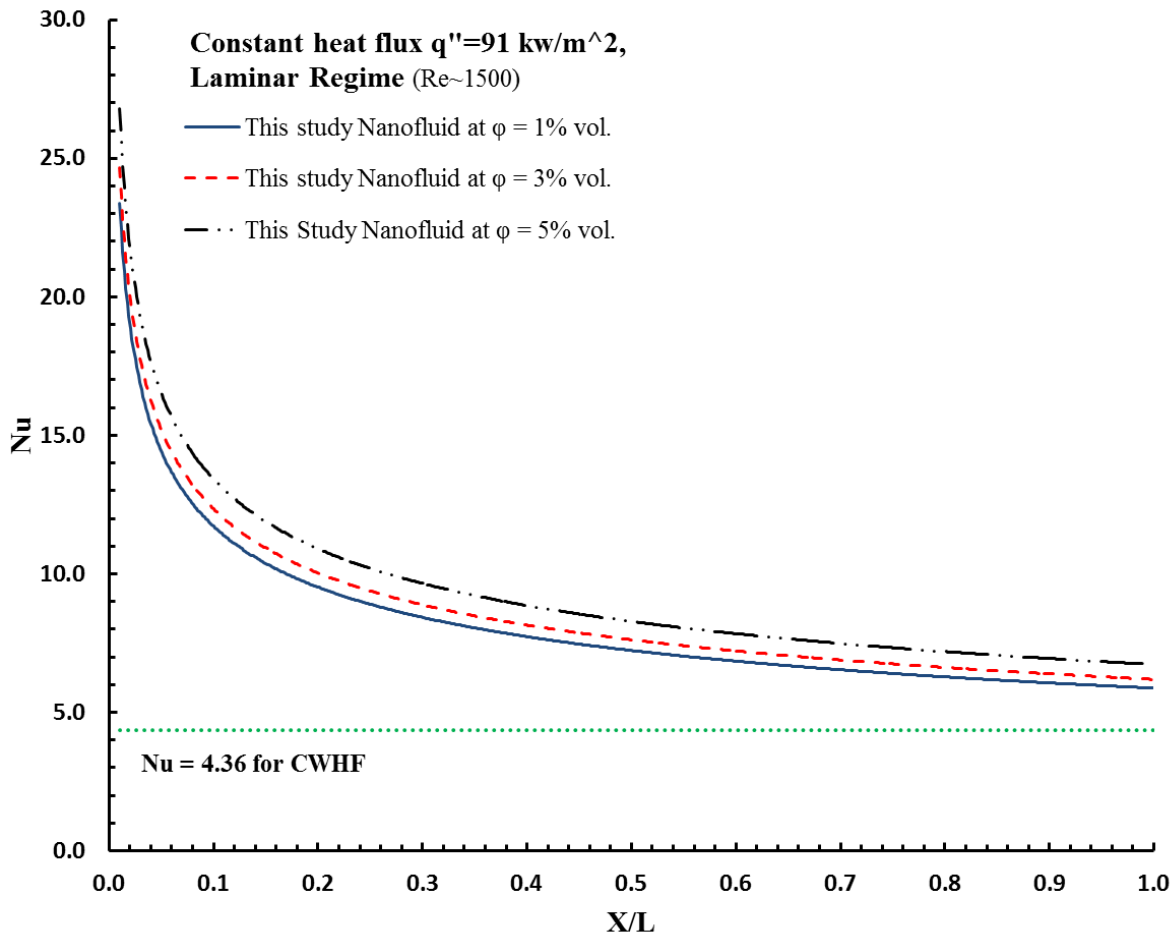


Figure 6.2 Nusselt number response at different volume fraction.

6.3 Comparison of Correlations from Literature

Different literature comes up with various correlation based on their experiment approach, numerical analysis or theoretical model. In this study we have compared the thermal performance of nanofluids based of different correlations developed by researchers for different nanofluids to compare the proximity for other studies.

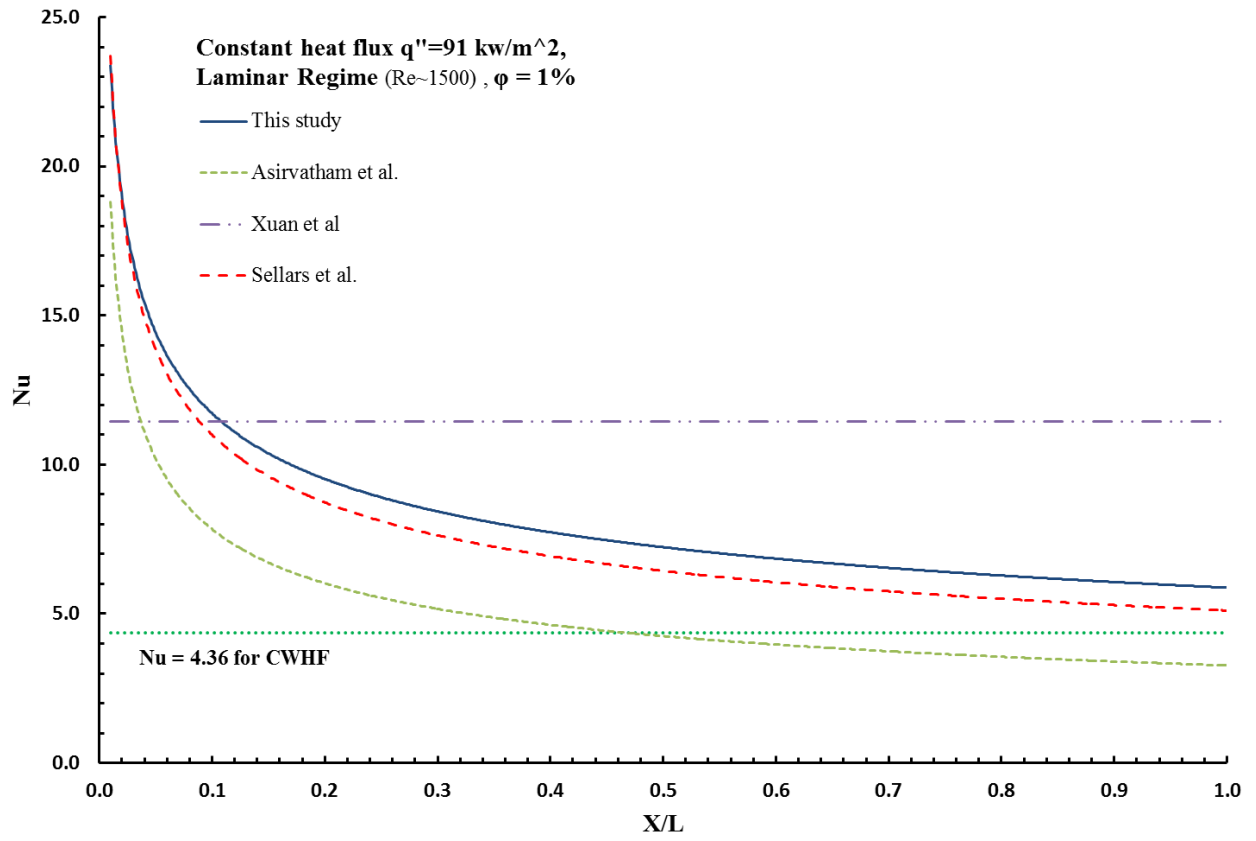


Figure 6.3 Nusselt number comparison of different models at $\phi=1.0\%$.

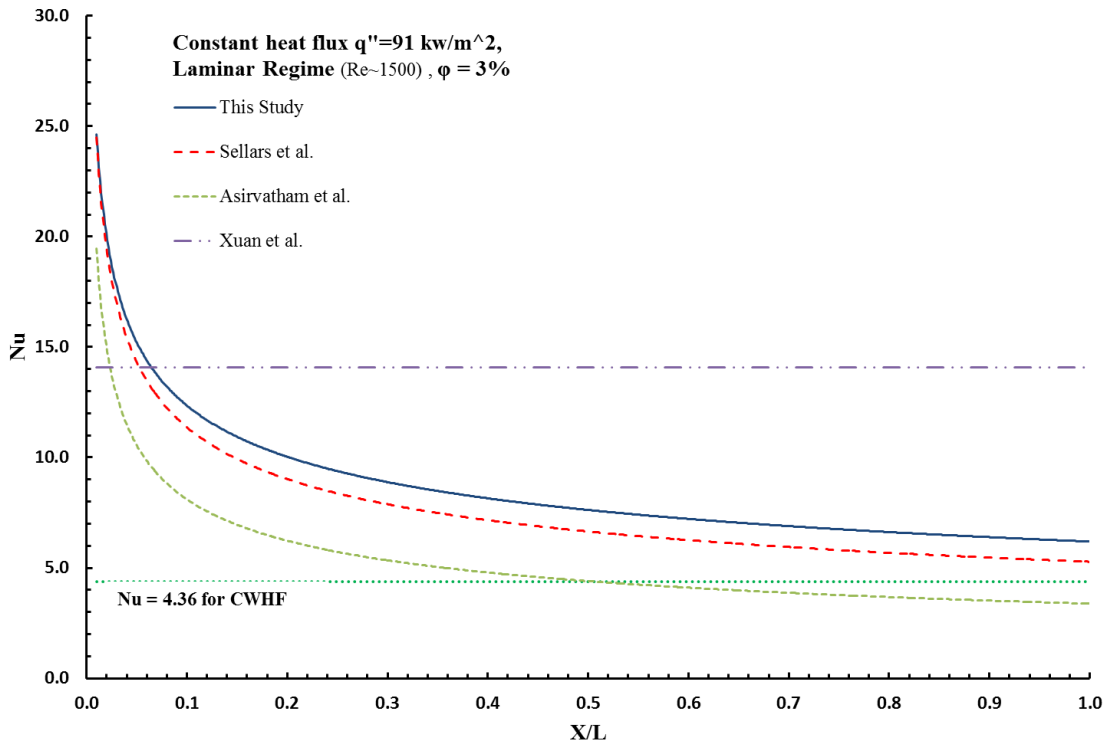


Figure 6.4 Nusselt number comparison of different models at $\phi=3.0\%$.

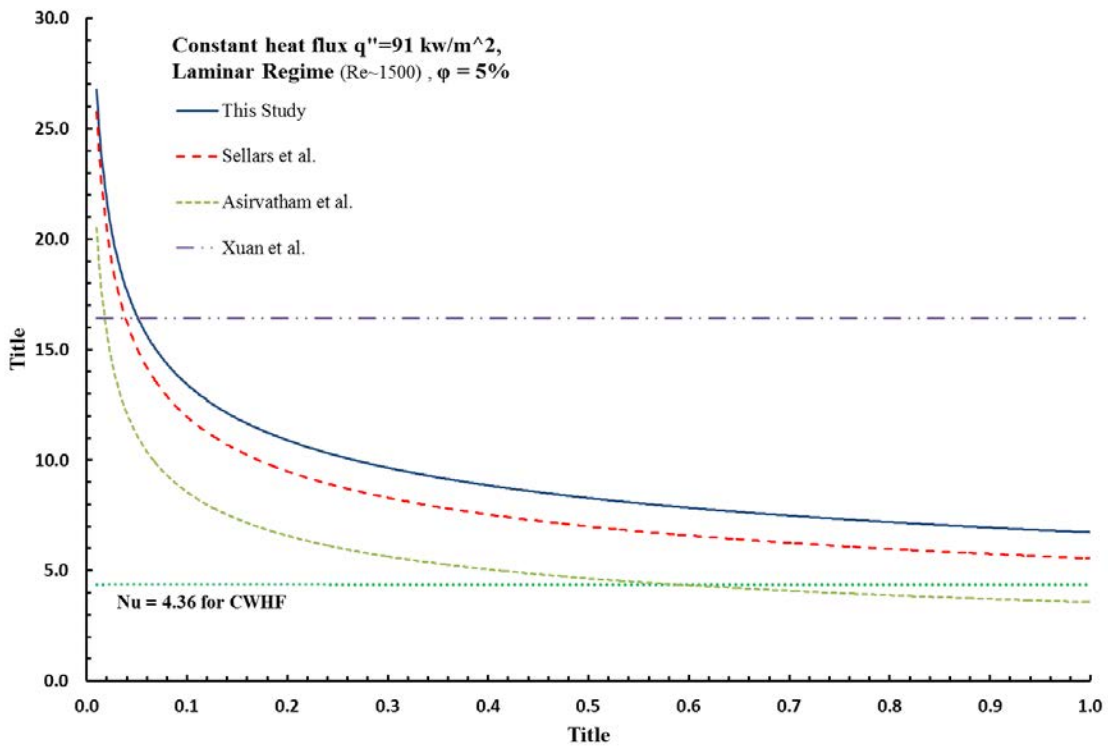


Figure 6.5 Nusselt number comparison of different models at $\phi=5.0\%$.

CHAPTER 7

CONCLUSION

Dispersed suspension of solid nanoparticles in a conventional base fluid is a novel technology that can lead to an advanced investigation which opens the gate for further exploitation of the untapped potential of nanofluids. For the past few decades, numerous researches are conducted a study on thermophysical, rheological, heat and mass transfer properties of a nanofluid and challenged to materialize the theoretical premises of a significant enhancement achieved in heat transfer and related fields. Although it is a fact that the thermal conductance of a fluid can be augmented by dispersing nanoparticles, literature doesn't report a consistent result on the enhancement attained. Discrepancies between studies results a vague cognition on the mechanism of heat transfer, and yet effort is needed to come up with a complete understanding of this phenomenon. In this research, sufficient experiments are gathered from literature and statistically compared to build a meaningful thermophysical and rheological model of nanofluids. And according to the conducted statistical and numerical study of heat transfer performance in nanofluid, a comprehensive explanation of heat transfer enhancement is delivered.

In this study, the significant effect of solid nanoparticle dispersions in a water base fluid is examined at different level of concentration and compared with previous studies from literature. Based on experimental results that are collected form researches, a new thermal conductivity and viscosity models are developed for water based nanofluids specifically with Al_2O_3 , CuO and TiO_2 nanoparticle suspensions. A decent agreement is observed between the predicted thermophysical and rheological model with the collected experimental sample points, which

supports the validity of the regressed equations. The developed equation is also compared to other classic theoretical and experimental models provided in literature to understand the deviation between studies.

Numerical analysis of nanofluid can be conducted based on different mathematical model approaches as it is briefly discussed on chapter 4 section 4.3. A homogenous single phase model approach is used in this research to estimate the heat transfer augmentation achieved from a nanofluid cooling. During the computational domain validation stage a Stollars [84] Nusselt equation used for error comparison via measuring the local Nusselt values at each section of the channel. Due to the short length copper channel used in this study (commonly used in microelectronics cooling systems) the flow at the entry of the channel will be thermally undeveloped which yields a thin thermal boundary layer on the entrance region. As a consequence, the heat transfer will be considerably higher at the inlet when compared to a measurement at the inlet. The computational fluid analysis is conducted for various combinations of volume fraction, inlet velocity (Reynolds at laminar flow regime) and type of nanoparticle. Post processed result from the numerical analysis demonstrates that a significant heat transfer enhancement is observed in all type of nanofluids used in this study. At 5% concentration of nanoparticle, Alumina, copper oxide and titania nanofluids shown an average heat transfer coefficient enhancement of 31.2%, 23.4% and 25.5% respectively when compared to the base fluid. According to the numerical results, the introduction of nanoparticles in to a conventional base fluid at different amount of concentration can significantly enhance the heat transfer performance of a cooling liquid.

The factors investigated in the literature such as fraction volume of nanoparticle, temperature, flow regime plays an important role in increasing the thermal conductivity of a

nanofluid, but according literature several additional factors which are not studied in this research are also linked with the thermal performance enhancement of a nanofluid. For instance shape of a nanoparticle, particle size and solution PH value are considered as significant factors in some researches. Although the research addresses the main factors in heat transfer enhancement, some key elements are also left out of the equation due to lack of experimental evidence.

Despite the weak theoretical foundation of the basic mechanism of heat transfer, experimental based understanding of nanofluid is comprehensively used in researches and industries. However, a complete cognition of a micro and atomic-scale-level heat transfer in nanofluids must be overcome in order to unlock the full potential of these novel heat transfer fluids. Development of a new theoretical model that considers the effect of various additional factors which enable us to explain the anomaly observed in present studies should be the ultimate goal of future researches.

REFERENCES

REFERENCES

- [1] J.A. Eastman, S. Phillpot, S. Choi, P. Keblinski, “Thermal transport in nanofluids.” *Annu. Rev. Mater. Res.* 34, (2004), pp.219–246.
- [2] Keblinski, P., Phillpot, S. R., Choi, S. U. S., and Eastman, J. A. “Mechanisms of heat flow in suspensions of nano-sized particles (nanofluids).” *International Journal of Heat and Mass Transfer* 45, (2002), pp.855–863.
- [3] Maxwell, J. C. “A Treatise on Electricity and Magnetism.”, Clarendon Press, Oxford, UK, second edition, (1873)
- [4] Bruggeman D. Berechnung “verschiedener physikalischer konstanten vonheterogenen substanzen.” *Ann. Phys.* 24, (1935), pp.636–79.
- [5] Hamilton R.L. & O.K. Crosser, “Thermal conductivity of heterogeneous two-component systems.” *I&EC Fundamentals* 1, (1962), pp.187–191.
- [6] Masuda H, Ebata A, Termae K, Hishinuma N “Alteration of thermal conductivity and viscosity of liquid by dispersing ultra-fine particles (Dispersion of Al₂O₃, SiO₂, and TiO₂ ultra-fine particles).” *Netsu Bussei* 7, (1993), pp.227-233.
- [7] K. Khanafer and K. Vafai. “A critical synthesis of thermophysical characteristics of nanofluids.” *International Journal of Heat and Mass Transfer* 54, (2011), pp.4410–4428.
- [8] Yu, W. and Choi, S. U. S. “The role of interfacial layers in the enhanced thermal of nanofluids: a renovated Maxwell model.” *Journal of Nanoparticle Research* 5, (2003), pp.167–171.
- [9] Xue, Q. and Xu, W.-M. “A model of thermal conductivity of nanofluids with interfacial shells.” *Materials Chemistry and Physics* 90, (2005), pp.298–301.
- [10] Xuan, Y., Li, Q., and Hu, W. “Aggregation structure and thermal conductivity of nanofluids.” *Aiche Journal* 49, (2003), pp.1038–1043.
- [11] Wang, X., Xu, X., and Choi, S. U. S. “Thermal conductivity of nanoparticle-fluid mixture.” *Journal of Thermophysics and Heat Transfer* 13, (1999), pp.474–480.
- [12] Kaufui V. Wong & Omar De Leon., “Applications of nanofluids: Current and Future, *Advances in Mechanical Engineering*,” *Advances in Mechanical Engineering*, (2010), pp.10
- [13] Yulong D.; Chen, H.S.; He, Y.R.; Alexei, L.; Mahboubbeh, Y.; Lidija Š.; Butenko Yuriy, V. “Forced convective heat transfer of nanofluids.” *Adv. Powder Technology* 18, (2007), pp.813-824.

REFERENCES (continued)

- [14] Choi, S. U. S., J.A Eastman “Enhancing thermal conductivity of fluids with nanoparticles.” *Developments and Applications of Non-Newtonian Flows* 66, (1995), pp. 99–105.
- [15] Buongiorno, J. “Convective transport in nanofluids.” *Journal of Heat Transfer* 128, (2006), pp.240–250.
- [16] Das, S. K., Putta, N., Thiesen, P., and Roetzel, W. “Temperature dependence of thermal conductivity enhancement for nanofluids.” *ASME Trans. J. Heat Transfer* 125, (2003), pp.567–574.
- [17] E.V. Timofeeva, Wenhua Yu, David M France, Dileep Singh, Jules L Routbort, “Nanofluids for heat transfer: an engineering approach.” *Nanoscale Res. Lett.* 6, (2011), pp. 1–7.
- [18] Lee, S., Choi, S. U. S., Li, S., and Eastman, J. A., “Measuring thermal conductivity of fluids containing oxide nanoparticles.” *Journal of Heat Transfer* 121,(1999), pp.280–289.
- [19] C. H. Chon, K. D. Kihm, S. P. Lee and S. U. S. Choi, “Empirical Correlation Finding the Role of Temperature and Particle Size for nanofluid (Al₂O₃) Thermal Conductivity Enhancement.” *Appl. Phy. Lett.* 87, (2005), pp.1-3.
- [20] Li, X., Zhu, D., and Wang, X., “Evaluation on dispersion behavior of the aqueous copper nano suspensions.” *Journal of colloid and interface Science*, 310, (2007), pp.456-463.
- [21] Xuan, Y. and Roetzel, W. “Conceptions for heat transfer correlation of nanofluids.” *International Journal of Heat and Mass Transfer* 43, (2000), pp.3701– 3707.
- [22] L.G. Asirvatham , N. Vishal, S. K. Gangatharan, D. M. Lal, “Experimental Study on Forced Convective Heat Transfer with Low Volume Fraction of CuO/Water nanofluid” *Energies* 2, (2009), pp.97-119.
- [23] Henderson, J.R. & F. van Swol, “On the interface between a fluid and a planarwall: Theory and simulations of a hard sphere fluid at a hard wall.” *Mol. Phys.* 51, (1984), pp.991–1010.
- [24] Evans W., Prasher R., Meakin P., Fish J., Phelan P., Keblinski P., “effect of aggregation on thermal conduction in colloidal nanofluids.” *Applied Physics Letters* 89, (2006),1431-1438.
- [25] Xue, Q.-Z., “Model for effective thermal conductivity of nanofluids.” *Physics Letters A* 307, (2003), pp.313–317.
- [26] R.Yajie, H. Xie, A. Cai, “Effective thermal conductivity of nanofluids containing spherical nanoparticles.” *J.Phys.D:Appl.Phys* 38, (2005), pp.3958-3961.

REFERENCES (continued)

- [27] Prasher R., Bhattacharya P. and Phelan P.E., "Thermal conductivity of nanoscale colloidal solutions (nanofluids)." *Physical Review Letters* 94, (2005), pp.025901,1-4.
- [28] Einstein A., "A new determination of the molecular dimensions." *Ann. Phys.* 19, (1906), pp.289-306.
- [29] Brinkman HC. "The viscosity of concentrated suspensions and solution." *J Chem Phys.* 20, (1952), pp.571-581.
- [30] Batchelor GK. "The effect of Brownian motion on the bulk stress in a suspension of spherical particles." *J Fluid Mech.* 831, (1977), pp.97-117.
- [31] Guth and R. Simha. "Untersuchungen uber die viskositat von suspensionen und losungen. 3. uber die viskositat von kugelsuspensionen." *Kolloid-Z.* 74, (1936), pp.266-275.
- [32] I.M. Krieger and T.J. Dougherty, "A mechanism for non-Newtonian flow in suspension of rigid spheres." *Trans. Soc. Rheol.* III, (1959), pp.137-152.
- [33] Kitano, T., Kataoka, T. & Shirota, T. "An empirical-equation of the relative viscosity of polymer melts filled with various inorganic fillers." *Rheol. Acta* 20, (1981), pp.207-209.
- [34] Thomas, D. G. "Transport characteristics of suspension: VIII. A note on the viscosity of Newtonian suspensions of uniform spherical particles." *J. Colloid Sci.*, 20, (1965), pp.267-277.
- [35] Pak, B. C. & Cho, Y. I. "Hydrodynamic and heat transfer study of dispersed fluids with submicron metallic oxide particles." *Experimental Heat Transfer* 11, (1998), pp.151-170.
- [36] Ho CJ, Liu WK, Chang YS, Lin CC, "Natural convection heat transfer of alumina-water nanofluid in vertical square enclosures: an experimental study." *Int J Therm Sci* 49, (2010), pp.1345-1353.
- [37] Zhou S-Q, Ni R "Measurement of the specific heat capacity of water-based Al₂O₃ nanofluid." *Appl Phys Lett* 92, (2008), pp.093123. 1-3.
- [38] Granqvist C. G., and R. A. Buhrman, "Ultrafine Metal Particles." *Journal of Applied Physics* 47, (1976), pp.2200-2219.
- [39] Yu W, France DM, Choi SUS, "Review and assessment of nanofluid technology for transportation and other applications." Argonne National Laboratory, Argonne, IL, (2007)
- [40] R. Saidur, K Y Leong and H A Mohammad "A review on applications and challenges of nanofluids." *Renew Sustain Energy Rev* 15, (2011), pp.1646-1668.

REFERENCES (continued)

- [41] S.C. Tzeng, C. W. Lin, and K. D. Huang, "Heat transfer enhancement of nanofluids in rotary blade coupling of four-wheel-drive vehicles." *Acta Mechanica* 179, (2005), pp.11-23.
- [42] M. J. Kao and C. R. Lin, "Evaluating the role of spherical titanium oxide nanoparticles in reducing friction between two pieces of cast iron" *J. Alloy. Compd.* 483, (2009), pp.456-459.
- [43] Senthilraja S., Karthikeyan M. and Gangadevi R., "Nanofluid applications in future Automobiles: Comprehensive review of existing data." *Nano-Micro Lett.* 2, (2010), pp.306–310.
- [44] M.J. Kao, H. Chang, Y.Y. Wu, T.T. Tsung, and H.M. Lin., "Producing aluminumoxide brake nanofluids using plasma charging system." *Journal of the Chinese Society of Mechanical Engineers* 28, (2007), pp.123–131.
- [45] S.L. Durham. 2009, "Researchers are Thinking Small." *Explorer* (online). August 2009.
- [46] Cheraghian G., Hemmmati M., Masihi M., Bazgir S., "An experimental investigation of drilling fluids using titanium dioxide and fumed silica nanoparticles." *Journal Of Nanostructure in Chemistry* 3, (2013), pp.78-87.
- [47] Kim, S. J., Bang, I. C., Buongiorno, J., and Hu, L. W. "Surface wettability change during pool boiling of nanofluids and its effect on critical heat flux." *International Journal of Heat and Mass Transfer* 50, (2007), pp.4105–4116.
- [48] C. T. Nguyen, G. Roy, N. Galanis, S. Suiro, "Heat Transfer Enhancement by using Al₂O₃-Water nanofluid in a Liquid Cooling System for Microprocessors." *Int. Conf. on Heat Transfer, Thermal Engineering and Environment*, (2006), pp. 103-108.
- [49] Y.H. Lin, S.W. Kang, and H.L. Chen., "Effect of silver nano-fluid on pulsating heat pipe thermal performance." *Applied Thermal Engineering* 28, (2008), pp.1312–1317.
- [50] Raj K Dash, T Borca-Tasciuc, A Purkayastha, and G Ramanath, "Electrowetting on dielectric-actuation of microdroplets of aqueous bismuth telluride nanoparticle suspensions" *Nanotechnology* 18, (2007), pp.475711 6-13.
- [51] Doina Bica, Ladislau Ve'ka' s, Mikhail V. Avdeev, Oana Marinica, Vlad Socoliuc, Maria Balasoiu, Vasil M. Garamus, "Sterically stabilized water based magnetic fluids: Synthesis, structure and properties." *Journal of Magnetism and Magnetic Materials* 311, (2007), pp.17–21.
- [52] J. Yan and J. Liu., "Nanocryosurgery and its mechanisms for enhancing freezing efficiency of tumor tissues." *Nanomedicine: Nanotechnology, Biology, and Medicine* 4, (2008), pp.79–87.

REFERENCES (continued)

- [53] Fei Duan, "Thermal Property Measurement of Al₂O₃-Water nanofluids, Smart Nanoparticles technologies", (2012), pp.335-356.
- [54] G. Paul, M. Chopkar, I. Manna, P.K. Das, "Techniques for measuring the thermal conductivity of nanofluids: A review", *Renewable and Sustainable Energy Reviews* 14, (2010), pp.1913-1924.
- [55] Haisheng Chen, Yulong Ding, and Chunqing Tan, "Rheological behaviour of nanofluids." *New Journal of Physics* 9, (2007), pp. 367-391.
- [56] Tavman, I., Turgut, A., Chirtoc, M., Schuchmann, H. and Tavman, S., "Experimental investigation of viscosity and thermal conductivity of suspensions containing nanosized ceramic particles." *International Scientific Journal* 34, (2008), pp.99-104.
- [57] H. Maddah, M. Rezazadeh, M. Maghsoudi, S. N.okhdan, "The effect of silver and aluminum oxide nanoparticles on thermophysical properties of nanofluids." *Journal Of Nanostructure in Chemistry* 3, (2013), pp.28-34.
- [58] Ronald L.Panton "Incompressible flow" John Wiley & Sons, Inc., New Jersey, Third Edition, (2005)
- [59] Madhusree Kole and T K Dey, "Thermal conductivity and viscosity of Al₂O₃ nanofluid based on car engine coolant." *J. Phys. D: Appl. Phys.* 43, (2010), 10pp.
- [60] A. Turgut, I. Tavman, M. Chirtoc, H. P. Schuchmann, C. Sauter, S. Tavman, "Thermal Conductivity and Viscosity Measurements of Water-Based TiO₂ nanofluids." *Int J Thermophys* 30, (2009), pp.1213–1226.
- [61] P. Namburu, D. Kulkarni, D. Misra, D. Das, "Viscosity of copper oxide nanoparticles dispersed in ethylene glycol and water mixture." , *Exp. Therm. Fluid Sci.* 32, (2007), pp.397–402.
- [62] D.P. Kulkarni, D.K. Das, G.A. Chukwu, "Temperature dependent rheological property of copper oxide nanoparticles suspension (nanofluid)", *J. Nanosci. Nanotechnol.* 6, (2006), pp.1150–1154.
- [63] M. Chandrasekar, S. Suresh, A. Chandra Bose, "Experimental investigations and theoretical determination of thermal conductivity and viscosity of Al₂O₃/water nanofluid", *Exp. Therm. Fluid Sci.* 34, (2010), pp.210–216.
- [64] M.T. Naik, G.R. Janardhana, K.V.K. Reddy, B.S. Reddy, "Experimental investigation into rheological property of copper oxide nanoparticles suspended in propylene glycol- water based fluids.", *ARPJ. Eng. Appl. Sci.* 5, (2010), pp.29–34.

REFERENCES (continued)

- [65] Zhu HaiTao, LI ChangJiang, Wu DaXiong, Zhang CanYing, Yin YanSheng, "Preparation, characterization, viscosity and thermal conductivity of CaCO₃ aqueous nanofluids." *Science China, Technological Sciences* 53, (2010), pp.360–368.
- [66] N. Putra, W. Roetzel, S.K. Das, "Natural convection of nano-fluids.", *Heat Mass Transfer* 39, (2003), pp.775–784.
- [67] N. Masoumi, N. Sohrabi, A. Behzadmehr, "A new model for calculating the effective viscosity of nanofluids.", *J. Phys. D Appl. Phys.* 42, (2009), pp. 055501 1-6.
- [68] Rostamani M, Hosseinizadeh SF, Gorji M and Khodadadi JM, "Numerical study of turbulent forced convection flow of nanofluids in a long horizontal duct considering variable properties." *Int. Commun. Heat Mass Transfer* 37, (2010), pp.1426-1431.
- [69] S. M. Sohel Murshed, Kai Choong Leong, Chun Yang, Nam-Trung Nguyen, "Convective heat transfer characteristics of aqueous TiO₂ nanofluid under laminar flow conditions." *International Journal of Nanoscience* 7, (2008), pp.325–331
- [70] P. Keblinski, J. Eastman, D. Cahill, "Nanofluids for thermal transport" *Mater Today* 8, (2005), pp.36–44.
- [71] H.E. Patel, S.K. Das, T. Sundararajan, A.S. Nair, B. George, T. Pradeep, "Thermal conductivities of naked and monolayer protected metal nanoparticle based nanofluids: manifestation of anomalous enhancement and chemical effects." *Appl. Phys. Lett.* 83, (2003), pp.2931–2933.
- [72] J.A. Eastman, U.S. Choi, S. Li, L.J. Thompson, S. Lee, "Enhanced thermal conductivity through the development of nanofluids." *Materials Research Society Symp.* 457, (1997), pp.3-11.
- [73] Li, C.H. & Peterson G.P., "Experimental investigation of temperature and volume fraction variations on the effective thermal conductivity of nanoparticle suspensions (nanofluids)". *J. Appl. Phys* 99, (2006), pp.1-8.
- [74] S. Lee, S. U.-S. Choi, S. Li, J. A. Eastman, "Measuring Thermal Conductivity of Fluids Containing Oxide Nanoparticles." *Journal of Heat Transfer* 121, (1999), pp.280-289.
- [75] Eastman JA, Choi SUS, Li S, Soyez G, Thompson LJ, Melfi RJD, "Novel thermal properties of nanostructured materials." *Mater Sci Forum*, (1999), pp.312-314.
- [76] X. Zhang, H. Gu, M. Fujii, "Effective thermal conductivity and thermal diffusivity of nanofluids containing spherical and cylindrical nanoparticles.", *J. Appl. Phys.* 100, (2006), pp.569-580.

REFERENCES (continued)

- [77] Angue Minsta, H., Roy, G., Nguyen, C.T., Doucet, D., “New temperature and conductivity data for water-based nanofluids.” *Int. J. Therm. Sci.* 48, (2009), pp.363–371.
- [78] Y. Hwang, Y. Ahn, H. Shin, C. Lee, G. Kim, H. Park, J. Lee, “Investigation on characteristics of thermal conductivity enhancement of nanofluids.”, *Curr. Appl Phys.* 6, (2006), pp.1068–1071.
- [79] Benigno Barbe’s, Ricardo Pa’ramo, Eduardo Blanco, Carlos Casanova, “Thermal conductivity and specific heat capacity measurements of CuO nanofluids.” *J Therm Anal Calorim* 115, (2014), pp.1883–1891.
- [80] Z. L. Wang, D.W. Tang, S. Liu, X. H. Zheng, N. Araki, “Thermal-Conductivity and Thermal-Diffusivity Measurements of nanofluids by 3ω Method and Mechanism Analysis of Heat Transport”, *Int J Thermophys* 28, (2007), pp.1255–1268.
- [81] John D. Anderson Jr. “Computational Fluid Dynamics: Theasics with application” McGraw Hill, (1995)
- [82] Timothy Barth, and Mario Ohlberger, “Finite volume methods: foundation and analysis” NASA Ames Research Center, John Wiley & Sons, Ltd, California, (2004)
- [83] E. Dick, “Introduction to Finite Element Methods in Computational Fluid Dynamics”, J.F wendt, (ed.), Third Edition, (2009), pp. 235-274.
- [84] Sellars, J.R., M. Tribus, and J.S. Klein, “Heat Transfer to Laminar Flow in a Flat - The Graetz Problem Extended,” *Trans. ASME* 78, (1956), pp.441-448.
- [85] M. R. Raveshi, A. Keshavarz, M. S.Mojarrad, S. Amiri, “Experimental investigation of pool boiling heat transfer enhancement of alumina-water-ethylene glycol nanofluids.”, *Exp. Thermal Fluid Sci.* 44, (2013), pp. 805-814.
- [86] H. O’Hanley, J. Buongiorno, T. McKrell, L. Hu, “Measurement and Model Validation of nanofluid Specific Heat Capacity with Differential Scanning Calorimetry” Hindawi Publishing Corporation, *Advances in Mechanical Engineering*, (2012) pp.6
- [87] Y. S. Muzychka, Edmond Walsh, Pat Walsh, “Simple Models for Laminar Thermally Developing Slug Flow in Noncircular Ducts and Channels.” *Journal of Heat Transfer*, Vol. 132, (2010), pp.10
- [88] S.E.B. Maiga, S.J. Palm, C.T. Nguyen, G. Roy, N. Galanis, “Heat transfer enhancement by using nanofluids in forced convection flows” *Int. J. Heat Fluid Flow* 26, (2005), pp.530–546.
- [89] Xuan Yimin and Li Qiang, “Convective heat transfer and flow characteristics of Cu-water nanofluid” *Science in China series E.* 45, (2002), pp.408-416.

REFERENCES (continued)

- [90] M. S Mojarrad, A. Keshavarz, A. Shokouhi, “Nanofluid thermal behavior analysis using a new dispersion model along with single-phase” *Heat mass Transfer* 49, (2013), pp. 1333-1343.
- [91] D.J. Jeffrey, “Conduction through a random suspension of spheres”, *Proc. Roy. Soc. (Lond.) A*335, (1973), pp. 355–367.
- [92] R.H. Davis, “The effective thermal conductivity of a composite material with spherical inclusions”, *Int. J. Thermophys* 7, (1986), pp. 609–620.

APPENDIX

APPENDIX

NANOFLUIDS THERMOPHYSICAL PROPERTIES

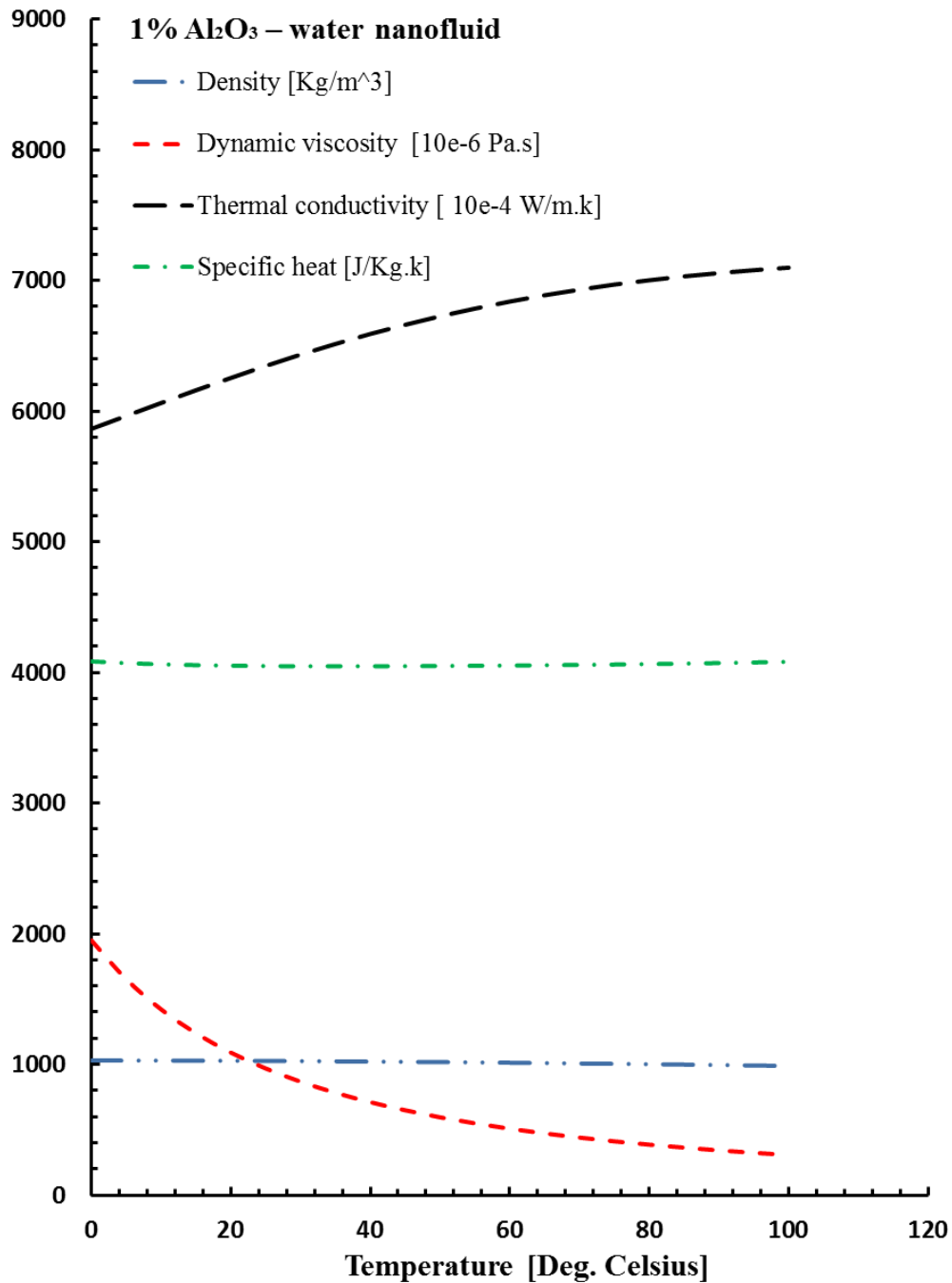


Figure A-1 Thermophysical properties of 1% Al₂O₃ – water nanofluid

APPENDIX (continued)

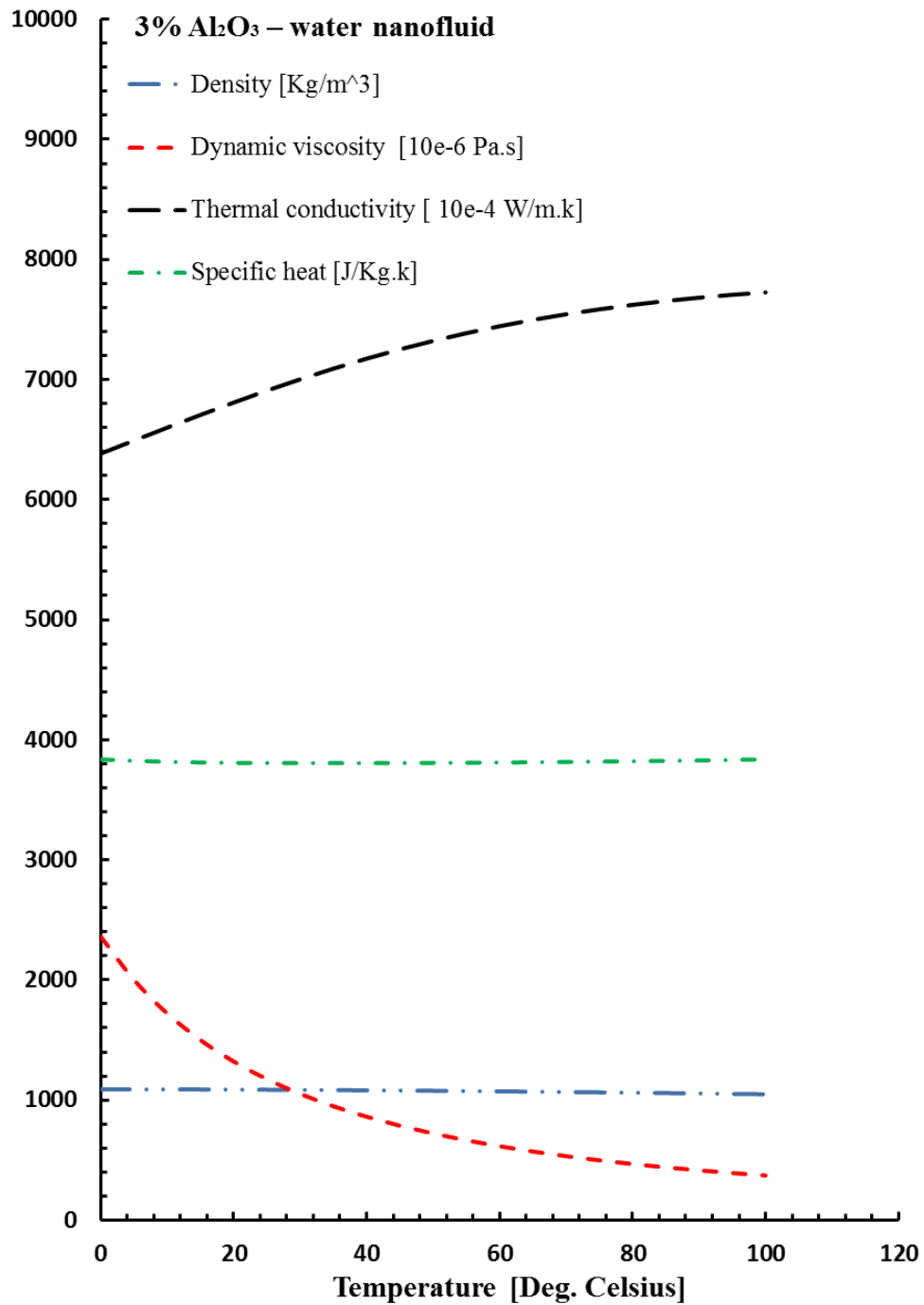


Figure A-2 Thermophysical properties of 3% Al₂O₃ – water nanofluid

APPENDIX (continued)

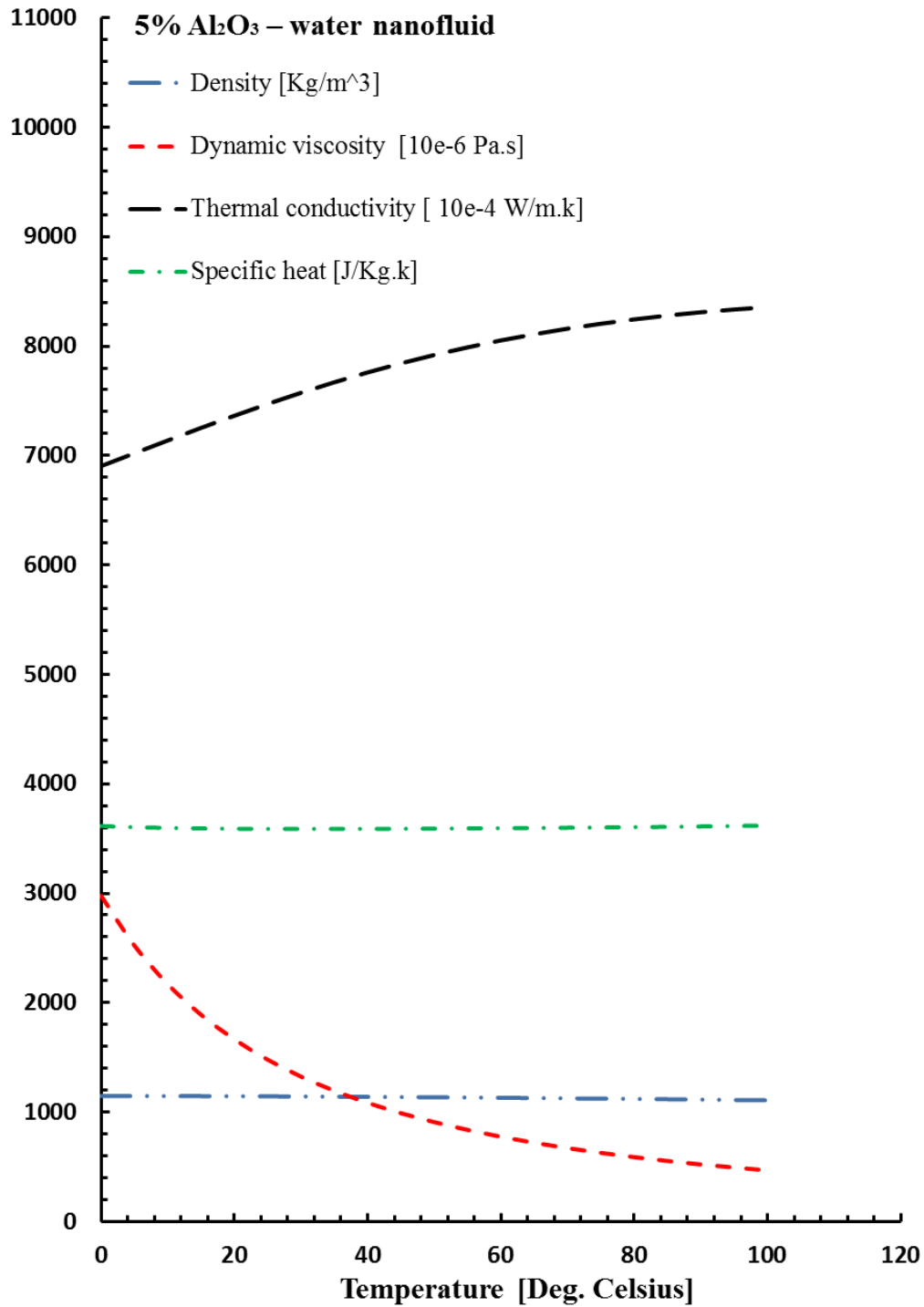


Figure A-3 Thermophysical properties of 5% Al₂O₃ – water nanofluid

APPENDIX (continued)

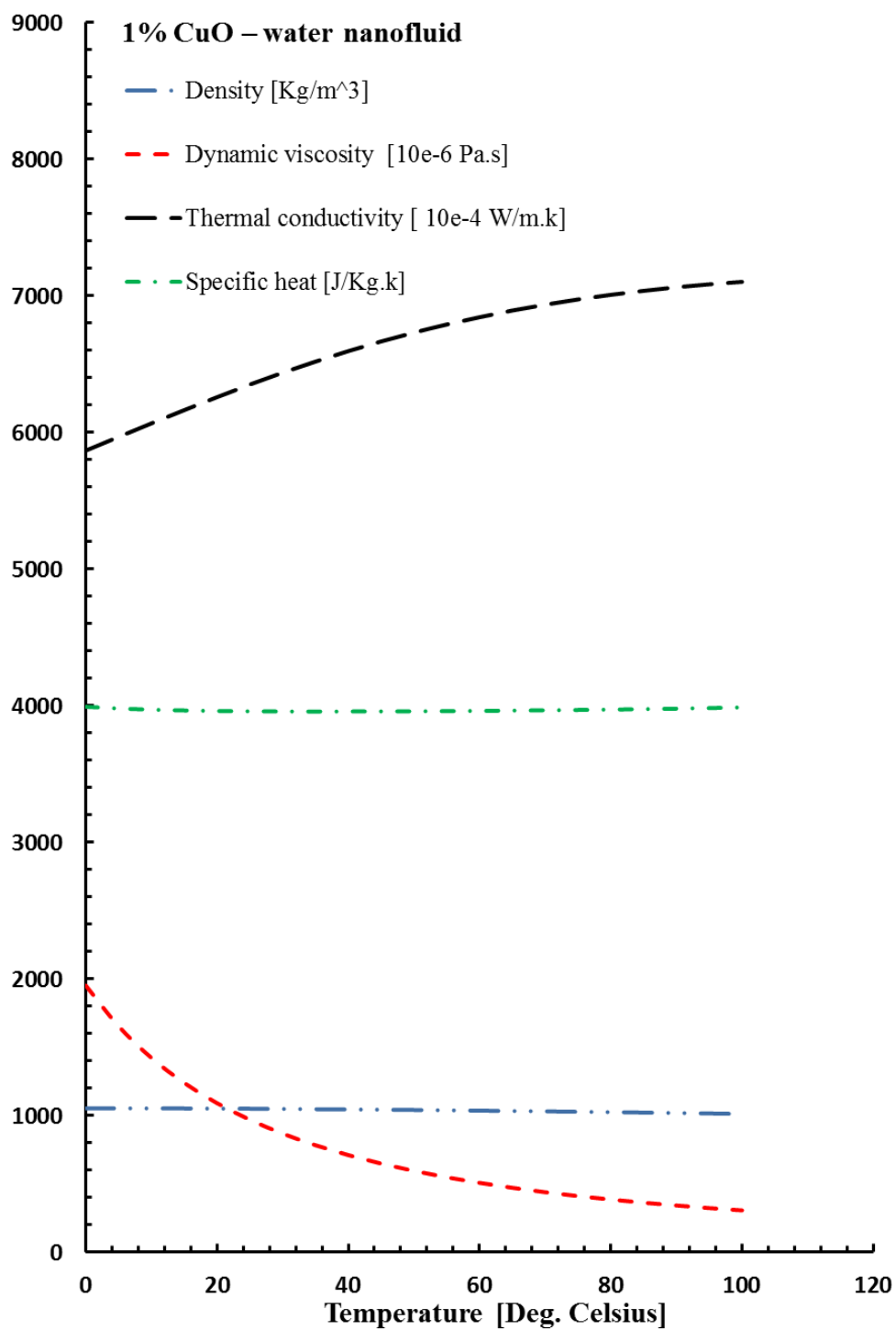


Figure A-4 Thermophysical properties of 1% CuO – water nanofluid

APPENDIX (continued)

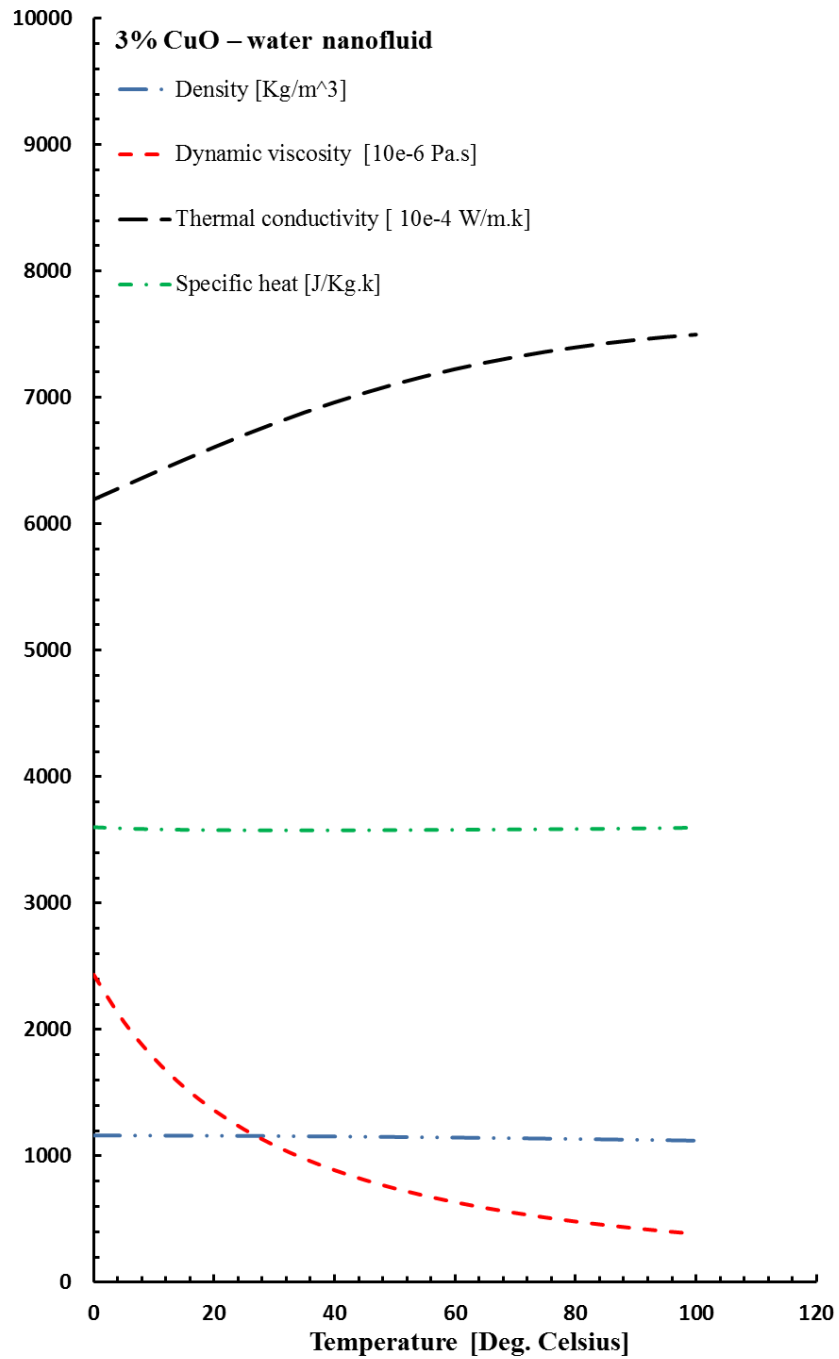


Figure A-5 Thermophysical properties of 3% CuO – water nanofluid

APPENDIX (continued)

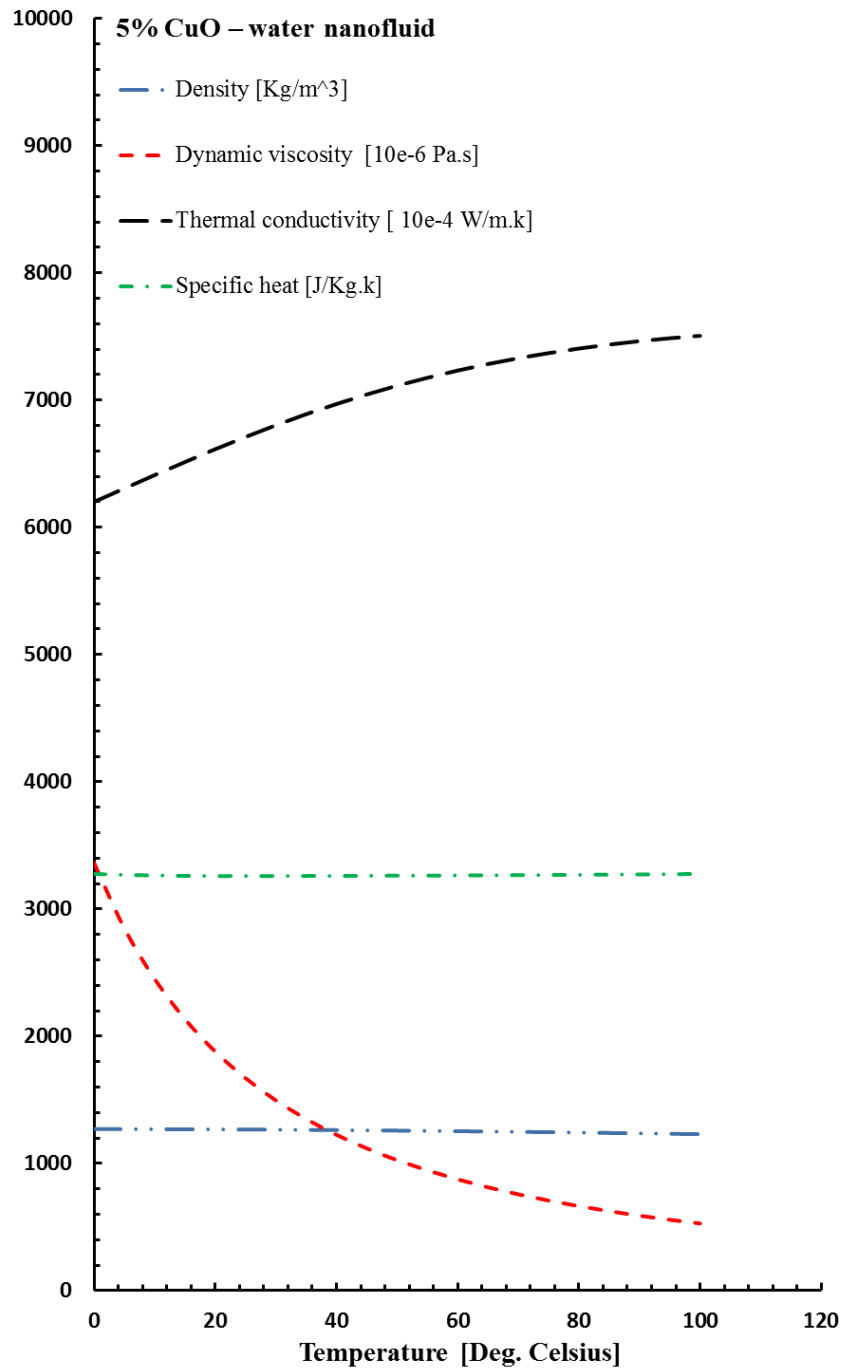


Figure A-6 Thermophysical properties of 5% CuO – water nanofluid

APPENDIX (continued)

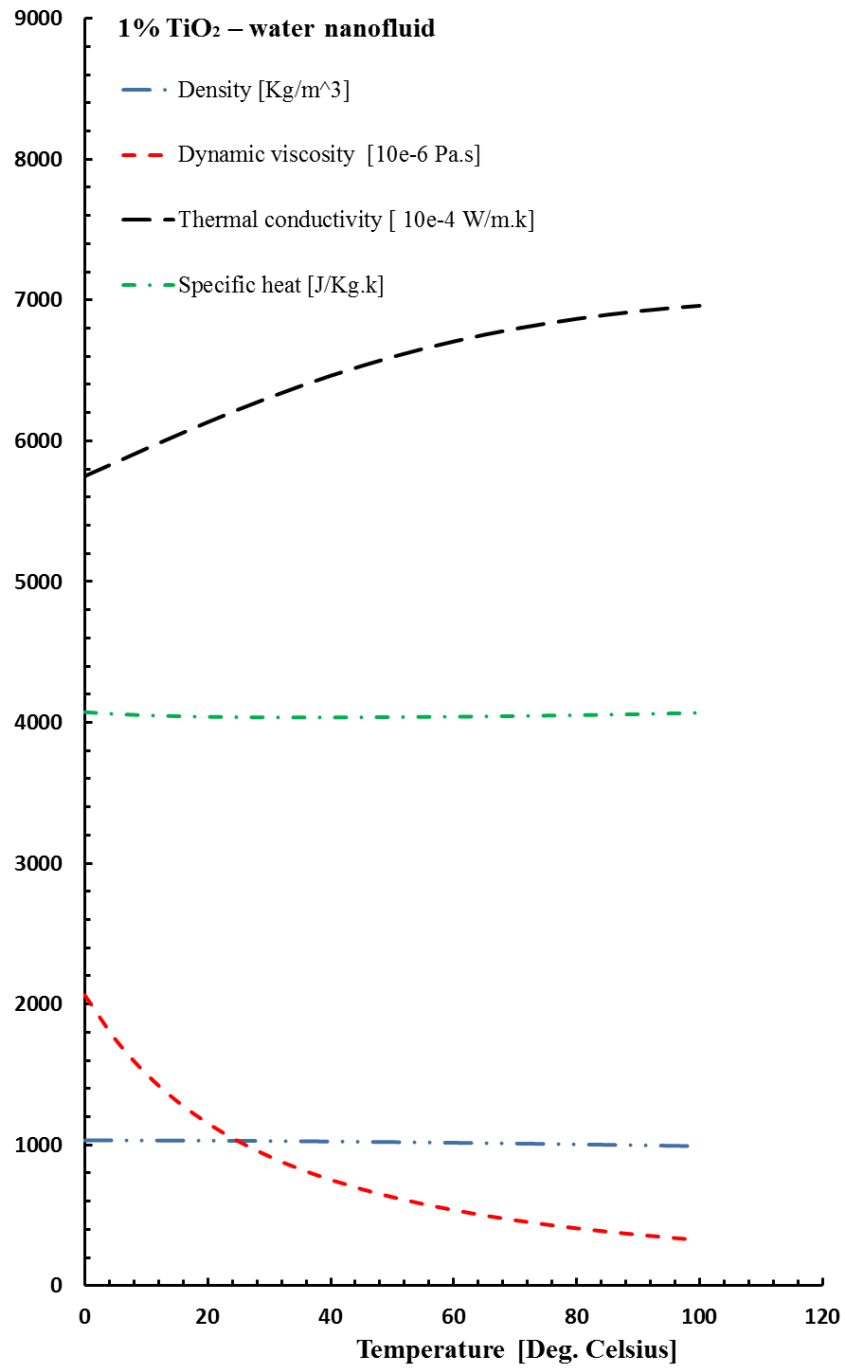


Figure A-7 Thermophysical properties of 1% TiO₂ – water nanofluid

APPENDIX (continued)

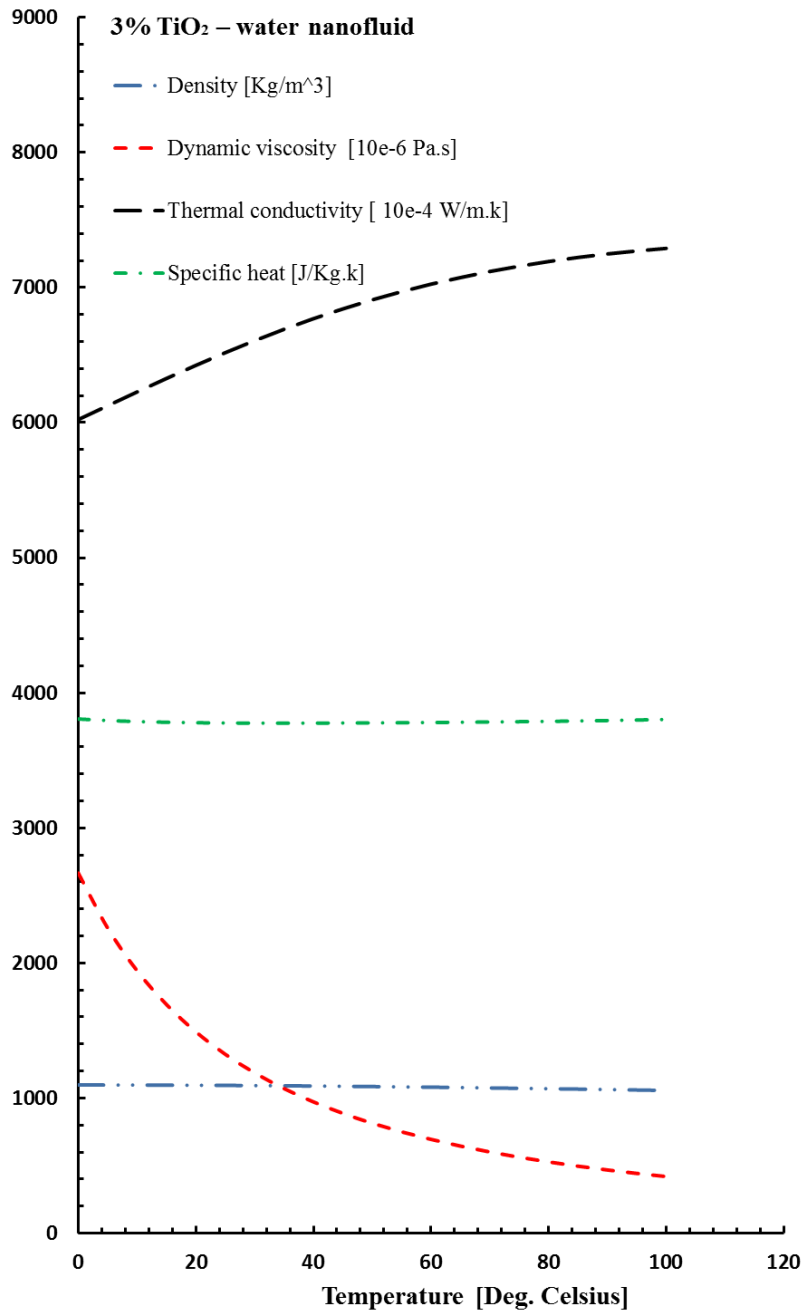


Figure A-8 Thermophysical properties of 3% TiO₂ – water nanofluid

APPENDIX (continued)

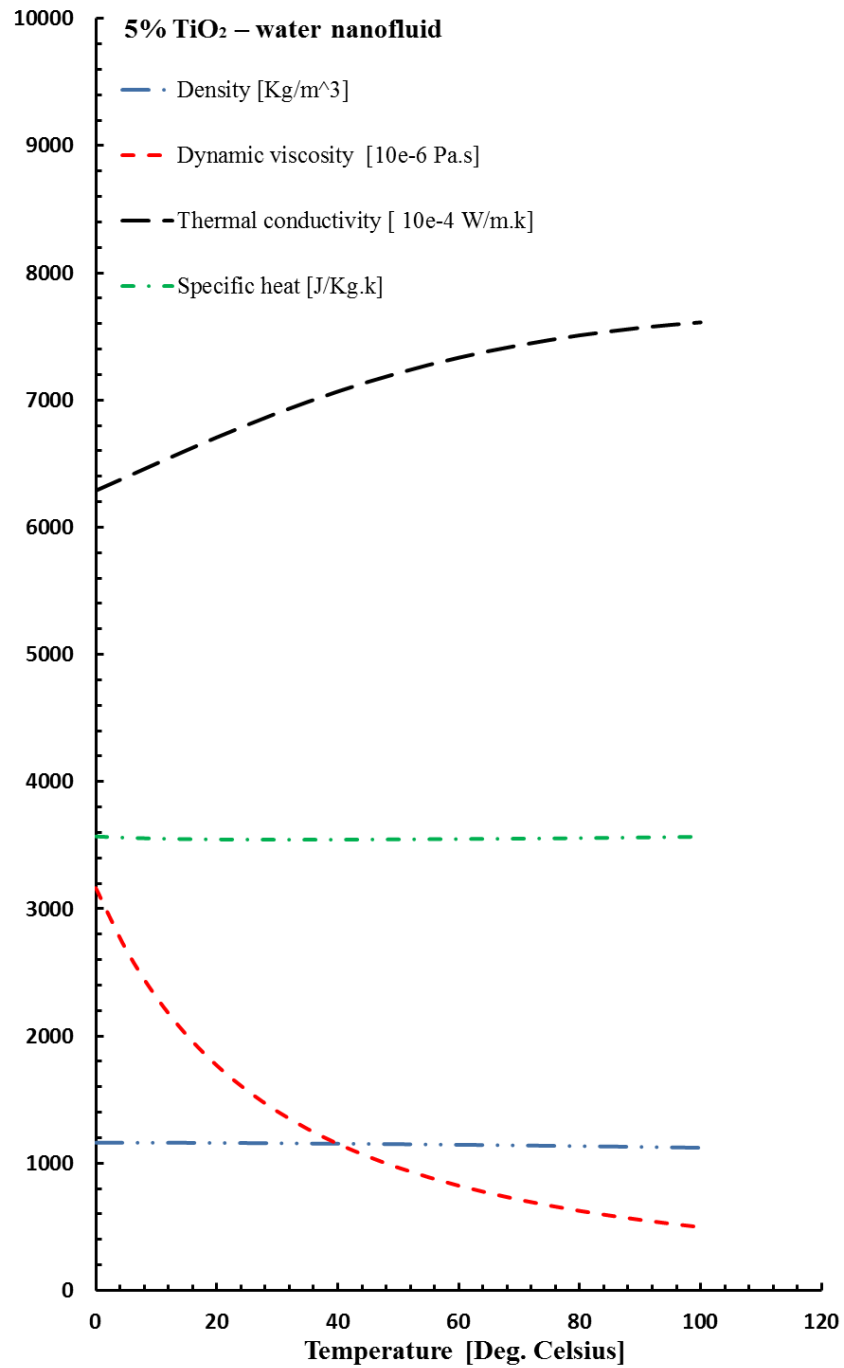


Table A-9 Thermophysical properties of 5% TiO₂ – water nanofluid